

# **Identification and functional characterization of cargo binding sites of plant myosins**

Inaugural Dissertation  
zur Erlangung des Doktorgrades  
der Mathematisch-Naturwissenschaftlichen Fakultät  
der Universität zu Köln

vorgelegt von  
Amirali Sattarzadeh Mohammadi  
aus Tabriz, Iran

Köln, 2006



Prüfungsvorsitzender: Prof. Dr. Wolfgang Werr  
Berichterstatter: Prof. Dr. Paul Schulze-Lefert  
Prof. Dr. Martin Hülskamp

Tag der mündlichen Prüfung: 30 Oktober 2006

## Abbreviations/acronyms

(v/v)	volume per volume
(w/v)	weight per volume
μ	micro
a.a	amino acid
Amp	ampicillin
At	<i>Arabidopsis thaliana</i>
ATP	adenosine 5-triphosphate
avr	avirulence
BDM	2, 3-Butanedione monoxime
<i>Bgh</i>	<i>Blumeria graminis</i> f.sp. <i>hordei</i>
bp	base pair(s)
C.C	coiled-coil
cDNA	complementary DNA
CFP	cyan fluorescence protein
CLSM	confocal laser scanning microscopy
dATP	deoxyadenosinetriphosphate
dCTP	deoxycytidinetriphosphate
ddH <sub>2</sub> O	deionised and distilled water
DEPC	diethylpolycarbonate
dGTP	deoxyguanosinetriphosphate
dicot	dicotyledonous
DIL	mouse <i>dilute</i> locus
DMF	dimethyl formamide
DMSO	dimethylsulfoxide
DNA	deoxyribonucleic acid
DNase	deoxyribonuclease
dNTP	deoxynucleosidetriphosphate
dpi	days post inoculation
<i>EDS1</i>	<i>Enhanced Disease Susceptibility 1</i>
EDTA	ethylenediaminetetraacetic acid
ER	endoplasmic reticulum
EST	expressed sequence tag
EtBr	ethidium bromide
EtOH	ethanol
FP	fluorescence protein
g	gram
GFP	green fluorescent protein
h	hour
hpi	hours post inoculation

HR	hypersensitive response
Hv	<i>Hordeum vulgare</i>
Kan	Kanamycin
Kb	kilobase(s)
kDa	kiloDalton(s)
KO	Knock-Out
l	litre
m	milli
M	Molar
Min	Minute(s)
mmol	millimolar
monocot	monocotyledonous
mRNA	messenger ribonucleic acid
N	amino
Nt	<i>Nicotiana tabacum</i>
ORF	open reading frame
Os	<i>Oryza sativa</i>
p	pico
PCR	polymerase chain reaction
PEG	polyethylene glycol
pH	negative decimal logarithm of the H
R	resistance
RFP	red fluorescent protein
RNA	ribonucleic acid
Rpm	rounds per minute
RT	room temperature
RT-PCR	reverse transcription- polymerase chain reaction
sec	second(s)
ssp.	Species
ST	Sialyl transferase
T-DNA	transfer DNA
TRIS	Tris-(hydroxymethyl)-aminomethane
TTSS	type III secretion system
U	unit
UV	ultraviolet
V	Volt
WT	wild-type
YFP	yellow fluorescence protein

**CONTENTS**

<b>ABBREVIATIONS/ACRONYMS.....</b>	<b>3</b>
<b>1 INTRODUCTION .....</b>	<b>8</b>
1.1 THE PLANT CYTOSKELETON AND THE INTRACELLULAR MOTILITY MEDIATED BY MOLECULAR MOTORS .....	9
1.2 THE SUPER FAMILY OF MYOSINS .....	10
1.3 ENZYMATIC ACTIVITY AND PRODUCTION OF MOVEMENT BY MYOSIN MOTORS .....	17
1.4 THE TAIL OF YEAST CLASS V MYOSIN (MYO2P) AS A MODEL FOR THE STUDY OF PLANT CLASS XI MYOSINS .....	20
1.5 MOLECULAR MOTORS IN PLANT CELLS .....	25
1.5.1 <i>Myosin motors in Arabidopsis thaliana</i> .....	25
1.5.2 <i>Myosin motors in Zea mays</i> .....	26
1.5.3 <i>Myosin motors in Oryza sativa</i> .....	26
1.5.4 <i>Myosin motors in Nicotiana tabacum</i> .....	27
1.5.5 <i>Domains in tails of plant myosins</i> .....	27
1.5.6 <i>Subcellular localization and function of plant myosins</i> .....	28
1.5.7 <i>Potential function of plant myosins</i> .....	29
1.6 OBJECTIVES OF THIS STUDY.....	31
<b>2 MATERIALS AND METHODS.....</b>	<b>34</b>
2.1. MATERIALS .....	34
2.1.1 <i>Plant Material</i> .....	34
2.1.2 <i>Bacteria / fungi / oomycetes /yeast</i> .....	34
2.1.3 <i>Media and Additives</i> .....	35
2.1.4 <i>Nucleic Acids</i> .....	38
2.1.5 <i>Enzymes, Buffers and Solutions</i> .....	42
2.1.6 <i>Chemicals and radiochemicals</i> .....	45
2.1.7 <i>Microscopes</i> .....	46
2.1.8 <i>Online Software</i> .....	47
2.2 METHODS .....	47
2.2.1 <i>Nucleic acids-related methods</i> .....	47
2.2.2 <i>Methods for the cultivation of bacteria and transformation of plants</i> ..	56
2.2.3 <i>Methods related to staining and microscopy</i> .....	61
2.2.4 <i>Methods related to Yeast transformation and two-hybrid assays</i> .....	61
2.2.5 <i>Methods related to fluorescence labeling of organelles</i> .....	64
<b>3 RESULTS.....</b>	<b>66</b>
3.1 CHARACTERIZATION OF PUTATIVE VESICLE BINDING SITES IN MYOSIN XI TAIL DOMAINS.....	66

3.1.1 Identification of putative vesicle binding sites in myosin XI tail domains .....	66
3.1.2 Subcellular localization of the DIL- and the LCP domain .....	70
3.1.3 Subcellular localization of class XI myosins from different subclasses .....	73
3.1.4 In planta expression of selected fragments of <i>S. cerevisiae</i> class V myosin, Myo2p .....	78
3.1.5 Transient expression and subcellular localization of selected fragments of AtMya1 .....	80
3.2 CHARACTERIZATION OF <i>ARABIDOPSIS THALIANA</i> CLASS VIII MYOSINS .....	81
3.2.1 Subcellular localization of ATM2 .....	83
3.2.2 Subcellular localization of ATM1 .....	91
3.3 SUBCELLULAR LOCALIZATION OF SELECTED MYOSIN CONSTRUCTS IN <i>A. THALIANA</i> .....	92
3.4 IDENTIFICATION OF PUTATIVE MYOSIN BINDING PROTEINS BY YEAST TWO-HYBRID SCREENING .....	93
3.4.1 Screening for Mya1 .....	93
3.4.2 Screening for ATM2 .....	95
3.5 <i>A. THALIANA</i> MYOSIN KNOCK-OUT LINES .....	96
3.5.1 Selection and identification of <i>A. thaliana</i> myosin knock-out lines .....	96
3.5.2 Phenotypic characterization of <i>Arabidopsis thaliana</i> class XI myosin knock-out lines .....	97
3.5.3 Phenotypic characterization of <i>Arabidopsis thaliana</i> class VIII myosin knock-out lines .....	99
3.6 STUDIES ON THE INVOLVEMENT OF MYOSINS IN PLANT DEFENCE RESPONSES .....	101
3.6.1 Non-host resistance (powdery mildew of barley) .....	101
3.6.2 Host resistance .....	103
3.6.3 Influence of BDM application on the defence response of barley .....	104
3.7 EFFECTS OF BDM ON THE SUBCELLULAR LOCALIZATION OF THE ATMYA1 DIL DOMAIN .....	105
3.8 EXPRESSION STUDIES OF BARLEY MYOSINS .....	106
3.8.1 Subcellular localization of myosins from barley .....	108
<b>4 DISCUSSION .....</b>	<b>110</b>
4.1 TRANSIENT OVEREXPRESSION OF MYOSIN FLUORESCENCE PROTEIN (FP) FUSIONS AS ASSAY SYSTEM FOR THE IN VIVO ANALYSIS OF CARGO BINDING SITES .....	110
4.2 SYSTEMATIC ANALYSIS OF <i>A. THALIANA</i> MYOSIN CLASS XI CARGO BINDING SITES .....	115
4.3 <i>IN PLANTA</i> EXPRESSION AND LOCALIZATION OF THE YEAST CLASS V MYOSIN (MYO2P) CARGO BINDING DOMAINS .....	118
4.4 SUBCELLULAR LOCALIZATION OF PLANT CLASS VIII MYOSINS .....	119
4.5 FUNCTIONS OF PLANT MYOSINS IN SUBCELLULAR TRANSPORT .....	124

---

4.5.1 Class XI myosins .....	124
4.5.1.1 Transportation of Peroxisomes .....	124
4.5.1.2 Transportation of Golgi stacks/vesicles .....	126
4.5.1.3 Motility of mitochondria and endoplasmic reticulum (ER) in plant cells .....	128
4.5.2 Class VIII myosins .....	130
4.6 POTENTIAL MYOSIN INTERACTING PROTEINS .....	132
4.6.1 Myosin class XI .....	132
4.6.2 Myosin class VIII .....	134
4.7 ANALYSIS OF MYOSIN KNOCK OUT LINES .....	135
4.7.1 Class XI myosins .....	135
4.7.2 Class VIII myosins .....	137
4.8 APPLICATION OF BDM AS MYOSIN INHIBITOR .....	137
4.9 POTENTIAL ROLE OF MYOSINS IN PATHOGEN DEFENCE .....	139
4.9.1 Effect of BDM on plant-pathogen interaction .....	139
4.9.2 Involvement of plant class XI myosins in host resistance .....	140
<b>5 SUMMARY .....</b>	<b>142</b>
5.1 SUMMARY (ENGLISH) .....	142
5.2 ZUSAMMENFASSUNG (DEUTSCH) .....	145
<b>6 OUTLOOK .....</b>	<b>148</b>
6.1 CLASS XI MYOSINS: .....	148
6.2 CLASS VIII MYOSINS .....	148
6.3 YEAST-TWO-HYBRID .....	149
<b>7 LITERATURE .....</b>	<b>150</b>
<b>8 ACKNOWLEDGEMENTS .....</b>	<b>172</b>
<b>9 EIDESSTATLICHE ERKLÄRUNG .....</b>	<b>174</b>
<b>10 LEBENSLAUF .....</b>	<b>175</b>

## 1 Introduction

Plants play directly or indirectly an essential role as a nutritional resource in extending our life. Improvements in crop yields need a better understanding of the mechanisms underlying intracellular trafficking in respect of carbohydrate, protein transport and plant interaction with the environment (Robinson, 2003). In respect to environment, plants are sessile organisms; therefore under stress conditions such as physical stresses like strong light, adverse temperature, dryness, wetness, high salt, or biological stresses like pathogen or herbivore attack, they can not escape but have to overcome the stress. Hence, plants evolved complicated adaptive responses at the organelle level as well as at the cell, tissue, and organ levels to avoid stresses (Nagai, 1993; Williamson, 1993). It is believed that intracellular organelle trafficking plays a crucial role in allowing plants to cope with environmental stresses and to propagate efficiently. Although each organelle type must have its own efficient mechanism for intracellular trafficking, however harmonic coordination between all these organelles is required to enable each organelle to accomplish its function (Wada and Suetsugu, 2004).

Furthermore, the increasing knowledge demonstrating that plants could serve as excellent bioreactors for the production of a variety of valuable proteins (Stoger et al., 2002; Fischer et al., 2004; Vitale and Pedrazzini, 2005) underlines the requirement for basic research on intracellular protein trafficking. Although the mechanisms underlying intracellular protein transport in animal and yeast cells are well known and many of the molecular players appear to be conserved among eukaryotes, however it

must to be taken into account that the plant endomembrane system has some features which are unique, e. g. decentralized Golgi apparatus consisting of a network of motile stacks which does not need fragment during mitosis, multiple vacuolar compartments including a protein storage compartment and a large central vacuole, cell-plate (phragmoplast) facilitated cytokinesis and cell division (Robinson, 2003; Hawes, 2005). Another specific feature of the intracellular transport in plant cells is cytoplasmic streaming which moves large quantities of cytoplasm (including organelles) around the cell and is most pronounced in larger, highly vacuolated cells (Nagai, 1979; Shimmen and Yokota, 1994). Cytoplasmic streaming has been studied extensively in characean algae (Nagai, 1979; Shimmen and Yokota, 2004). Studies of streaming events in the past have relied on visualization of moving organelles with phase-contrast microscopy. The nature of the organelles was therefore mostly unknown. However it is been shown that cytoplasmic streaming is mostly driven by the acto-myosin system (Shimmen and Yokota, 2004).

### **1.1 The plant cytoskeleton and the intracellular motility mediated by molecular motors**

The cytoskeleton is playing an important role in a variety of cellular functions of plant cells such as intracellular transport, signaling, cell division and generation as well as maintenance of cell shape (Williamson, 1986; Volkmann and Baluska, 1999; Mathur et al., 2003; Mathur et al., 2003). In eukaryotes the cytoskeleton consists of three types of filaments called actin filaments or micro filaments, intermediate filaments and

microtubules. Notably, so far the presence of intermediate filaments has not been confirmed in plants (Meagher and Fechheimer, 2003).

Actin filaments and microtubules are polar filaments, the ends of which are referred to as *plus* and *minus* ends. Both types of filaments provide the tracks for motor based transport. Transport along microtubules occurs in both directions and is performed by kinesins and dyneins. Kinesins are generally plus-end directed (Vallee and Sheptner, 1990) motor proteins. Movement along actin filaments is accomplished by members of the myosin super family (Sellers, 2000). Myosin mediated movement is mainly plus-end, although recently myosin VI (Wells et al., 1999) has been shown to move in the opposite direction. All these motors utilize energy from the hydrolysis of ATP to move in association with the cytoskeleton. ATP hydrolysis generates a small conformational change in the motor domain that is amplified and translated into movement with the assist of structural motifs ( reviewed by Schilwa and Woehlke, 2003).

## **1.2 The super family of myosins**

Myosins comprise a large super family of proteins that share common domains which have been shown to interact with actin, hydrolyze ATP and produce movement in all cases examined to date. All myosins have typically three functional domains as shown in Figure 1: (I) the motor domain which interacts with actin and binds ATP and is responsible for force production, (II) the neck or regulatory domain which binds light chains or calmodulin, and (III) the tail domain which is thought to be important for subcellular localization and cargo binding (reviewed by Seller, 1999). However for most myosins its precise cellular function is still obscure. The motor

domains are highly conserved with the exception of several surface loops and the amino-terminus. With one known exception (Heintzelman and Schwartzman, 1997), the motor domain is linked to the C-terminal tail domain by the neck domain of variable length that contains sites for binding of regulatory light chains or calmodulin (Mermall et al., 1998). The neck consists of a characteristic helical sequence termed the IQ motif with a consensus sequence of IQXXRGXXR (Cheney and Mooseker, 1992). The number of IQ motives present in the neck of different myosins can vary between zero and six. The tail domain is the most divergent domain among the different myosin classes varying widely in length and in sequence. Functional motives, such as kinase domains, GTPase-activating domains, SH3, GAP, FERM and pleckstrin homology (PH) domains are sometimes found in the tails of myosins known to function in signal transduction, membrane binding, or protein–protein interactions (Mermall et al., 1998; Oliver et al., 1999). In addition, the tails of many myosins contain coiled-coil forming sequences which allow the molecules to dimerize and produce two-headed molecules. In general, the tail domains of myosins are believed to be largely responsible for class-specific functions. In Table 1.1 some of the most important domains found in the tail of unconventional myosins are listed.

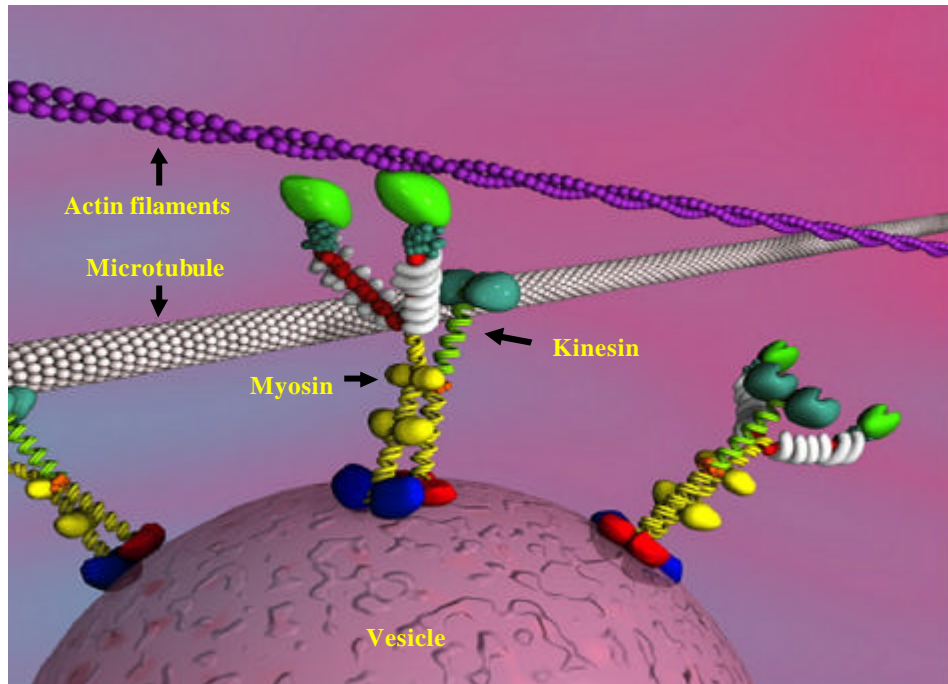


**Figure 1:** Major structure features of myosin molecular motors with their corresponding track (actin filaments) are shown. Myosin head domain (green), IQ domain (white) and tail domain (yellow and blue) are shown (Fig from Cell motility and Cytoskeleton 2000, 45-4).

The myosins are subdivided into an ever-increasing number of classes (17 at the last count) according to phylogenetic analyses of the motor domains (Hodge and Cope, 2000). Traditionally they have been segregated into two categories: the conventional (muscle and nonmuscle myosins, class II) and the unconventional myosins, which include all other myosins. Class II reviewed by (Seller, 2000) was discovered over 60 years ago and is found in muscles and in the cytoplasm of animal cells. Class I myosins were next discovered and the subsequent classes were numbered in order of the discovery of the founding member of the class (Mermall et al., 1998). Not

all types of myosins are expressed in one organism. For example class VIII, XI and XIII are plant specific myosins and plants do not have any other myosins from other classes. However even the simplest of eukaryotes express multiple myosins (Reddy and Day, 2001). The budding yeast, *Saccharomyces cerevisiae*, for example has five myosin genes: one conventional class II myosin and two of each classes I and V (reviewed in Pruyne et al., 2004). The number of myosin genes present in mammals is conservatively estimated at 25–30 from classes I, II, III, V, VI, VII, IX, X and XV. In any case, all eukaryotic animal cells examined contain at least one myosin II gene and, usually, multiple myosin I genes. In addition, myosin V genes are found widely, if not universally (Mermall et al., 1998; Oliver et al., 1999).

Although most family trees are constructed by analysis of the motor domains, analysis of the whole molecule or of the tail domains alone generally gives similar relationships (Cope et al., 1996). While relatively little is known about the detailed cellular functions of most of the unconventional myosins, their importance is highlighted by the discovery that mutations in unconventional myosins can lead to severe defects as deafness, blindness, seizures or even death (Table 1.1, Mermall et al., 1998).

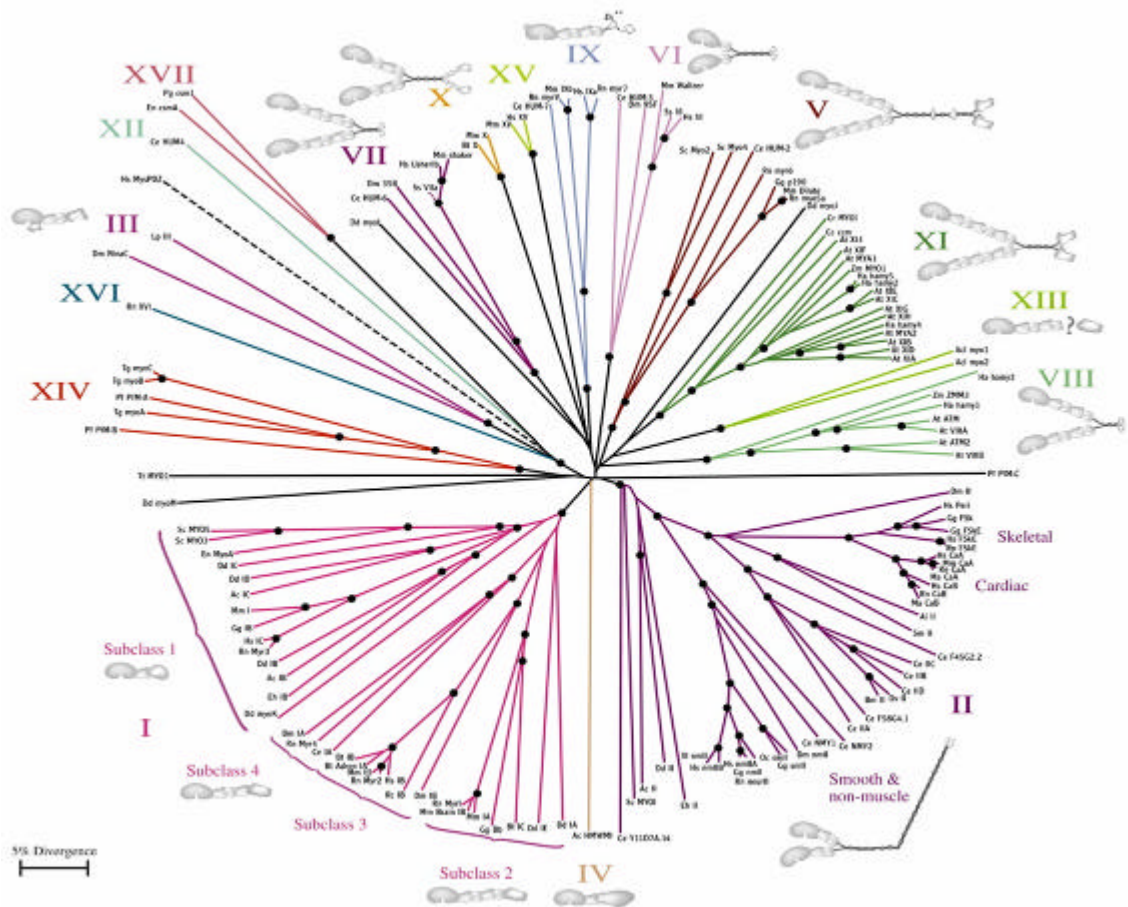


**Figure 1.1:** An unrooted phylogenetic tree of the myosin superfamily based on head domain protein sequences. Myosin classes are shown in roman numerals. Sequence divergence is proportional to the length of the connecting branches. The large globular domains represent heads, smaller globular structures represent neck and tail motifs, and twisted lines denote coiled-coils (Fig from Hodge and Cope, 2000).

Generally, the tail domain structure is conserved within each class but differs between classes (Mermall et al., 1998). In light of the high degree of conservation between the motor domains, the myosin tail is thought to determine the specificity of the protein, both for interactions such as dimerization and for the type of cargo it will carry. In contrast to the motor

domain, which has been extensively studied in both conventional and several of the unconventional myosins, the functions of the individual tail domains are by far less well understood (Mermall et al., 1998). There are multiple ways in which motor proteins may be regulated: regulation of enzymatic activity, regulation of affinity to the cytoskeleton, regulation of protein levels and regulation of affinity to the cargo in the cell (Howard, 2001; Schliwa and Woehlke, 2003). The regulatory pathways involved appear to be highly complex, and are just at the beginning of characterization. In a few studies it has been demonstrated that phosphorylation, G proteins, and calcium/calmodulin are signals involved in myosin regulation (Reilein et al., 2001; Legesse-Miller A et al., 2006). For instance, in case of myosin V, the closest homologue of class XI myosins, it has been shown that organelle transport by myosin V is down-regulated during mitosis by myosin-V phosphorylation (Karcher et al., 2001). Using mass spectrometry phosphopeptide mapping the authors showed that the tail of myosin-V was phosphorylated in mitotic *Xenopus* egg extracts on a single serine residue localized in the carboxyl-terminal organelle-binding domain which resulted in the release of the motor from the organelle. Interestingly, the phosphorylation site matched the consensus sequence of calcium/calmodulin dependent protein kinase II (CaMKII), and inhibitors of CaMKII prevented myosin-V release. However, to understand how these multiple pathways and mechanisms are coordinated to regulate a single motor in other motor proteins remains a question to be solved in the future (Karcher et al., 2001).

<b>Class</b>	<b>Function</b>	<b>Domains</b>	<b>Dis</b>	<b>Disease</b>
I	Cell growth and development, Cell movement, Endocytosis	Basic,SH3,GPA	E(NP)	
II	cytoplasmic Cytokinesis, phagocytosis, cell shape and polarity	N-terminal SH3 like	E(NP)	FHC
III	Rhabdomere function (Drosophila), photoadaptation	PK, Basic	Meta	Deafness
IV	<i>Acanthamoeba</i> species only.	MyTH4,SH3	Ac	
V	Vesicle transport, mRNA transport, Chitin localization	DIL	E(NP)	Pigmentation disorder
VI	Stabilizing and anchoring, Endocytosis	Reverse Gears	Meta	Deafness
VII	Sensory epithelia	FERM,MyTH4,SH3	Meta	Deafness
VIII	?	-	Plants	
IX	Signal transduction, Leukocyte differentiation	RA, RhoGAP, DAG_PE	Meta	
X	Signal transduction	PH,MyTH4,FERM	Vert	
XI	Vesicle transport	DIL	Plants	
XII	?	MyTH4	Ce	

XIII	?	-	Acl	
XIV	<i>Toxoplasma</i> and <i>Plasmodium</i> species only	-	Prot	
XV	Auditory	FREM,MyTH4,SH3	Mamm	Deafness
XVI	Neuronal cell migration	ANK	Mamm	
XVII	chitin synthase <i>Pyricularia</i> and <i>Emiricella</i> species only.	Chitin synthase	Fungi	

**Table 1.1:** The most important features of the unconventional myosins including identified or potential functions and related diseases are summarized in the table. Dis: Distribution, known or inferred occurrence in different organisms., E(NP): Eukaryotes (not plants) , Meta: Metazoa, Mamm: Mammals, Vert: Vertebrates, Prot: Protozoan parasites, Acl: *Acetabularia cliftonii*, Ac: *Acanthamoeba castellanii*, Dd: *Dictyostelium discoideum*, Tt: *Tetrahymena thermophila*, Pf: *Plasmodium falciparum*, Ce: *Caenorhabditis elegans*, FHC: Familial Hypertrophic Cardiomyopathy (Mermall et al., 1998; Oliver et al., 1999).

### 1.3 Enzymatic activity and production of movement by myosin motors

Essential attributes of the actomyosin ATPase cycle were derived from transient kinetic studies using actin filaments and myosin motor domain fragments in solution and by comparing the results with those obtained from mechanical, optical and structural measurements on rate processes in intact muscle fibers (Bagshaw et al., 1974; Geeves et al., 1984; Goldman, 1987; Lombardi et al., 1995; Piazzesi et al., 2002). These studies demonstrated clearly that the conserved myosin motor domain is the active partner in the interaction with actin filaments and confirmed that myosin is a product-

inhibited ATPase that is strongly stimulated by actin (Reedy M. K., 1965; Huxley, 1969; Lynn and Taylor, 1971).

Several models have been proposed for the acto-myosin ATPase cycle. However, that the sliding of the filaments was driven by consumption of ATP by the myosin molecule itself was not demonstrated convincingly until 1962 (Cain and Davies, 1962). Later on, the 'sliding filament model' was refined to the 'swinging cross-bridge' model with the help of molecular engineering, single molecule approaches, and X-ray crystallography to the currently accepted 'swinging lever-arm model' (Rayment et al., 1993; Anson et al., 1996; Uyeda T. Q., 1996; Suzuki et al., 1998; Spudich, 2001). The swinging lever-arm model expects that the motor domain binds to actin with almost regular geometry and that small actin- and nucleotide-dependent conformational changes within the motor domain are amplified at its distal end by the extended and rigid lever arm domain (Fig 1.2). The fact that reverse-direction movement of myosins can be achieved simply by rotating the direction of the lever arm 180° support this model. During the acto-myosin ATPase cycle, weak actin-binding states (ATP and ADP-Pi states) rotate with strong actin-binding states (ADP states and nucleotide-free or rigour state; Fig 1.2). Biochemical, kinetic and mechanical studies on muscle myosins have established that ATP binding dissociates the acto-myosin complex, and that ATP hydrolysis is rapid when myosin is not associated with actin. Pi release conduct ADP release and both product release steps are accelerated considerably upon actin binding. Force development occurs when myosin binds strongly to actin and is associated with actin-induced acceleration of Pi release (Geeves et al., 2005).

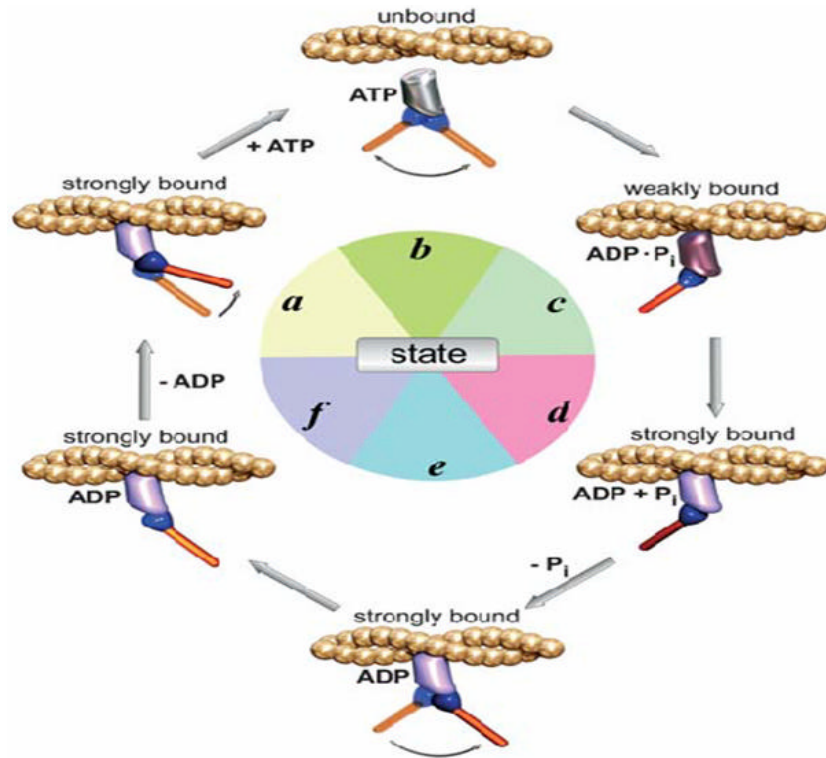


**Figure 1.2:** A minimal mechanochemical scheme for the actomyosin cross-bridge cycle. Starting from the rigor complex, A·M (state *a*), ATP binds to rapidly dissociate the complex and the lever arm is reprimed to the pre-power-stroke position (state *b*).

This is followed by hydrolysis. The preceding three states have been well defined by crystallography, electron microscopy and solution kinetics. The exact sequence of biochemical, structural and mechanical events is more speculative. The M·D·Pi complex rebinds to actin, initially weakly (state *c*) and then strongly (state *d*). Binding to actin induces the dissociation of Pi and the power stroke (state *e*). The completion of the tail swing (state *f*) is followed by ADP release to return to the rigor-like complex (state *a*); in some myosins (e.g. smooth-muscle myosin-II, myo1b or myosin-V) ADP dissociation is associated with a further displacement of the lever arm. Actin monomers are shown as golden spheres. The motor domain is coloured metallic grey for the free form, purple for the weakly bound form and violet for the strongly bound form. The converter is shown in blue and the lever arm in orange (Fig from Geeves et al., 2005).

### **1.4 The tail of yeast class V myosin (Myo2p) as a model for the study of plant class XI myosins**

Since this dissertation focuses on myosins from plants the emphasis here will be on the unconventional myosins, particular attention will be paid to the interesting protein domains found in the tail of class V myosins, the closest homologue of plant class XI myosins (Kinkema and Schiefelbein, 1994). This structural homology is supported by other studies. For instance based on phylogenetic tree construction and studies on the evolutionary history of the myosin superfamily it was hypothesized that myosins V and XI evolved from a common myosin II-like ancestor, but the two families diverged to either the plant XI or animal V lineage (Thomson and Langford, 2002). Indeed, Myosin V and myosin XI have similar sequences and structural properties (Kinkema and Schiefelbein, 1994). Both are dimers, meaning two-headed molecules, that move processively hand over hand on helical actin filaments (Kinkema and Schiefelbein, 1994; Tominaga et al., 2003), they both have 4-6 IQ repeats and possess a DIL domain within the C terminal part of the tail (with two exceptions in class XI). In figure 1.3 a scheme of the structure of myosin V is depicted. Moreover, their functions appear to be related: both act as organelle motors (Mermall et al., 1998).

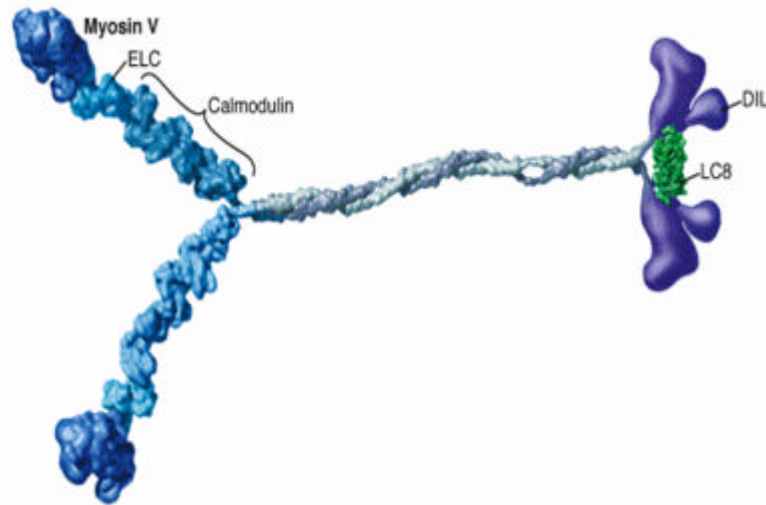


**Figure 1.3:** The structure of the myosin V protein, closest homologue of plant class XI myosins. It forms a dimer and walks processively on actin filaments. The motor domain is shown in dark blue, the legs working as mechanical amplifiers are in light blue, and the stalk in grey. The stalk, formed by dimerization of alpha helical domains of monomers, connects the head regions and contains a cargo-binding domain in its tail (violet and green; Fig from Vale, 2003).

Myosin V is suggested to be the most ancient class of myosins, being present in the fungal and animal kingdoms (Berg et al., 2001). Work in the yeast system has provided the strongest evidence for involvement of class V myosins in transport of vesicles (reviewed in Pruyne et al. 2004). The first myosin V to be identified, the yeast Myo2p, is also the only yeast myosin essential for viability (Johnston et al., 1991) and his deletion (*myo2-66*) causes cells to arrest in an enlarged, unbudded state, with an accumulation of secretory vesicles and disorganization of the actin cytoskeleton (Johnston et al., 1991). Further studies have shown that the *S. cerevisiae*, Myo2p, attaches to at least six types of cargo, including secretory vesicles, the vacuole/lysosome, late Golgi elements, peroxisomes, mitochondria, and

microtubules (Govindan and Bowser, 1995; Hill et al., 1996; Catlett and Weisman, 1998; Schott et al., 1999; Beach et al., 2000; Yin et al., 2000; Hoepfner et al., 2001; Rossanese et al., 2001; Boldogh et al., 2004; Itoh et al., 2004). Additionally overexpression causes a dominant-negative phenotype. For example it has been shown that the carboxyl-terminal tail of Myo2p is sufficient for localization to sites of polarized cell growth and overexpression of the tail of Myo2p causes mislocalization of the endogenous Myo2p, suggesting that some critical and limiting localization determinant for Myo2p exists in the cell (Govindan and Bowser, 1995; Govindan et al., 1995; Reck-Peterson et al., 1999).

The identification of six different cargoes for Myo2p implicates that these cargoes can move to distinct locations at different times. Thus, regulation of cargo attachment/detachment and/or regulation of motor activity must specify the appropriate movement of each cargo. Indeed, the discovery of organelle-specific myosin V receptors demonstrates that organelle-specific myosin V receptors play a major role in the regulation of cargo attachment/detachment. Only a few such receptors have been characterized: melanophilin on melanosomes (Wu et al., 2002), Vac17p on the yeast vacuole (Ishikawa et al., 2003) and more recently Inp2p as peroxisomes specific receptor (Fagarasanu et al., 2006).

The cargo-binding domain of Myo2p is composed of subdomains I and II. These domains, amino acid residues 1131–1345 (subdomain I) and residues 1346–1574 (subdomain II), were defined by mild proteolysis of the Myo2p globular tail (residues 1087–1574; Pashkova et al., 2005; Legesse-Miller et al., 2006). Through random mutagenesis of this globular tail, Catlett et al. (2000) isolated six new single point mutants defective in vacuole

inheritance, but not polarized growth. Surprisingly, all the residues required for Myo2p attachment to the yeast vacuole reside within subdomain I, whereas many of those predicted to be required for Myo2p attachment to secretory vesicles reside within subdomain II. These point mutations cluster to four amino acids in an 11-amino acid (1285-1307) span, suggesting that this region is important for vacuole movement (Catlett and Weisman, 1998; Schott et al., 1999; Catlett et al., 2000). In addition, through characterization of *myo2- D AflIII*, a deletion of amino acids 1,459–1,491, they identified a second region of the globular tail specifically required for polarized growth.

For the other member of class V myosins in *S. cerevisiae*, Myo4p, there is no indication for involvement in vesicle trafficking so far. Further studies, have been shown that it is required for mRNA transport into the bud (Long et al., 1997; Takizawa et al., 1997).

Mammals have three myosin V genes that encode myosin Va, myosin Vb and myosin Vc (Berg et al., 2001). The first which has been discovered was myosin Va, the product of the mouse *dilute* locus (Mercer et al., 1991), which is important for mouse coat color among other functions.

The DIL domain, named after the locus *dilute* in mammals which codes for a class V myosin (Mercer et al., 1991) is highly conserved among all class V myosins and, strikingly, also among class XI myosins of plants (Ponting, 1995). Remarkably, this domain can also be found in the tail region of the microtubule-based motor kinesin and in some kinesin-like proteins (Ponting, 1995). The function of the full-length DIL domain is not known. However, the data available so far suggest the capacity of this domain to contain cargo binding sequences. Several studies demonstrated an important role for myosin Va in vesicle trafficking so far. For example,

myosin Va together with Rab 27 has been shown that it is involved in movements of secretory granules through the actin-rich cortex of neuroendocrine and chromaffine cells (Desnos et al., 2003), with the assist of the melanophilin-like myosin-rab-interacting protein (Desnos et al., 2003; Rudolf et al., 2003). Furthermore, myosin Va is involved in movements of smooth ER into neuronal dendrites (Takagishi et al., 1996) and his association with synaptic vesicles through binding to synaptobrevin II and synaptophysin has been demonstrated (Prekeris and Terrian, 1997). For another member of myosin class V, mammalian myosin Vb, it has been demonstrated that it is associated with plasma membrane–recycling compartments in nonpolarized and polarized cells (Lapierre et al., 2001; Hales et al., 2002).

Although the mammalian myosins V are extensively studied, the function of myosin Vc is still not clear. It has been shown that overexpression of its tail results in its colocalization with a membrane compartment containing the transferrin receptor and Rab8 (Rodriguez and Cheney, 2002; Pruyne et al., 2004).

All this indicates that there might be some common rules in regulation of myosin V in respect to their organelle trafficking. Considering the high homology between class V and class XI myosins, it will be worthwhile to consider the well studied class V myosins as a model for further analysis of the class XI myosins.

## 1.5 Molecular motors in plant cells

In contrast to non-plant motors which have been extensively characterized, our knowledge about the function of motor proteins in plant cells is very limited. With completion of the sequence of the *A. thaliana* and *Oryza sativa* genomes as model systems for plants, the plant cell biologists was given a great opportunity for to study the presence and function of motor proteins.

### 1.5.1 Myosin motors in *Arabidopsis thaliana*

Shortly after completion of the *A. thaliana* genomic database, Reddy and Day (2001) analyzed the *A. thaliana* myosin-related sequences. As the myosin motor domain is highly conserved, the sequence from one myosin motor can be used to search a database for all other myosins. The authors concluded that there were only 17 myosin motor-related sequences in *Arabidopsis* including the 5 already reported myosins. They also found that *Arabidopsis* has the lowest percentage (0.068%) of myosin genes out of the total number of genes, as compared to *S.cerevisiae* and *S. pombe* with 0.080 % and 0.093 %, respectively, and *C.elegans* with 0.11 % and *D. melanogaster* with 0.096 %. An analysis of their exon/intron junctions and sequence similarities indicates that all *A.thaliana* myosins are highly conserved and some may represent gene duplication events (Reddy and Day, 2001). Sequence tree building divided the higher plant myosins into two classes, those still closely related to algal myosins (myosin class VIII) and a group of higher plant myosins (myosin class XI). None of the plant sequences were more related to animal myosins than they were to each

other, although animal myosin V sequences remain one of the closest outgroups consistent with the findings of (Berg et al., 2001). In other words, it is most probable that the *A. thaliana* (plant) myosins are all related to one common ancestral plant or algal myosin sequence, and the myosin family variation all occurred after plants and their protist green algal ancestors diverged from other eukaryotes (Meagher and Fechheimer, 2003).

### **1.5.2 Myosin motors in *Zea mays***

The five reported myosin genes from *Zea mays* were the first monocotyledon myosin genes to be analyzed (Liu et al., 2001). Later on immunofluorescence studies using a specific antibody against an isoform of class XI myosins from maize, showed localization on plastids and mitochondria (Wang and Pesacreta, 2004).

### **1.5.3 Myosin motors in *Oryza sativa***

Analysis of the so far released sequences of *Oryza sativa* cv. Nipponbare revealed that there are at least 14 myosin genes (12 out of 14 belong to class XI and 2 others to class VIII myosins; (Jiang and Ramachandran, 2004). Interestingly, the authors reported that among these 14 class XI genes, 11 genes were expressed in three major organs including leaves, panicles, and roots. The existence of these two classes, class VIII and class XI, in both monocotyledons and dicotyledons suggests that the origin of plant myosins might date before the divergence of dicotyledons and monocotyledons (Jiang and Ramachandran, 2004).

#### **1.5.4 Myosin motors in *Nicotiana tabacum***

So far only two myosins from *Nicotiana tabacum* have been isolated and characterized (Yokota et al., 1999). Further studies showed that one of the identified myosins belongs to class XI myosins (Yokota et al., 1999; Tominaga et al., 2003). Tominaga et al., 2003 have measured its ATPase characteristics, *in vitro* motility and, using optical trap nanometry, forces and movement developed by individual myosin XI molecules. Interestingly, like myosin V, this myosin XI from *N. tabacum* moves processively (can move along the actin filament for a long distance without detachment from it) along actin filaments with 35 nm steps at 7  $\mu\text{m/s}$ , the fastest known processive motion.

#### **1.5.5 Domains in tails of plant myosins**

In plant class VIII and XI myosins the tail consists of one or several  $\alpha$ -helical coiled-coil regions and a carboxy-terminal region. The only significant domain among the tails of class XI myosins is the DIL domain (Ponting, 1995). The DIL domain is missing in the class VIII myosins. The presence of an  $\alpha$ -helical coiled-coil region suggests that the two heavy chains can associate by twisting this region together into a coiled-coil to form a stable dimer that has two heads and a tail, as seen with other myosin subfamily members (see Fig 1.3). In contrast, no conserved domain could be found in the tail domain of class VIII myosins. The most characteristic feature of myosin VIII sequences is their unique C-terminus that contains

several predicted phosphorylation sites for protein kinases A and C (Baluska et al., 2001).

### **1.5.6 Subcellular localization and function of plant myosins**

Subcellular localization studies of plant myosins based on immunocytology could be divided into two different categories. First, use of heterologous antibodies and second, more recently, use of plant myosin specific antibodies. As a heterologous antibody the polyclonal myosin (skeletal and smooth) antibody (Sigma M7648) was extensively used. Such studies have identified proteins of various sizes from different plants in a variety of tissues such as isolated root cells (Parke et al., 1986; Qiao et al., 1989; Qiao et al., 1994; Baluska et al., 2000), chara internodal cells (Grolig et al., 1988; Grolig et al., 1996); Qiao et al., 1989; Qiao et al., 1994), chara rhizoid cells (Braun, 1996), and for pollen tubes (Heslop-Harrison and Heslop-Harrison; Tang et al., 1989; Miller et al., 1995; Tirlapur et al., 1995; Tang et al., 2003), tendrils of *Luffa cylindrical* (Zhao et al., 2002), cultured cells of tobacco (Yokota, 2000), and root of maize (Baluska et al., 2000). It has been shown that labeling mostly resulted in a punctate pattern in the cytoplasm that presumably was associated with endoplasmic reticulum, nuclei, plasma membrane and several types of small organelles.

These results obtained by applications of heterologous antibodies which suggested that class XI myosins may be involved in vesicle trafficking, were later supported by biochemical and immunocytochemical experiments using specific antibodies for class XI myosins. These experiments showed that class XI myosins both colocalize and cofractionate with cytoplasmic

organelles. First Wang and Pesacreta (2004) showed that a subclass of myosin XI is associated with mitochondria, plastids, and the molecular chaperone subunit TCP-1 in maize. And more recently, Hashimoto et al. (2005), using an antibody against an isoform of *A. thaliana* class XI myosin, showed specific localization of this isoform on peroxisomes. Although ATM1 belonging to class VIII myosins was the first myosin that have been characterized using PCR based approaches in *A. thaliana*, little is known about its subcellular localization and function. Immunofluorescence studies showed that ATM1 is concentrated mostly at newly formed cross walls at the stage in which the phragmoplast cytoskeleton has depolymerized and the new cell plate is beginning to mature (Reichelt et al., 1999). Due to the fact that these walls are rich in plasmodesmata the authors suggest that ATM1 is involved in maturation of the cell plate and the re-establishment of cytoplasmic actin cables at sites of intercellular communication (Reichelt et al., 1999).

### **1.5.7 Potential function of plant myosins**

Considering the fact that myosin motors use actin filaments as their track and actin-based movement in plant cells plays a critical role in a broad variety of cellular processes, the potential functions of myosins in plant cells should relate to actin functions. The demonstrated or proposed roles of actin in different plant processes that could be also related to the function of myosins include (reviewed by Volkmann and Baluska, 1999):

I) Intracellular movements

- Short-range transport: directed and salutatory
- Movements of vesicles and organelles long-range mass transport:  
Cytoplasmic streaming

II) Plastid division

III) Cytomorphogenesis and growth processes

- Mitosis, Cytokinesis, Cell elongation, Tip growth

IV) Cell to cell interactions

- Plasmodesmata as actomyosin supported channels

V) Sensing and signaling related to environmental factors

- Chloroplast positioning by light
- Multisensory guard cells: Stomatal movements
- Mechanosensing: Gravi-orientation and responses to touch
- Plant host-pathogen interactions
- Wound-healing

## 1.6 Objectives of this study

As described (see 1.5.6), using several heterologous antibodies and recently a few homologous antibodies for plant specific myosins, immunocytochemical studies have attempted the identification of the nature of translocated vesicles by plant myosins. However the exact relationship between myosins and specific organelles including cargo binding sites or interacting partners and the difference between subclasses of class VIII and XI was not investigated, leaving the function of myosin VIII and XI in obscure. The most poorly understood aspects of plant myosin-dependent trafficking is the identity of the membranous cargo each motor carries and the nature of the motor–cargo interactions. It is believed that motor–cargo interactions may require three players: the motor proteins, a cargo-bound receptor and accessory components. Thus some of the unresolved key questions are as follows:

- Which are myosin tasks in plant cells?
- Are there distinct functions for class VIII and XI?
- Do members belonging to the same class have differential functions or are they redundant?
- What are their cargoes (binding sites, binding proteins)?

Based on the published immunocytochemical data for class XI myosins and the hypothesis that their involvement in transport of vesicles is similar to class V myosins, one of the most attractive questions was which type of vesicles they carry and in which pathway they might be involved. While, as described in the last chapter, in the past several different plants have been used in studies of plant myosins, recently many labs have focused on the

model plant *A. thaliana*. In this dissertation, because of the amount of sequence information *A. thaliana* was an excellent subject for characterizing myosin based movement.

The primary goal of this project was to identify the cargo binding sites of *A. thaliana* class VIII and XI myosins using a combination of high resolution *in vivo* microscopy (confocal laser scanning microscopy), molecular biology and *in vivo* biochemistry. In order to achieve the primary objective, the following topics had to be studied:

1. Bioinformatic sequence analysis of class VIII and XI family members.
2. Phenotypical analysis of *A. thaliana* knock-out lines for class VIII and XI myosins.

On the basis of results obtained from the above analysis, a specific candidate for class VIII (ATM2) and XI (MYA1) had to be selected for further in detail characterization to address the following questions:

1. Which cargoes do class VIII and class XI are transporting?
2. Where are the cargo binding sites of class VIII and class XI located?
3. What are the direct/indirect interacting proteins for both classes?

Subsequently, due the high homology between the different subclasses of class VIII and XI and based on the obtained results for ATM2 and Mya1 other *A. thaliana* class VIII and XI isoforms (one from each subclass as a representative for each subclass) have been tested to confirm or compare the

obtained results from ATM2 and Mya1. Later, the identified cargo from *A. thaliana* has been tested with a barley myosin as a representative for monocots.

Finally, combining the results obtained from the *in vivo* binding assay and the functional analysis of myosin knock-out lines and a yeast-two-hybrid screening for identification of potential interacting proteins should help to get some clues about the questions concerning plant myosin function.

During this study *in vivo* binding biochemistry together with confocal laser scanning microscopy should be used to answer the above listed questions and to attempt to provide a road map for future research that will help to better understand myosin-based intracellular movement in plant cells.

## 2 Materials and Methods

### 2.1. Materials

#### 2.1.1 Plant Material

*Arabidopsis thaliana*: *A. thaliana Col-0* genetic background has been used in this study for transient expression. All analyzed myosin knock-out lines belong also to *Col-0* genetic background. Plants were grown at 22° C under a 12 h light/ 12 h darkness cycle in pathogen-free chambers.

*Hordeum vulgare*: The 5-6 days old barley leaves used belong to *Hordeum vulgare* Golden Promise (*Mlo*) and Ingrid (*mlo-3* genetic background).

*Nicotiana benthamiana*: Leaves of 4-6 weeks old *N. benthamiana* plants grown at 22° C under a 16 h light/ 8 h have been used for transformation as described.

#### 2.1.2 Bacteria / fungi / oomycetes /yeast

##### *E. coli*

DH5 a: Genotype: *supE44 DlacU169 hsdR17, recA1, endA1, gyrA96, thi-1, relA1, F* (Hanahan, 1983).

DB3.1: Genotype: F<sup>-</sup> *gyrA462 endA1.(sr1-recA) mcrB mrr hsdS20(rB-, mB-) supE44* (Invitrogen, Heidelberg).

XL1-Blue MRF': Genotype: *(mcrA) 183 .(mcrCB-hsdSMR-mrr)173 endA1 supE44 thi-1 recA1 gyrA96 relA1 lac [F' proAB lacI q Z .M15 Tn10 (Tet r )]* (Stratagene, USA).

XLOLR: Genotype :(*mcrA*)183 .(*mcrCB-hsdSMR-mrr*)173 *endA1 thi-1*  
*recA1 gyrA96 relA1 lac* [F' *proAB lacI q Z .M15 Tn10* (Tet r )] Su –  
(nonsuppressing) ? r (lambda resistant)(Stratagene,USA).

### ***Agrobacterium tumefaciens***

GV3101 *pMP90RK* (Koncz et al., 1990).

## **Pathogens**

### **Bacterial pathogens**

*Pseudomonas syringae* pv. *tomato* DC3000 (Whalen et al., 1991).

### **Fungal Pathogens**

*Blumeria graminis* f. sp. *hordei* (*Bgh*) (kindly provided by Ralph Panstruga MPIZ-Koeln).

### **Yeast Strains**

AH109: Genotype: *MATa*, *trp1-901*, *leu2-3, 112*, *ura3-52*, *his3-200*, *gal4D gal80D*, *LYS2::GAL1 UAS-GAL1 TATA-HIS3*, *MEL1 GAL2 UAS-GAL2TATA-ADE2*, *URA3::MEL1 UAS-MEL1TATA-acz* (James et al., 1995).

Y187: Genotype: *MATa*, *ura3- 52*, *his3- 200*, *ade 2- 101*, *trp 1- 901*, *leu 2- 3, 112*, *gal4D met-*, *gal80D URA3::GAL1UAS-GAL1TATA-lacZ*, *MEL1* (Harper et al., 1993).

## **2.1.3 Media and Additives**

### **Media for Bacteria**

LB medium (Sambrook): 5g yeast extract, 10g trypton, 10g NaCl, pH=7.5.

SOC medium (Sambrook): 5g yeast extract, 20g trypton, 20 mM glucose, 0.5g NaCl, 2.5 mM CaCl<sub>2</sub>, pH=7.5.

YEB medium: 10g yeast extract, 10g peptone, 5g NaCl.

Antibiotics were supplemented to the following final concentration if required:

Ampicillin 50 mg/l

Carbenicillin 100 mg/l

Gentamycin 10 mg/l

Rifampicin 100 mg/l

Kanamycin 50 mg/l

Spectinomycin: 100mg/ml

### **Media for plants**

MS-medium: 4.7g MS salt, 500 µl vitamins, 5-10 g glucose, 15 g Agar pH 5.7-5.8. Media were diluted in deionized 1L H<sub>2</sub>O.

### **Media for Lambda ZAP express**

LB Broth with Supplements: following filter-sterilized supplements prior to use were added to LB Broth: 10 ml of 1 M MgSO<sub>4</sub>, 3 ml of a 2 M maltose solution

SM Buffer: 5.8 g of NaCl, 2.0 g of MgSO<sub>4</sub> · 7H<sub>2</sub> O, 50.0 ml of 1 M Tris-HCl (pH 7.5), 5.0 ml of 2% (w/v) gelatin

NZY Broth: 5 g of NaCl, 2 g of MgSO<sub>4</sub> · 7H<sub>2</sub> O, 5 g of yeast extract, 10 g of NZ amine (casein hydrolysate), pH 7.5 with NaOH (15 g of agar for solid media if required).

NZY Top Agar: 0.7% (w/v) Agarose added to NZY broth.

### **Media for Yeast**

YPD medium: 20 g/L Difco peptone, 10 g/L Yeast extract, 20 g/L Agar (for plates only), pH to 6.5, sterile carbon source, dextrose (glucose) added to end concentration 2%,

SD medium: 0,67 SD minimal agar base without –Leu/–Trp/–Histidin DO supplement (Clontech, Germany); 6.7 g Yeast nitrogen base without amino acids; 20 g Agar (for plates only), pH to 5.8, sterile carbon source, dextrose (glucose) added to 2%.

1 M 3-AT (3-amino-1, 2, 4-triazole; Sigma #A-8056); prepared in deionized H<sub>2</sub>O and filter sterilized.

1M Sorbitol (Sigma S-3889): 100,21 mg Sorbitol prepared in deionized H<sub>2</sub>O and filter sterilized.

PEG and LiAc solution (polyethylene glycol and lithium acetate): were prepared fresh just prior to use.

YPD with 10% PEG 6000: 50 g PEG 6000 was diluted in 500 ml YPD.

50% PEG 3350 (Polyethylene glycol, avg. mol. wt. = 3,350; Sigma #P-3640) prepared with sterile deionized H<sub>2</sub>O

10X TE buffer: 0.1 M Tris-HCl, 10 mM EDTA, pH 7.5. Autoclave.

10X LiAc: 1 M lithium acetate (Sigma #L-6883), pH 7.5 with dilute acetic acid and autoclaved.

### 2.1.4 Nucleic Acids

#### Plasmids

Plasmids used for the generation of constructs described in this thesis are listed below:

*pDONR<sup>TM</sup> 201* (Invitrogen, Heidelberg) kan R

*pDONR<sup>TM</sup> 221* (Invitrogen, Heidelberg) kan R

*pAM-PAT 35S YFP-GW-Terminator* amp R\*

*pAM-PAT 35S CFP-GW-Terminator* amp R\*

*pAM-PAT 35S cCFP-GW-Terminator* amp R\*

*pAM-PAT 35S GW-YFP-Terminator* amp R\*

*pAM-PAT 35S GW-CFP-Terminator* amp R\*

*pAM-PAT 35S GW-cCFP-Terminator* amp R\*

*pAM-PAT 2x35S GW-mRFP-Terminator* amp R\*\*

*pAM-PAT 2x35S mRFP-GW-Terminator* amp R\*\*

The constructs indicated with \* are kindly provided by Dr. Riyaz Baht from the group of Dr. Ralph Panstruga, MPIZ, Cologne and constructs indicated with \*\* kindly provided by Dr. Imre Sommsich group , MPIZ, Cologne.

#### Oligonucleotides

Listed below are primers used in the present study and were synthesized by Invitrogen with the exception mentioned specifically. The universal Gateway – compatible extensions for the BP recombination reactions

(between an attB-flanked PCR product and a donor vector containing attP sites to create an entry clone) were:

GWF (*attB1*) 5' *ggggacaagtttgtaaaaaagcaggctta*3'

GWR (*attB2*) 5' *ggggaccactttgtacaagaaagctgggtc*3'

Primer sequences are in 5' to 3' direction.

### Mya1 (At1g17580)

Mya1-F	(GWF)TCATGGCTGCTCCAGTCATAAATTGT
Mya1Tail-F	(GWF)TCATGCTGAAAATGGCTGCAAGAGA
Mya1KPF	(GWF)TCAAGCCTGTTGCTGCCTGTCTG
Mya1veak-F	(GWF)TCGTTGAAGCTAAATATCCTGCTTTG
Mya1veak-R	(GWR)CTCACTGAATGCAAGAAGCAAGCAGAG
Mya1DIL-F	(GWF)TCGTGTTCCGGCAGATATTTTCATT
Mya1INVQ-F	(GWF)TCATCAATGTTTCAGCTGTTAACAGC
Mya1LCP-F	(GWF)TCCTTTGTCCGGTGCTTAGCATT
Mya1LCP-R	(GWR)CTCATATCACCTCTGTAGATACGCTATG
Mya1DIL*-F	(GWF)TCGTGTTCCAGCAGATATTTTCATTTA
Mya11/2DIL-R	(GWR)CTCAAACAAACTCCTCCGTTGCATCATG
Mya11/2DIL-F	(GWF)TCAAGCACATTAGACAAGCTGTTG
Mya1-354-F	(GWF)TCAATGAAAACTGCAACAGCAT
Mya1-354-R	(GWR)CTCAATCTTTGTTCTTGTCGATGAA
Mya1-356-F	(GWF)TCGAAGCATTGGAATGCAAAAAC
Mya1-356-R	(GWR)CTCAAACACGGGACCTCTCCAGCAGA
Mya1-R	(GWR)CTCAATCTGACCTTTCCAACAAGAAC

### Class XI VEA, DIL and LCP domains

At4g33200Veak-F	(GWF)TCATAGAAGCAAGATATCCAGCA
At4g33200Veak-R	(GWR)CTCAACCATAAATCTTCTCCACAC
At5g43900Veak-F	(GWF)TCGTGGAGGCAAAGTACCCGGC
At5g43900Veak-R	(GWR)CTCACCCAAACATTTTCTCAACATA
At1g4600Veak-F	(GWF)TCGTAGATGCTAGATATCCTGC
At1g4600Veak-R	(GWR)CTCATCCATACATTGTTTCAACAT
At1g4600DIL-F	(GWF)TCGATGTTTCAGCCAAACTTTCCA
At1g4600DIL-R	(GWR)CTCATCCATCGTCTTTGTCTTGCAG

At1g4160DIL-F (GWF) TCATGTGCATTCAGGCACCGAGA  
 At1g4160DIL-R (GWR) CCTAGTGCAAGAATACGAATTCTG  
 At4g33200DIL-F (GWF) TCAACTTGTGACTCAGGTTTTCTC  
 At4g33200DIL-R (GWR) CTCAATCCATATTTATCATCCCAGTACA  
 At5g20490DIL-F (GWF) TCAAGTATTCACACAAATATTCTC  
 At5g20490DIL-R (GWR) CTCAGCCATATTTGTCATCCCAGTAC  
 At5g20490LCP-R (GWR) CTCAAAATAACATCTGAAGAAACACTA  
 At5g43900LCP-F (GWF) TCTTTGCCCGGTCCTCAGTGT  
 At5g43900LCP-R (GWR) CTCACATATCACTTCTTGTGAGACGCTT  
 At5g43900DIL-F (GWF) TCCTTAGTGCAAGAATACAAATGCTG  
 At5g43900DIL-R (GWR) CTCATATACTCTCAAACCTTCTCATA

## Class VIII myosins

ATM2 (At5g54280)  
 ATM2Full-F (GWF) TCATGTTGTCCACTGCAAATGTTG  
 ATM2Full-R (GWR) CCTAGCCTCTTTTTCCCCACCA  
 ATM2Tail-F (GWF) TCATGCAAAGACAAAAAGAACTACG  
 ATM2Tail-RS (GWR) CTCACCTCTTTTTCCCCACCATTTTC  
 ATM2Tail-R (GWR) CCCTCTTTTTCCCCACCATTTTC  
 ATM2-816-F (GWF) TCATGTCTGATCTCCAGAAACGGAT  
 ATM2-816-R (GWR) CTCATCTATGGAGTCTTGCTTTAGTA  
 ATM2-815-R (GWR) CAGACATAGATGTTGGTTGAACT  
 A350\_ATM2 AGCTGGGAAAACCTGAGACTG  
 A351\_ATM2 ATACCTACCTGAGCCAGAGT  
 A352-ATM2 AGGGATGGAATAGCAAAATT  
 A353-ATM2 AACTGATTTGACCTTTGCCA  
 A354\_ATM2 GTCCTCACTTCATTCGATGCA  
 A355-ATM2 ATTTCCGTGGTCACTTGTCT

ATM1 (At1g19960)  
 ATM1tail-F (GWF) TCATGAAATCAATGGAAGAAATCTG  
 ATM1tails-R (GWR) CTCAATACCTGGTGCTATTTCTC  
 ATM1tail-R (GWR) CATACCTGGTGCTATTTCTCCTT

## Barley myosin

VIIIItail-F (GWF) TGCCTGCAGGAAGAAAAGGAATCT  
 VIIIItial-R (GWR) TCACTTGGAGCTCTTCTTCCCCCA  
 X3DIL-F (GWF) TTACTAACCCTAAATGTTTTCTATG  
 X3DIL-R (GWR) CTCAGCCGTTTCATGTTCGTCCCAGTA

X6DIL-F (GWF) TCAAGATATTTACCCAGATTTTCTC  
 X6DIL-R (GWR) CTCAATATTTGTCATCCCAGTACTGCGT  
 HM11-F (GWF) TCAGGGAACCTCAGGAACTTAAAATGG  
 HM11-R (GWR) CTTATTCAGGGGGCGGCAACAAGA

## Yeast myosin V (Myo2p) primers

Myo2pVeak-F (GWF) TCAAGGAGTATGTTTCATTGGTC  
 Myo2pVeak-R (GWR) CTCAGTTATATATAT TATAACTTAG  
 Myo2pDIL-F (GWF) TCGTCACAACCTTATTGAATTATGT  
 Myo2pDIL-R (GWR) CTTACTCATAGTCTGCCACCTGGT  
 Myo2pLCP-F (GWF) TCGAGGAATTTGTTATTTCGC  
 Myo2pLCP-R (GWR) CTTAGATTTCTGTGGAATTGGAGA

## Arabidopsis genes identified by yeast-two-hybrid

PAS2-F (At5g10480) (GWF) TCATGGCGGGCTTTCTCTCCGTT  
 PAS2-R (At5g10480) (GWR) CTTCCCTCTTGGATTTGGAGAGA  
 Integ-F (At4g15620) (GWF) TCATGGAACACGAGGGCAAGAAC  
 Integ-R (At4g15620) (GWR) CAGGAAGCTTAATAGCGTCAAGA

*Arabidopsis thaliana* myosin Knock-out lines

219-F (At3g19960) GGTGGAGAACATTGCTGATAGA  
 219-R (At3g19960) CCTCCTTCGTAACCTCAGCAAACCT  
 604-F (At5g54280) GAACAAGAGGAATATGAAGAAG  
 604-R (At5g54280) GAACAAGAGGAATATGAAGAAG  
 N522-F (At5g54280) CGACCATTGCAGTAGTTTCTTT  
 N522-R (At5g54280) ACAAGAACTGAGAATAGAAG  
 N51-R (At1g17580) GGTATCCAATTCGCCACATT  
 N51-F (At1g17580) TTAGAAATTAGCAAGGAAGGCAC  
 403-F (At1g04160) GTTATGTAAGAAATCGGACAAAA  
 403-R (At1g04160) ACTCAGATTCAATCAAAAACGACA  
 135E-F (At1g04160) CGTTTTTGCCTAGACTCCATACTT  
 135E-R (At1g04160) CACCCCTCCCCACTCAGA  
 622E-F (At1g04600) GCTGCTTCAGCCAAAGTAACGGT  
 622E-R (At1g04600) ACAACCTAAGAAACAAATGCATCA  
 754-F (At1g08730) TTATCCAATACCTCGACACTCCTA  
 754-R (At1g08730) ATGAATGAGAATATCTGCGTAAACA  
 115C-F (At5g43900) GAAACCATCACAAAACTCTTGA

115C-R	(At5g43900)	ATATCTTGATTGTCTACGAACTCT
N584-F	(At4g33200)	GTACCCTCGTTCTTCATTTCG
N584-R	(At4g33200)	GGAGGTTCTATTTCTGATGGG
N594-R	(At2g33240)	GCAGCCATTGCACGCAACC
N594-F	(At2g33240)	GGGTCATGGAAGCCATTAGG
N589-F	(At1g54560)	ACAAAGGCTGCTACAACCTATTC
N589-R	(At1g54560)	CTTTTTCTTTCTGTCCCTCGCT
232-F	(At2g20290)	ATGGTCTTTAAGGTTTTCTCATTTG
232-R	(At2g20290)	CAACTGCAAACGGATGGGGAC
Actin-F	(At5g09810)	TGGCACCCGAGGAGCACC
Actin-R	(At5g09810)	GTAACCTCTCTCGGTGAG
TDNA-SALK		GCGTGGACCGCTTGCTGCAACT
TDNA-GABI		CCCATTTGGACGTGAATGTAGACAC

others

RFP-F		ATGGGATGGCCTCCTCCG
RFP-R		TCTACGTAGGCGCCGGTG
YFP-F	(GWF)	TCATGGTGAGCAAGGGCGAGGAG
YFP-R	(GWR)	CCTTGACAGCTCGTCCATGC
Ara6-F	(GWF)	TCATGGGATGTGCTTCTTCTCTTCC
Ara6-R	(GWR)	CTGACGAAGGAGCAGGACGAGGT
GOL-F	(GWF)	TCATGATTCATACCAACTTGAAGAA
GOL-R	(GWR)	CGGCCACTTTCTCCTGGCTCT

### 2.1.5 Enzymes, Buffers and Solutions

If not indicated otherwise, enzymes used for experiments in this thesis were obtained from Roche and New England Biolabs. 10 x buffers for enzymes (nucleic acid modifying enzymes) were accompanied with the enzymes supplied by manufacturers.

#### Enzymes

*Accu prime* Taq DNA polymerase(Invitrogen)

*Taq* DNA Polymerase (Biolab)

*Pfx* DNA-Polymerase (Invitrogen)

BD Advantage 2 PCR enzyme (BD Bioscience)

RNase A (DNase-free) (Qiagen)

RNase DNase free set (Qiagen)

SuperScript TM II RNase H - (Invitrogen)

Shrimp Alkaline Phosphatase (Amersham Pharmacia Biotech)

Exonuclease I (Invitrogen, Carl bath, APPROX)

### **Solutions**

Aniline Blue solution: 150mM KH<sub>2</sub>PO<sub>4</sub> (pH 9,5) containing 0.01% Aniline Blue

Coomassie staining solution: Coomassie Blue 0.6 % in methanol

C-TAB solution: 100mM Tris-HCL pH8, 1,4 M NaCl, 20m MEDTA, 2% CTAB ,0.2% mercaptoethanol

Leaves clearing solution: (1 x Lactic acid, 2x Glycerol and 1x H<sub>2</sub>O). Stock solution was diluted 1: 2 with 70 % ethanol

Propidium Iodide solution: 2.5 % manitol, 0.01 % silwet, 0.5% propidium iodide

### **Buffers**

Denaturation Buffer: 0.5 M NaOH , 1 M NaCl

DNA extraction buffer: 0.1 M NaCl 0.01 M Tris-HCl, pH 7.5 1 mM EDTA 1% SDS.

Lysis buffer for Yeast DNA extraction: 10 mM Tris, pH 8.0 1 mM EDTA 100 mM NaCl 1% SDS 2% Triton X-100

Hybridization buffer: 150ml 20x SSPE, 0.1 % SDS, 0.2 g PVP, 0.2 g Ficoll 400

Neutralization Buffer: 3 M NaCl, 0.5 M Tris pH 7.5

Pre-Hybridization Buffer: 300ml 20xSSPE, 0.1 %SDS, 0.2 g PVP 360, 0.2 g Ficoll 400

5x RNA Loading Buffer: 16 µl saturated aqueous bromophenol blue solution

80 µl 500 mM EDTA, pH 8.0 720 µl 37% (12.3 M)

10x RNA Gel running buffer: 200 mM 3-[N-morpholino]propanesulfonic acid

(MOPS) (free acid) ,50 mM sodium acetate, 10 mM EDTA pH to 7.0 with NaOH

Solution I (Resuspension buffer): 50 mM Tris pH 7.5; 10mM EDTA; 100µg/ml (DNAase free) RNAaseA

Solution II (Lysis buffer): 0.2 M NaOH, 1% SDS

Solution III (Neutralization buffer): 1.32 M Potassium Acetate, pH 4.8

20x SSC: 2 M NaCl 0.3 M Sodium citrate Adjust pH to 7.0 ith HCl

20x SSPE: 174 gNaCl, 27,6g NaH<sub>2</sub>PO<sub>4</sub>, 7,4 g EDTA , 13ml 5M NaOH, pH 7,4

20x TAE: 800 mM Tris 20 mM EDTA 2.3% (v/v) Glacial cetic acid

TE Buffer: 10mM Tris, 0.1mM EDTA

Washing Buffer: 2x SSPE, 0.1% SDS

### 2.1.6 Chemicals and radiochemicals

Chemicals and radiochemicals used for experiments in this thesis were obtained from Amersham Buchler GmbH & Co KG, J.T. Baker Chemicals, BioRad, Difco Laboratories, Fluka, Merck AG, Serva Feinbiochemica GmbH & Co, Sigma Aldrich GmbH, other specifications are indicated.

Acetosyringon (Roth, Germany)

Adenine (Sigma-Aldrich, Munich, Germany)

Autoradiofilm XOMAT AR - Kodak

BDM (Sigma -Aldrich, Munich, Germany)

BP-Clonase (Invitrogen, Heidelberg)

Exosap-IT (USB, USA)

First Strand cDNA Synthesis Invitrogen

Gel Extraction Kit (QIAGEN)

Hybond N (Amersham Pharmacia Biotech)

LR-Clonase (Invitrogen, Heidelberg)

Lyticase (Sigma-Aldrich, Munich, Germany)

Miniprep® Kit (QIAGEN)

Miniprep® Kit (Macherey and Nagel)

Parafilm M (American National Can.)

Petridishes (Greiner GmbH)

Pipette tips (Greiner GmbH)

Propanoid iodid (Sigma -Aldrich, Munich, Germany)

Reaction tubes (Eppendorf)

RNAwiz extraction reagent (Ambion)

RNeasy Plant Mini® Kit (QIAGEN)

Silwet L77 (lehle seeds, USA)

Shreng 1ml (B+D)

Sterile filtration units (Millipore)

Whatman 3MM paper (Whatman)

### **2.1.7 Microscopes**

Confocal laser scanning microscopy (CLSM): Analysis of intracellular fluorescence was performed by a TCS SP2 confocal system (Leica Microsystems, Heidelberg ) and a LSM 510 META microscopy system (Zeiss, Germany). An 514 nm argon laser was used to excite YFP, a He/Ne laser at 562 nm for dsRed and /or propidium iodide. The CFP was excited by using a 405 nm diode laser or the argon laser with the 456 nm line. The emitted light was collected in the lambda spectrum mode between 494 and 644 nm. Reference spectra of CFP, YFP, dsRed, and/or propidium iodide were used to linearly unmix the relevant spectra. Light emission was detected in the range of 570–634 nm for RFP constructs and 535–545 nm for YFP constructs. Images were recorded and processed by using LSM 510 3.2 software (Carl Zeiss, Jena, Germany) and LCS Lite version 2.5 (Leica Microsystems, Heidelberg, Germany).

As conventional fluorescence microscope a Zeiss Axiophot 1 equipped with epifluorescence and a DISKUS imaging system was used.

### **2.1.8 Online Software**

BLAST and Bioinformatics NCBI, MIPS, TAIR and TIGER

Cluster analysis NASC "EPCLUST"

MultAlign software Corpet, INRA Toulouse, France, BCM

Mutant search tools GABI PoMaMo Database, SALK, NASC

## **2.2 Methods**

If not indicated otherwise, the methods employed in this study were taken from Sambrook, J. et al., eds. (1989) *Molecular cloning — a laboratory manual*, 2nd ed. Cold Spring Harbor, NY: Cold Spring Harbor Laboratory Press).

### **2.2.1 Nucleic acids-related methods**

#### **DNA isolation**

DNA was isolated by the C-TAB method (modified protocol of (Shahjahan et al., 1995). 200-300 mg plant material was ground in liquid N<sub>2</sub> and transferred into a 1.5 ml microfuge tube. 300 µl hot (pre-heated at 65°C) C-TAB was added as extraction buffer and the tubes were incubated for 15 minutes. 600 µl of Chloroform:Isoamyl-alcohol (24:1) was added and mixed on a shaker for 15 minutes. The samples were centrifuged at 13000 rpm for 5 minutes. The supernatant was transferred to a new tube containing an equal volume (600µl) Isopropanol. The samples were thoroughly mixed and

placed at  $-20^{\circ}\text{C}$  for 15 minutes. The supernatant was discarded and the pellet was washed with 70% cold Ethanol. Finally, the dry pellet was resuspended in 100 $\mu\text{l}$  TE Buffer. The quality and quantity of DNA was measured by comparison of the band- intensity on ethidium bromide stained agarose gels with the 1kb ladder DNA size marker (Invitrogen). After electrophoresis, DNA was visualized on a transilluminator under UV light (254 nm). Subsequently, DNA concentration was measured by an Eppendorf BioPhotometer based on DNA absorbance at 260 nm.

**DNA isolation from Yeast** (modified protocol after Rose et al., 1990)

5 ml of overnight yeast culture of strain AH109 at  $28^{\circ}\text{C}$  (200 rpm shaking) was centrifuged for 3 minutes. Then, 0.3 glass beads (Sigma), 0.2 ml of lysis buffer and 0.02 ml of a 1:1 mix of phenol and chloroform was added to the cell pellet in an Eppendorf tube and vortexed at maximum speed for 2 min, then 0.2 ml of TE buffer were added and vortexed again for a few seconds. The tubes were centrifuged for 5 min (room temperature) at maximum speed in an Eppendorf centrifuge and the upper phase transferred to a fresh eppendorf tube. 2 volumes of 100% ethanol was added at room temperature and mixed thoroughly and centrifuged for 23 min. The supernatant was discard and the pellet was rinsed with 0.5 ml of cold, 70 % ethanol and centrifuged for 3-5 sec. The supernatant was removed and finally the pellet was resuspended in 50  $\mu\text{l}$  TE buffer.

**Quick DNA preparation for PCR amplification of *A.thaliana* myosin knock-out lines** (according to Weigel and Glazerbrook, 2002)

Although this procedure yields a small quantity of poorly purified DNA, however, many samples can be processed in a short time, and the DNA is generally of sufficient quality for PCR amplification. The following steps have been performed:

The cap of an eppendorf tube was closed onto a leaf to clip out a section of tissue and 400 µl of extraction buffer was added to the tube. A micropestle has been used to grind the tissue in the tube. The tube was centrifuged at maximum speed for 5 minutes in a microcentrifuge, and 300 µl of the supernatant has been transferred to a clean tube. 300 µl of isopropanol was added, mixed by shaking and centrifuged at maximum speed for 5 minutes. The supernatant was carefully discarded. The pellet was rinsed with 70% ethanol, drained and dried. Finally, the pellet was dissolved in 40 µl of TE.

**RNA isolation**

Total RNA was isolated from 50-200 mg fresh tissue. The tissue was flash-frozen and ground in liquid nitrogen. Total RNA was extracted using the RNA plant Qiagen Kit following the supplier's protocol.

**PCR amplification**

Routine PCRs were carried out according to a standard protocol amplifying in 25 µl PCR reactions containing 50 ng of template DNA, in the presence of 20 mM Tris-HCl pH 8.4, 2.5 mM of MgCl<sub>2</sub>, 50 mM of KCl, 200 nM of

each primer, 100  $\mu$ M of each dNTP, and 0.4-1 units of Taq DNA polymerase. Standard cycling conditions were as follows: initial denaturation step of 4 min at 94 °C, followed by 30 cycles of 1 min denaturation at 94 °C, 1 min annealing at the appropriate  $T_m$ , and 1 min extension at 72 °C. After cycling, PCR reactions were incubated for 8 min at 72 °C. PCR products were analyzed by electrophoresis on agarose gels in 1 x TAE or TBE buffer and visualized by ethidium bromide staining.

### **Proof reading PCR**

During this thesis *AccuPrime Pfx* (Invitrogen, Heidelberg) DNA polymerase was used for amplification of PCR fragments which have been used in producing entry clones. This DNA polymerase posses 3' to 5' exonuclease activity that provides higher fidelity than *Pfu* DNA polymerase. The PCR amplification has been performed according to the manufacturer's protocol.

### **Purification of gel-extracted**

DNA fragments: PCR products were purified using Macherey and Nagel PCR Fragments Purification Kit or Macherey and Nagel Gel Extraction Kit (Mc NAgel, Hilden, USA) following the manufacturer's protocol.

### **PCR products enzymatic purification**

ExoSAP-IT has been used for enzymatic purification of PCR products before sequencing. ExoSAP-IT is added directly to the PCR product. The enzymes are active in the buffer used for PCR; hence no buffer exchange is required. After treatment, ExoSAP-IT is inactivated by heating to 80 °C for

15 minutes. 10 µl of the PCR was incubated with 1U Shrimp Alkaline Phosphatase (Amersham Pharmacia Biotech, Piscataway, NJ, the USA) and 1U Exonuclease I (Invitrogen, Carl bath, APPROX., the USA) in 37°C for 30 min. Finally the reaction mixture was heated for 15 min at 80°C.

### **DNA sequencing**

DNA sequences were performed by the DNA core facility (ADIS) of the Max-Planck Institute for Plant Breeding Research, Cologne. The ABI PRISM Dye Terminator cycle Sequencing Ready Reaction Kit was used (Applied Biosystems) for sequencing on an Applied Biosystems 377 DNA Sequencer (Applied Biosystems). Sequence analyses were performed using sequence analysis software package GCG (Wisconsin University, Version 9.1, UNIX, September 1997). NCBI and TAIR data-base were searched for the sequences of functional genes available in the databases. For sequence comparison, the Gene Runner was used.

### **RT-PCR**

Reverse transcription-polymerase chain reactions (RT-PCR) were carried out with total RNA templates, isolated and purified as described above. 2mg RNA was used as starting template material for first strand cDNA synthesis using SuperScript TM II RNase H - (Invitrogen) as described in the manual provided with the SuperScript TM II RNase H. For subsequent RT-PCR analyses, 2 µl of the above mixture as template was used and reactions were standardized using actin primers, specific to actin 7 of *Arabidopsis thaliana*.

**Amplifying the cDNA library**

(The library was obtained from epidermis cells of barley leaves 16 h after infection with *Bgh* in Lambda ZAP express and was kindly provided by Dr. H. Thordal Christensen Royal Veterinary and Agricultural University, Copenhagen, Denmark.).

A 50-ml overnight culture of XL1-Blue MRF' cells (as a host) in LB broth with supplements was grown at 30°C with shaking. In second day, the XL1-Blue MRF' cells were gently spun down (1000 x g) and the cells were resuspended in 25 ml of 10mM MgSO<sub>4</sub>. The OD<sub>600</sub> of the cell suspension was measured and then the cells were diluted to an OD<sub>600</sub> of 0.5 in 10 mM MgSO<sub>4</sub>. Aliquots of the library suspension containing  $\sim 5 \times 10^4$  pfu of bacteriophages were combined with 600  $\mu$ l of XL1-Blue MRF' cells at an OD<sub>600</sub> of 0.5 in polypropylene tubes. The tubes containing the phage and host cells were incubated for 15 minutes at 37°C to allow the phages to attach to the cells. 6.5 ml of NZY top agar, molten and cooled to  $\sim 48^\circ\text{C}$ , was mixed with each aliquot of infected bacteria and spread evenly onto a freshly poured 150-mm NZY agar plate. The plates were allowed to set for 10 minutes. The plates were inverted and incubated at 37°C for 6-8 hours. Subsequently, the plates were overlayed with 10 ml of SM buffer and stored overnight at 4°C. The bacteriophage suspension was recovered from each plate and pooled into a sterile polypropylene container and then chloroform to a 5% (v/v) final concentration was added and mixed well and incubated for 15 minutes at room temperature. Subsequently, the cell debris was removed by centrifugation for 10 minutes at 500  $\times$  g. The supernatant was

recovered and transferred to a sterile polypropylene tube. Finally, chloroform was added to a 0.3% (v/v) final concentration and stored at 4°C. The titer of the amplified library using host cells and serial dilutions of the library has been performed according to the supplier protocol (Stratagene).

### **Performing plaque lifts**

The equivalent of  $5 \times 10^4$  pfu/plate and 600  $\mu$ l of freshly prepared XL1-Blue MRF' cells at an OD600 of 0.5 were combined and the mixture of the bacteria and phages was incubated at 37 °C for 15 minutes to allow the phages to attach to the cells. Then, 6.5 ml of NZY top agar (~48°C) was added to the bacteria and phage mixture and quickly poured onto a dry, prewarmed 150-mm NZY agar plate containing kanamycin 30mg/l. Finally, the plaques from NZY plates containing the cDNA library was spotted on Hybond N+ nylon membrane (Hybond N - Amersham Pharmacia Biotech) by the DNA core facility (ADIS) of Max-Planck Institute for Plant Breeding Research, Cologne using a Micro Gid II (Biorobotics).

### **Lambda cDNA library hybridization**

Pre-hybridization and hybridization have been performed with spotted Nylon membrane in pre-hybridization and hybridization solutions in glass tubes (30 cm x 4 cm) at 65°C under continuous rotation in a hybridization oven (Bachofer, Reutlingen, Germany). The pre-hybridization was performed for 4 hours. Upon adding the denatured radio-active probe, the hybridization was performed for 16- 20 hrs. After hybridization the filter was washed accordingly:

1. twice 50 ml 2 x SSC + 0.1 % SDS at RT for 15 minutes
2. twice 50 ml 1 x SSC + 0.1 % SDS at 65°C for 15 minutes
3. once 50 ml 0.1 x SSC + 0.1 % SDS at 65°C for 30 minutes

Finally, the Nylon membrane was wrapped in thin plastic foil and exposed overnight to a phosphoimager screen (Molecular Dynamics) in a cassette at room temperature. Radioactively labeled probe preparation for plasmid labeling was used in this protocol according to Amersham Bioscience protocol.

Probe was later on purified using Qiagen PCR purification Kit according to the manufacturer's manual.

### **Cloning strategies**

Cloning strategies performed in the course of this thesis are described below. Plasmids and primers used for cloning procedures are listed in materials section.

### **Generating entry clones**

CDNA sequences of interest were amplified using the *attB* primers extension sites by *Accu prime* Taq DNA polymerase to generate PCR products that are flanked by *attB* sites. Separate BP recombination reactions with the donor vector (*pDONR201or*, *pDONR.221*) were performed to generate entry clones containing DNA sequences of interest. Reactions were incubated at 25°C for at least 12 h before completely transformed into *E. coli* strain DH5  $\alpha$ . Insert size was verified by PCR amplification. The entry clone plasmid DNA was extracted using Plasmid Isolation Mini Kit (Qiagen, Germany) and verified by sequencing.

**BP reaction**

<i>attB</i> -PCR Product (50 ng/μl)	0.5 μl
GATEWAY ® BP clonase	0.5 μl
BP reaction buffer (5x)	0.5 μl
pDONR™201 vector (50 ng/μl)	0.5 μl
TE Buffer PH 8.0	0.5 μl

The LR reaction was used to transfer the insert from entry clones pDONR 201 or 221 to the described destination vectors according to the manufacturer's instructions (Invitrogen). The products of LR reactions were transformed into an electro-competent strain of *E. coli* (DH5 a) and plated on selective agar-media. The insert sizes were verified by PCR amplification. The expression clone plasmid DNA was extracted using the company's protocol (Qiagen-Germany/Mc-Nagel-USA).

**LR reaction**

Entry clone (50 ng/μl)	0.5 μl
GATEWAY ® LR clonase	0.5 μl
LR reaction buffer (5x)	0.5 μl
Destination vector (50 ng/μl)	0.5 μl
TE Buffer PH 8.0	0.5 μl

### **2.2.2 Methods for the cultivation of bacteria and transformation of plants**

The *Agrobacterium* strain GV3101 was used for all the below described transformations. The strain has a C58C1 chromosomal background marked by a rifampicin resistance mutation, and carries pMP90RK, a helper Ti plasmid encoding virulence functions for T-DNA transfer from *Agrobacterium* to plant cells (Koncz et al., 1990).

#### **Transformation of electro-competent *E. coli* cells**

For each transformation, one aliquot of electro-competent cells of DH5 was thawed on ice and 0,5 µl of BP reaction or 25 ng plasmid DNA was added. DNA and cells on ice were mixed and the mix was transferred to a prechilled electroporation cuvette.

The electroporation was carried out as recommended for *E.coli* by a Bio-Rad electroporator using the following conditions with a 2 mm cuvette:

Capacitance: 25 µF, Voltage: 2.4 kV, Resistance: 200 Ohm, Pulse length: 5 msec

Immediately after electroporation 1 ml of LB/SOC was added to the cuvette and the bacterial suspension was transferred to a 2 ml culture tube and incubated for 2 hours at 37°C with gentle agitation. A fraction (~ 150-200 µl) of the transformation mixture was plated out onto selection media plates. Transformed colonies were isolated.

#### **Small scale plasmid isolation from *E. coli***

Small scale plasmid isolation from *E.coli* was performed by alkaline lysis according to Sambrook and Fritsch, 1998, using Plasmid Isolation Mini Kit

(Qiagen, Germany) or following the described protocol based on Promega Wizard-based DNA plasmid miniprep.

First, 2 ml of the O/N culture was centrifuged at 13000 rpm for 1 minute. The pellet was resuspended in 200  $\mu$ l of solution I. Then 200  $\mu$ l of solution II (Lysis buffer) was added and inverted 3 times and was left for 5 minutes at room temperature. Subsequently, 200  $\mu$ l of solution III (neutralization buffer) was added and inverted 3 times. Then the tube was centrifuged for 5 minutes at 13000 rpm. Subsequently, the supernatant (600 $\mu$ l) was placed in a tube containing 300  $\mu$ l isopropanol, mixed and centrifuged for 10 minutes at 13000 rpm. The supernatant was discarded and 1ml 70% ethanol was added to the pellet, the tube was inverted and centrifuged again for 3 minutes. The Pellet was dried for 3-5 minutes in a speed vacuum heater and finally resuspended in 40  $\mu$ l of sterile water.

#### **Preparation of electro-competent *A. tumefaciens***

A single colony of *A. tumefaciens* was inoculated into 5 ml of YEB medium and grown o/n at 28°C. The o/n culture was used to inoculate 400 ml of YEB medium and grown to A600nm=0.5. Cells were harvested by centrifugation at 5000 rpm and sequentially resuspended in 200 ml, 100 ml and 10 ml of ice-cold 1 mM Hepes (pH=7.5). Finally cells were resuspended in 800  $\mu$ l of 1 mM Hepes (pH=7.5) and 10% v/v glycerol, aliquoted and frozen at -80°C.

#### **Transformation of elctro-competent *A. tumefaciens* cells**

The same procedure was used as described for electro-competent *E.coli* transformation. The only difference was that after electroporation cells were

incubated at 28 ° for at least 2 hours and later were plated out onto selection media plates. Transformed colonies were identified by PCR amplification.

### **Transformation of Arabidopsis plants**

*Agrobacterium* clones carrying respective plasmids were grown in 5 ml of YEB medium with gentamycin (25 mg/l), kanamycin (25 mg/l), carbenicillin (50 mg/l) and rifampicin (50 mg/l) o/n at 28°C. The o/n culture was used to inoculate 400 ml of YEB medium and grown for another 16-20h. 5% sucrose solution was added to the bacterial solution and continued with mixing. Before transformation Silwet L-77 (500 µl/l) were added to the *A. tumefaciens* culture. Arabidopsis WT-*col* plants were grown under greenhouse conditions at a density of 5 plants/pot (9 cm diameter). Transformation was performed 5-10 days after clipping. The plants were dipped for 30-45 s into *A. tumefaciens* culture and covered with a plastic dome for 24 hrs to maintain high humidity. After removal of the plastic domes, plants were transferred to a growth-chamber with high humidity conditions for two days and then to the greenhouse until seeds were harvested.

### **Transient transformation of *N. benthamiana* leaves**

Extracted plasmids were electroporated into *A. tumefaciens* GV3101 and selected on agar plates containing the described required antibiotics. Colonies usually appeared after 3-day incubation at 28 C, and plates were kept at 4° C for up to 2 weeks. Transformation of *N. benthamiana* leaves by *Agrobacterium* directly from plates has been performed. Cultures were resuspended in 10 mM MgCl<sub>2</sub>, 10 mM MES pH5.6 and 150 µM

acetosyringone to an OD of 0.5, incubated for 2–5 h at 28 ° C in dark conditions, and infiltrated with a needleless syringe from the abaxial side into leaves of 3-4 week-old *N.benthamiana* plants.

### **Transient transfection assay in Arabidopsis epidermal cells using particle delivery system**

(The following protocol was applied according to the department of Molecular Plant-Microbe Interactions of the MPIZ).

First, 30mg of 1µm gold microcarrier (Bio-Rad) was weighed and transferred into a 1.5ml Eppendorf tube. After adding 1ml of 70% ethanol, the suspension was vigorously vortexed for 3-5 minutes. Subsequently, 15 minutes break to allow the particles soaking. Micro-particles were centrifuged for 5 seconds to pellet. After the complete removal of supernatant, 1ml sterile H<sub>2</sub>O was added.

Afterward, rigorous vortexing was performed for 1 min and then allowing the particles to sediment for 1min. Subsequently, gold particles were centrifuged very briefly to remove the supernatant.

These steps were repeated three times for proper washing of micro-particles. Finally, micro-particles were suspended in 500µl sterilized 50% glycerol solution. These washed micro-particles were stored at 4°C and used within 2 weeks.

### **Coating Microcarriers with DNA**

Pre-washed micro-carriers in 50% glycerol (60mg/ml) were vortexed for 5 min to resuspend and disrupt agglomerated particles. For one bombardment,

50µl was aliquoted into a new Eppendorf tube and subsequently in the following order 5µl DNA (1µg/µl), 50µl 2.5M CaCl<sub>2</sub> were and 20µl 0.1M spermidine added. Subsequently, the tubes were vortexed vigorously for additional 2-3 min. Finally the microcarriers were left to stand for 1 min for sedimentation.

Micro-carriers were centrifuged for 2 seconds and after discarding the supernatant, 140µl 70% EtOH was added. The next step was done at low speed to vortex the micro-carriers for 2 seconds and spun down for 2 seconds. Supernatant was removed and 140µl 100% EtOH was added. The step was repeated one more time and micro-carriers were resuspended in 48 µl 100% EtOH. DNA coated gold particles were kept on ice until bombardment.

### **Transient transfection assay**

Arabidopsis or barley leaves were cut and placed on agar plates (1%). These leaves could be stored at 4°C up to 2-3 days. Macrocarriers were situated in the appropriate seven places of the macrocarrier holder and fixed tightly with a holder. 7 µl of DNA coated microcarriers was taken after mixing and added on pre-placed microcarriers. When the ethanol was fully evaporated, the macrocarrier holder was positioned inside the BioRad particle delivery system (Biolistic-PDS-1000/He) and fixed tightly. A vacuum of 27 mm Hg was applied.

The bombardment process have been performed under constant 900 psi pressure with exploding the rupture discs. Finally, the bombarded leaves were incubated in a light chamber at 18°C for 24-48 h to allow the protein expression.

### **2.2.3 Methods related to staining and microscopy**

**Callose staining:** The cleared leaves were rinsed for 48 h in Annilin blue staining solution

**Clearing of plant leaves:** Leaves incubated for at least 48 hours in clearing solution, changing the solution after 24 hours if necessary.

**Fungus staining:** The leaves were incubated for ca. 10 sec in Coomassie Blue solution.

**Propidium iodide staining:** The leaf tissue was mounted on a drop immediately before microscopy.

### **2.2.4 Methods related to Yeast transformation and two-hybrid assays**

**LiAc-mediated yeast transformation** (according to Ito et al., 1983; Gietz et al., 1995)

In the LiAc transformation method, yeast competent cells are prepared and suspended in a LiAc solution with the plasmid DNA to be transformed, along with excess carrier DNA. Polyethylene glycol (PEG) with the appropriate amount of LiAc is then added and the mixture of DNA and yeast is incubated at 30°C. After the incubations, the cells are heat shocked, which allows the DNA to enter the cells. The cells are then plated on the appropriate medium to select for transformants containing the introduced plasmid(s). Because, in yeast, this selection is usually nutritional, an appropriate synthetic dropout (SD) medium is used.

Five ml of YPD with several colonies was inoculated for overnight. One ml of ON culture was transferred into a flask containing 50 ml of YPD and

incubated at 30°C for 3-5 hr with shaking at 250 rpm and the OD600 of the diluted culture was checked to bring the OD600 up to 0.2–0.3. The cells were placed in 50-ml tubes and centrifuged at 3,000 x g for 5 min at room temperature. The supernatants were discarded and resuspended in sterile distilled H<sub>2</sub>O and immediately were centrifuged at 3,000 x g for 5 min at room temperature. The supernatant was discarded and the cell pellet was resuspended in 1 ml of freshly prepared, sterile 100mM LiAc. For transformation, 0.5 µg of plasmid DNA and 2mg/ml of herring testes carrier DNA were added to a fresh 1.5-ml tube and mixed. Later, 0.1 ml of yeast competent cells were added to each tube and mixed well by vortexing. Additionally, 0.24 ml of sterile PEG/LiAc solution to each tube were added and vortexed at high speed for 10 sec to mix. The tube was incubated at 30°C for 30 min with shaking at 200 rpm and mixed well by gentle inversion.

The mixture was heat shocked for 25 min in a 42°C water bath and was chilled on ice for 1–2 min and was centrifuged for 10 sec at 14,000 rpm at room temperature. The supernatant was removed and the cells were resuspended in 1 ml of sterile 1M Sorbitol. Finally, 200 µl from each transformant was plated on SD agar plates and incubated up-side-down, at 30°C until colonies appeared.

### **Yeast two-hybrid**

Yeast two-hybrid screens were performed as described by Soellick and Uhrig, 2001. The cDNAs encoding for different myosin domains were recombined into the bait vector pCD2attR (J.F. Uhrig, unpublished). The Gal4BD-fused myosins proteins were used as bait proteins to screen an

*Arabidopsis* cDNA-library (Clontech). The screening procedure was performed by liquid mating of the bait proteins with pre-transformed frozen prey-library yeast cells. The following protocol was optimized by the group of Dr. Uhrig (MPIZ, Cologne, Germany). For this purpose each bait was used to inoculate 25 ml SD-Trp containing 4% Glucose and was incubated at 30 °C O/N with shaking at 200 rpm. The next day, the library was thawed very fast in water bath at 42 °C and subsequently was incubated for 1 h in YPD medium with shaking at 200rpm in 30 °C. Later, the OD600 of the library and the baits were measured. The equivalent amount of the bait and the library was mixed (each 10 OD) and was centrifuged for 5 min at 4000 rpm. Then, the supernatant was discarded and the sediment was resuspended in 20 ml YPD with 10% 6000 PEG and incubated O/N at 30 °C with shaking at 80 rpm. The next day the solution was centrifuged at 4000 rpm at 20 °C and the sediment was resuspended in 500 ml SD-LWH3 (SD lacking leucine, tryptophan, and histidine) with 0.05% Gelrite. Subsequently, 20 µl from the resuspended solution was mixed with 20ml SD-LW with 0.05% Gelrite for producing the titer plates. The rest was distributed into 20 SD-HLW3 plates containing 0.05% Gelrite and 50mM MES. All plates were incubated for 1 week at 30 °C. After three days the titer plates were counted. The emerged positive candidates after 1 week were transferred into 96 micro titer plates (MTP) and the MTP plates were covered and incubated O/N at 30°C. Later, the clones grown on SD-HLW3 plates were transferred to new plates using stamp and incubated O/N at 30 °C. After 6 days candidates were analyzed by PCR and the insert was sequenced.

### **2.2.5 Methods related to fluorescence labeling of organelles**

#### **Actin filaments**

During the present study actin filaments were visualized using a construct which was kindly provided by the group of Dr. F. Baluska, Bonn University, Germany. The construct is consisting of RFP fused to the C-terminal half of *A. thaliana* fimbrin 1 (Voigt et al., 2005).

#### **Endosomal compartments**

In the course of this thesis, for the visualization of the endosomes related compartments, the RFP fusion protein of the FYVE domain, which recently has been shown that it is labeling plant endosomes, has been used (Voigt et al., 2005). The construct was kindly provided by the group of Dr. F. Baluska, Bonn, Germany.

#### **Mitochondria**

The construct pGJ1425 which is obtained from the group of Prof. D. Leister, Munich, Germany, has been used for visualization of mitochondria in transient expression systems. The construct is a fusion between the N-terminus of At5g52520 (Prolyl-tRNA synthetase) and the RFP and has been shown recently to localize on mitochondria (Pesaresi et al., 2006).

#### **Peroxisomes**

For visualization of peroxisomes the construct RFP-TS has been used. The construct was obtained from the group of Dr. Komberink, MPIZ, Cologne. In this construct RFP is extended by the canonical major PTS1 tripeptide -SRL (RFP-SRL). The construct has been shown currently that it

successfully targeted to the peroxisomes in plant cells (Schneider et al., 2005).

### **Construction of fluorescence markers labeling Golgi and endosome compartments**

The Entry clone pDNOR201-ST and pDNOR201-Ara6 lacking the stop codon were obtained by PCR using ST-GFP (Boevink et al., 1998) and Ara6cDNA (Ueda et al., 2001) respectively. ST-GFP was kindly provided by the group of Prof. Hawes, Oxford, UK and the full length Ara6-cDNA was obtained from Nottingham Arabidopsis Stock Centre (NASC), Nottingham, UK. For PDNOR201-ST the two oligonucleotides 5' (GWF)TCATGATTCATACCAACTTGAA-3' and 5' (GWR)CGGCCACTTTCTCCTGGCTCT-3' and for pDNOR201-Ara6 the following two oligonucleotides 5' (GWF)TCATGGGATGTGCTTCTTCTCTTCC-3' and 5'-(GWR)CTGACGAAGGAGCAGGACGAGGT -3' have been used.

The amplified fragments were cloned into the *pDONR201* (Invitrogen) using the Gateway cloning technique. The PCR products were verified by sequencing at ADIS Service Unit in the MPIZ, Cologne with ABI Prism BigDye Terminator Cycle Sequencing kits according to the manufacturer's instructions. The verified pDNOR201-STentry clone was subcloned into the destination vectors 35S-GW-CFP/mRFP and the pDNOR201-Ara6 into destination vectors 35-GW-YFP/RFP using the Gateway cloning technique (Invitrogen, Heidelberg).

## 3 Results

### 3.1 Characterization of putative vesicle binding sites in myosin XI tail domains

#### 3.1.1 Identification of putative vesicle binding sites in myosin XI tail domains

As pointed out in the introduction, it has been shown recently that the globular tail of the yeast myosin Myo2p contains a vacuole and a secretory vesicle binding site (Catlett et al., 2000). The latter is part of the DIL domain which is conserved among all class V myosins from animals and yeast. By multiple alignments of the amino acid sequences of the tail domains of plant class XI myosins and animal and yeast class V myosins, I could identify in 11 of the 13 class XI myosins from *Arabidopsis thaliana* a region in the C-terminal part of the tail domain that is homologous to the DIL domain from animal and yeast class V myosins. The genes AT3g58160 and AT4g28710 do not possess this DIL domain homolog. Within this plant DIL domain homolog a segment could be identified (LCP domain) which is highly homologous to the secretory vesicle binding site described in the *Saccharomyces cerevisiae* class V myosin Myo2p (Fig 3.1.1 A, C). The DIL domains of class XI myosins from *A. thaliana* are highly conserved. Based on the protein sequence comparison to the Mya1 DIL domain, this homology varies between 88 % (for AT5g20490) and 55 % (for AT2g33240, Table 3.1.1).

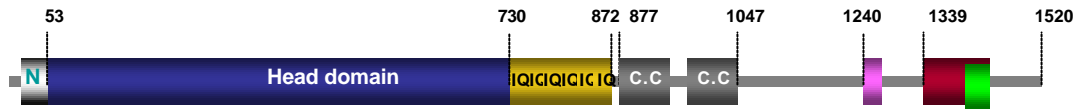
Further analysis revealed that the full length protein sequence, the complete tail domain and the DIL domain of Mya1 are showing 51 %, 40 % and 48 % homology to the full length sequence, the complete tail and the DIL domain of Myo2p, respectively.

<b>Gene code</b>	<b>DIL</b>	<b>VEAK</b>
At5g20490	88	100
At1g54560	86	91
At1g08730	83	91
At4g33200	73	82
At2g31900	70	78
At5g43900	70	78
At1g04160	69	82
At2g20290	58	69
At1g04600	58	73
At2g33240	55	78
Myo2p	22	21

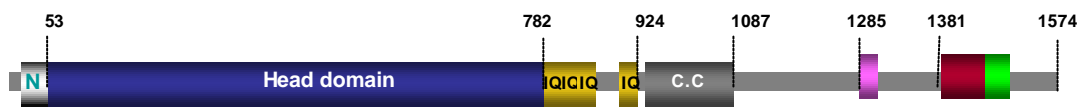
**Table 3.1.1:** Comparison of the amino acid sequences of the DIL and VEA domains from *A. thaliana* class XI myosins and the yeast class V myosin Myo2p with the DIL and VEA domains of AtMya1. The percentages of identical amino acids are shown.

In contrast to this secretory vesicle binding site I could not find a domain in class XI myosin tail regions that is highly homologous to the yeast Myo2p vacuole binding site (Catlett et al., 2000). However, in 11 of the 13 class *A. thaliana* XI myosins a highly conserved segment (VEAK domain) could be identified in a region corresponding to the position of the vacuole binding site in the yeast Myo2p. In this region the yeast Myo2p sequence displays at 5 distinct positions identical or homologous amino acids. The sequence and the alignment of these segments are shown in the (Fig 3.1.1 B). It is important to state, that the two *A. thaliana* class XI myosins At4g28710 and At3g58160 do neither have a VEA or DIL a domain.

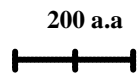
## A) AtMya1 tail domain



AtMya1



Myo2-Yeast



## B)

MYo2p	1285	K	E	Y	V	S	L	V	T	E	L	K	D	D	F	E	A	L	S	Y	N	I	Y	N	1307
At4g33200	1233	I	E	A	R	Y	P	A	L	L	F	K	Q	Q	L	T	A	C	V	E	K	I	Y	G	1259
At1g54560	1250	V	E	A	K	Y	P	A	L	L	F	K	Q	Q	L	T	A	Y	V	E	K	I	Y	G	1272
At1g08730	1259	V	E	A	K	Y	P	A	L	L	F	K	Q	Q	L	T	A	Y	V	E	K	I	Y	G	1281
At5g20490	1264	V	E	A	K	Y	P	A	L	L	F	K	Q	Q	L	T	A	F	L	E	K	I	Y	G	1286
At1g17580	1240	V	E	A	K	Y	P	A	L	L	F	K	Q	Q	L	T	A	F	L	E	K	I	Y	G	1262
At2g33240	1427	V	D	A	R	Y	P	A	L	L	F	K	Q	Q	L	T	A	Y	I	E	T	I	Y	G	1449
At1g04600	1407	V	D	A	R	Y	P	A	L	L	F	K	Q	Q	L	T	A	Y	V	E	T	M	Y	G	1429
At1g04160	1231	V	E	A	K	Y	P	A	L	L	F	K	Q	Q	L	A	A	Y	V	E	K	I	F	G	1253
At5g43900	1236	V	E	A	K	Y	P	A	L	L	F	K	Q	Q	L	A	A	Y	V	E	K	M	F	G	1258
At2g20290	1233	V	D	A	K	D	P	A	L	H	F	K	Q	Q	L	E	A	Y	V	E	K	I	L	G	1255
At2g31900	1272	V	E	A	K	Y	P	A	L	L	F	K	Q	H	L	A	A	Y	V	E	K	T	Y	G	1294

C)

```

Myo2p      AVVTLLNLYVDAIC FNELIMKRNFLSWKRGLQINYNVTRLEEWC . . . KTHGLTDG
At2g20290  KIFSQAFSLINVQV CNSLWTRPDNCSFINGEYLKSGLEKLEKWC CETKEEYAGSS
At4g33200  KLVTQVFSFINLSL FNSLLLRRECCTF SNGEYVKSGLI SELEKWI ANAKE EFAGT S
At1g17580  KVFTQIFSFINVQLFNS LLLRRECCSF SNGEYVK TGLAELEKWC HDATEEFVGS A
At5g20490  KVFTQIFSFINVQLFNS LLLRRECCSF SNGEYVKAGLAELEQWC IEATDEYAGS A
At1g54560  KVFTQIFSFINVQLFNS LLLRRECCSF SNGEYVKAGLAELEHWC YNATDEYAGSS
At1g08730  KVFTQIFSFINVQLFNS LLLRRECCSF SNGEYVKAGLSELEHWC FKATNEYAGSS
At2g31900  KLHQQVFSYINVQLFNS LLLRRECCSV SNGEYLMGLHELEQWC LKADDEATRSP
At5g43900  KIYSQTF SYINVQLFNS LLLRRECCTF SNGEYVKSGLAELELWC CQA .KEYSGP S
At1g04160  KIHTQTF FSFVNVQLFNS LLLRRECCTF SNGEYVKSGLAELELWC GQV .NEYAGP S
At1g04600  KMFSQTF QYINVQLFNS LLLRRECCTF VMGIVKAGLDELESWC SQATEEFVGS S
At2g33240  KIFCQTF QDINVQLFNS LLLRRECCTF IMGKKNVWVWNELESWC SQATEDFVGS S

```

```

Myo2p      TECLQHLIQTAKLLQV . RKYTTEDIDL RGICYSLTPAQLQKLSIQYQVADYE . . SPIPQEI
At2g20290  WDELKHTRQAVGFL LIHKKYNI SYDEIANDLCPNLQIQHF KLCTLYKDEIYNTKSVSQDVI
At4g33200  WHELNYIRQAVGFL VIHQKPKKSL DEIRQDLCPVLTIRQIYRISTMYWDDKYGTQSVSSEV
At1g17580  WDELKHIRQAVGFL VIHQKPKKSL KEITTELCPVLSIQQLYRISTMYWDDKYGTHSVSTEVI
At5g20490  WDELRHIRQAVGFL VIHQKPKKTL DEITRELCPVLSIQQLYRISTMYWDDKYGTHSVSDVI
At1g54560  WDELKHIRQA IGFLVIHQKPKKTL DEISHELCPVLSIQQLYRISTMYWDDKYGTHSVSPDVI
At1g08730  WDELKHIRQA IGFLVVIHQKPKKTL DEISHDLCPVLSIQQLYRISTMYWDDKYGTHSVSPDVI
At2g31900  WDELQHIRQAVMFL VSHQKTKSL DEITAKEICPVLSIPQVYRIGTMFWDKYGTQGLSPEVI
At5g43900  WEELKHIRQAVGFL VIHQKYRISY DEIANDLCPVLSVQQLYRICTLYWDDSYNTRSVSQEVI
At1g04160  WDELKHIRQAVGFL VIHQKYRVS YDDIVHDLCPILSVQQLYRICTLYWDDCYNTRSVSQEVI
At1g04600  WDELKHTRQAVLL LVTEPKST ITYDDLTLINLCSVLSTEQLYRICTLCKDKDDGDHNVSPVI
At2g33240  WDELKNTRQA LVLVTEPKST ITYDDLTTNLCPALSTQQLYRICTLCKIDHDHQNVS PDVI

```

**Figure 3.1.1:** Identification of conserved, putative binding regions in the tail domain of plant class XI myosins. Shown are the representatives alignments of the DIL domain containing *A. thaliana* class XI myosins and the class V myosin Myo2p from yeast.

**A:** Scheme of the AtMya1 (class XI) and yeast Myo2p full length protein. The position of the DIL domain is depicted in red, the position of the LCP domain in green and of the VEA domain in pink.

**B:** Alignment of the VEA domains from *A. thaliana* class XI myosins in comparison to the corresponding region in the yeast class V myosin Myo2p (vacuole binding site). The conserved amino acids are written in bold. The identified amino acids in the yeast Myo2p sequence that are required for vacuole transport are underlined. The identical or homologous a.a. at the same positions in the yeast and the plant sequences are marked in pink.

**C:** The alignment of the DIL domains from *A. thaliana* class XI myosins and the class V myosin Myo2p from yeast. Marked in blue is the LCP domain (Identical a.a. in bold).

In order to test the class XI tail domain and the identified putative binding regions (DIL domain, LCP domain, VEAK domain) for their potential capacity to bind to vesicular cargo, the following approach has been taken: with help of the Gateway technology constructs containing the complete AtMya1cDNA (representative for class XI), the cDNA subsequence coding only for the tail domain and a systematic array of tail domain subsegments containing the putative cargo binding sequences were generated and fused at the N-terminus to the YFP-cDNA (Fig 3.1.1.2.; Table 3.1.1.2). These constructs were used for transient expression in *A. thaliana* (after biolistic transformation) and in *Nicotiana benthamiana* (*Agrobacterium* mediated transformation).

### **3.1.2 Subcellular localization of the DIL- and the LCP domain**

*N. benthamiana* leaves were transiently transformed with AtMya1 LCP (see Table 3.1.1.2) and AtMya1 DIL (Table 3.1.1.2) that were tagged with YFP at their N-terminus. The expression of these fluorescent fusion proteins and their subcellular targeting was monitored and analyzed in epidermal cells by confocal laser scanning microscopy. The AtMya1 LCP domain labeled small vesicular structures that co-localized with peroxisomes which were marked with dsRed (Fig 3.1.2). In contrast, the AtMya1 DIL domain labeled vesicles that were shown to co-localize with dsRed-tagged Golgi stacks/vesicles (Fig 3.1.2).

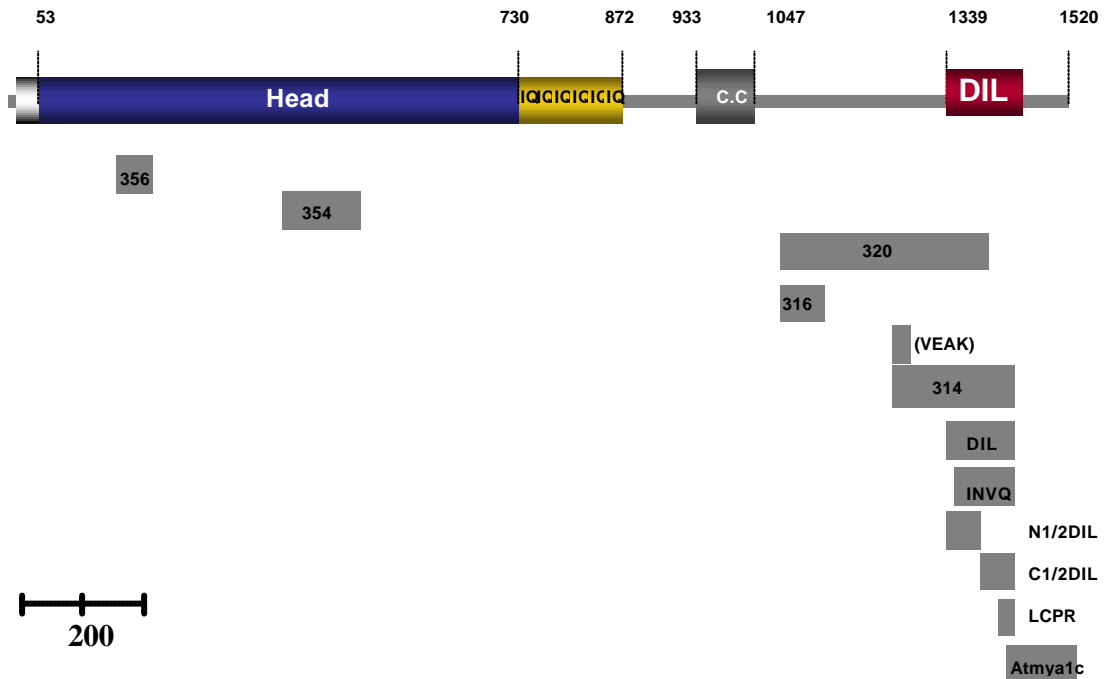


**Fig 3.1.1.2:** The amino acid positions and lengths of the of the most important fragments subcloned from the AtMya1 full length cDNA

Position	Name of fragment	Localization
1-1520	AtMya1 full	Not determined
196-241	AtMya1 356	Cytoplasmic
452-564	AtMya1 354	Cytoplasmic
1122-1377	AtMya1 320	Cytoplasmic
1122-1281	AtMya1 316	Cytoplasmic
1240-1454	AtMya1 314	Golgi
1240-1281	AtMya1 VEAQ	Not determined
1339-1454	AtMya1 DIL	Golgi
1339-1454	AtMya1 DIL*	Cytoplasmic
1339-1389	AtMya1 N 1/2DIL	Golgi
1347-1454	AtMya1 INVQ	Cytoplasmic
1423-1454	AtMya1 LCP	Peroxisomes
1438-1520	AtMya1 C	Cytoplasmic

**Table 3.1.1.2:** The length and amino acid positions and the names of the fragments subcloned from AtMya1 and Nterminally fused to YFP and their subcellular localization are listed. In the construct indicated with \*, the residue 1341, glycine, is replaced by threonine.

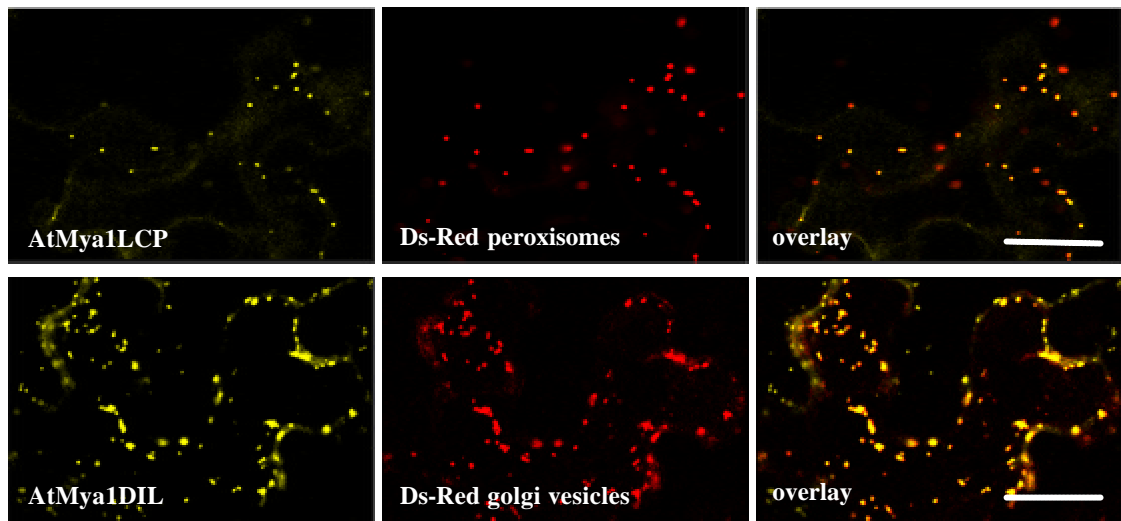


**Fig 3.1.2:** Subcellular localization of AtMya1 LCP and DIL domain (Table 3.1.1.2). The YFP-tagged tail subsegments were used for transient expression in *Nicotiana bentamiana*. Plasmid constructs appropriate for the fluorescent tagging of peroxisomes and Golgi stacks/vesicles with dsRed were co-expressed. AtMya1LCP co-localized with peroxisomes and the *AtMya1* DIL domain with Golgi stacks/vesicles. Bar, corresponds to 20  $\mu$ m.

Importantly, upon deletion of the N-terminal first six amino acids from the AtMya1 DIL domain (subsegment INVQ; Table 3.1.1.2) this fusion protein lost its targeting to Golgi stacks/vesicles and was detected just in the cytoplasm (Fig 3.1.2.1 C). Furthermore, when the amino acid in position 4 from the N-terminus of the DIL domain, which is glycine in the May1 sequence in contrast to all other *A. thaliana* class XI myosin sequences, was replaced by threonine, this mutated version, fused to YFP (May1DIL\*, Fig 3.1.2.1 B), was also distributed throughout the cytoplasm. However, the N-terminal half of the DIL domain (native N-terminus; Table 3.1.1.2) was colocalizing with Golgi stacks/vesicles upon coexpression of the respective YFP and CFP fusions (Fig 3.1.2.1 D, E, F). Thus, both the deletion of the first N-terminal 8 amino acids and the single amino acid exchange (G to T) within this sequence stretch caused loss of Golgi stack/vesicle targeting.

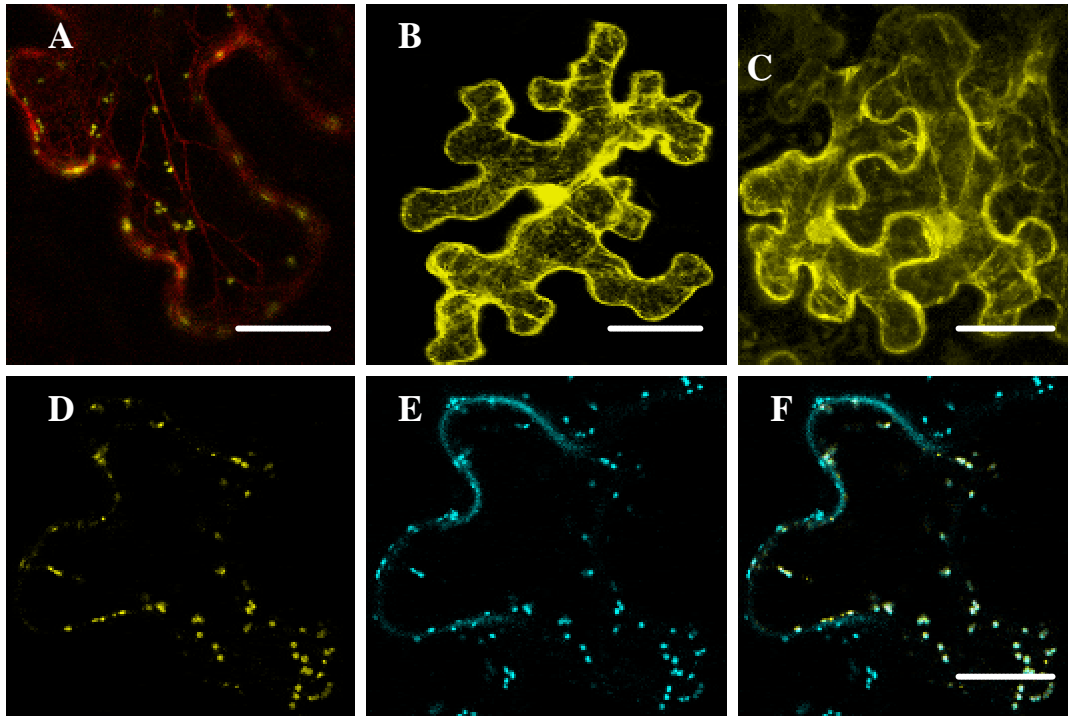


**Figure 3.1.2.1:** The fragments Mya1DIL (A), Mya1DIL\*(B), Mya1INVQ(C) and Mya1N1/2DIL (D) (Table 3.1.1.2) were N terminally fused to YFP and used for transient expression in *Nicotiana benthamiana*. (A), co-expression of Mya1DIL with plasmid constructs appropriate for the fluorescent tagging of actin filaments with dsRed; (E), co-expression of Mya1N1/2 DIL with plasmid constructs appropriate for the fluorescent tagging of Golgi stacks/vesicles with CFP. Their localization in epidermal cells was examined by confocal laser scanning microscopy. The N terminal YFP fusion protein of Mya1DIL\* (B) and Mya1INVQ (C) showed cytoplasmic localization. In contrast Mya1N1/2DIL localized on Golgi stacks/vesicles (F). Bar correspond to 20, 25, 25 and 10  $\mu\text{m}$  in A, B, C and F, respectively.

### 3.1.3 Subcellular localization of class XI myosins from different subclasses

The Identification of the binding sites (DIL and LCP domains) for either Golgi stacks/vesicles or peroxisomes within the tail domain of *AtMya1* as a

representative for class XI myosins raised important questions: do homologs of these sites in other *A. thaliana* class XI myosins also have binding capability and if so, do they bind to the same vesicles? To approach these questions, the tail domains of all *A. thaliana* class XI myosins were subjected to a phylogenetic analysis. According to the resulting phylogenetic tree, the 13 class XI myosins of *A. thaliana* can be grouped into 4 subclasses, Mya1 – Mya4 (Fig 3.1.3). As mentioned above already, Mya3 (AT3g58160) has no DIL domain and AT4G28710 has no or only a very short tail domain and is not included in this tree, but also belongs to the Mya3 subclass. Representatives from the subclasses Mya1, Mya2 and Mya4 were then analyzed for their capabilities to bind to the different vesicles (peroxisomes or Golgi stacks/vesicles). Because of lack of the DIL domain, Mya3 was not further tested.

For this purpose *N. benthamiana* leaves were transiently transformed with the following fusion proteins: AT5g43900LCP (subclass MYA2), AT4g33200DIL (subclass MYA 4) and At1g04160DIL (subclass MYA2; Table 3.1.3; Fig 3.1.3.1) which were tagged with YFP at their N-terminus. The expression of these fluorescent fusion proteins and their subcellular targeting was monitored and analyzed in epidermal cells by confocal laser scanning microscopy. Interestingly, all the above mentioned YFP fusion proteins labeled small vesicular structures which were moving and additional co-localization studies showed that the labeled vesicular structures with all these three above described constructs represent peroxisomes (see Fig 3.1.3.1).

In Table 3.1.3 the observed subcellular localization patterns or co-localizations with the VEA, DIL or LCP domains of *A.thaliana* class XI myosins are summarized.

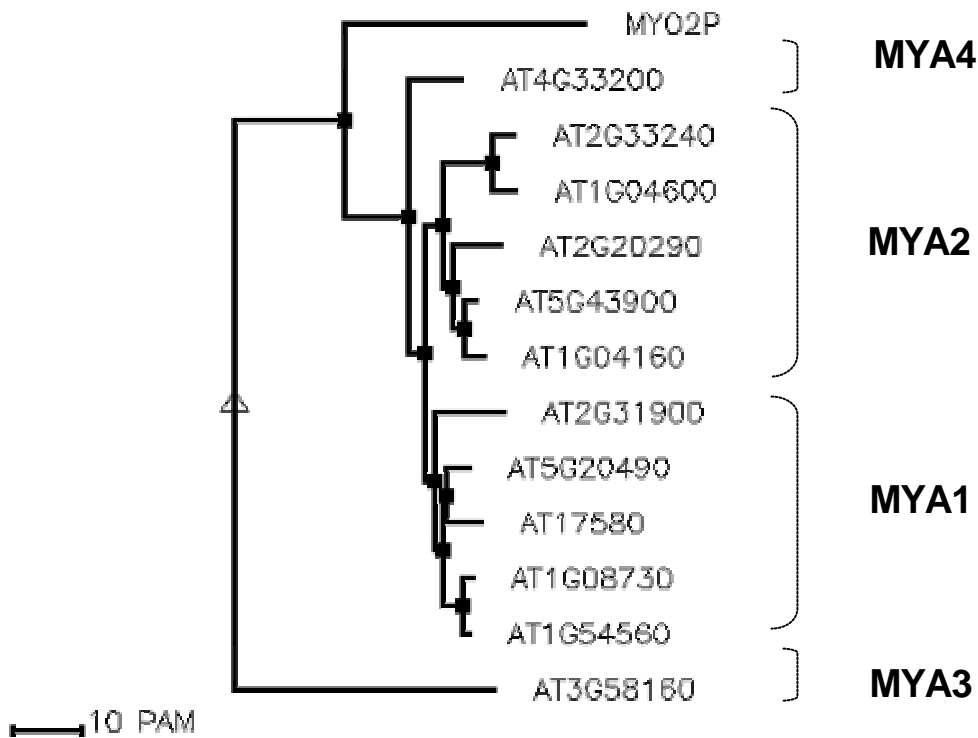


**Figure 3.1.3:** Alignment and phylogenetic tree of the complete tail domains of Myo2p and all class XI myosins from *A. thaliana* were performed by using Multalin (version 5.4.1) with hierarchical clustering method (Corpet 1988.).

Subclass	Gene code	DIL domain	LCP domain	VEAK domain
MYA 1	AT1g17580	Golgi	Peroxisomes	not tested
MYA 1	AT5g20490	Peroxisomes	not tested	not tested
MYA 2	AT5g43900	not tested	Peroxisomes	cytoplasmic
MYA 2	AT1g04160	Peroxisomes	not tested	not tested
MYA 4	AT4g33200	Peroxisomes	not tested	cytoplasmic

**Table 3.1.3:** Localizations of the vesicle binding domains of selected subclass members of the class XI myosins from *A. thaliana* are listed.

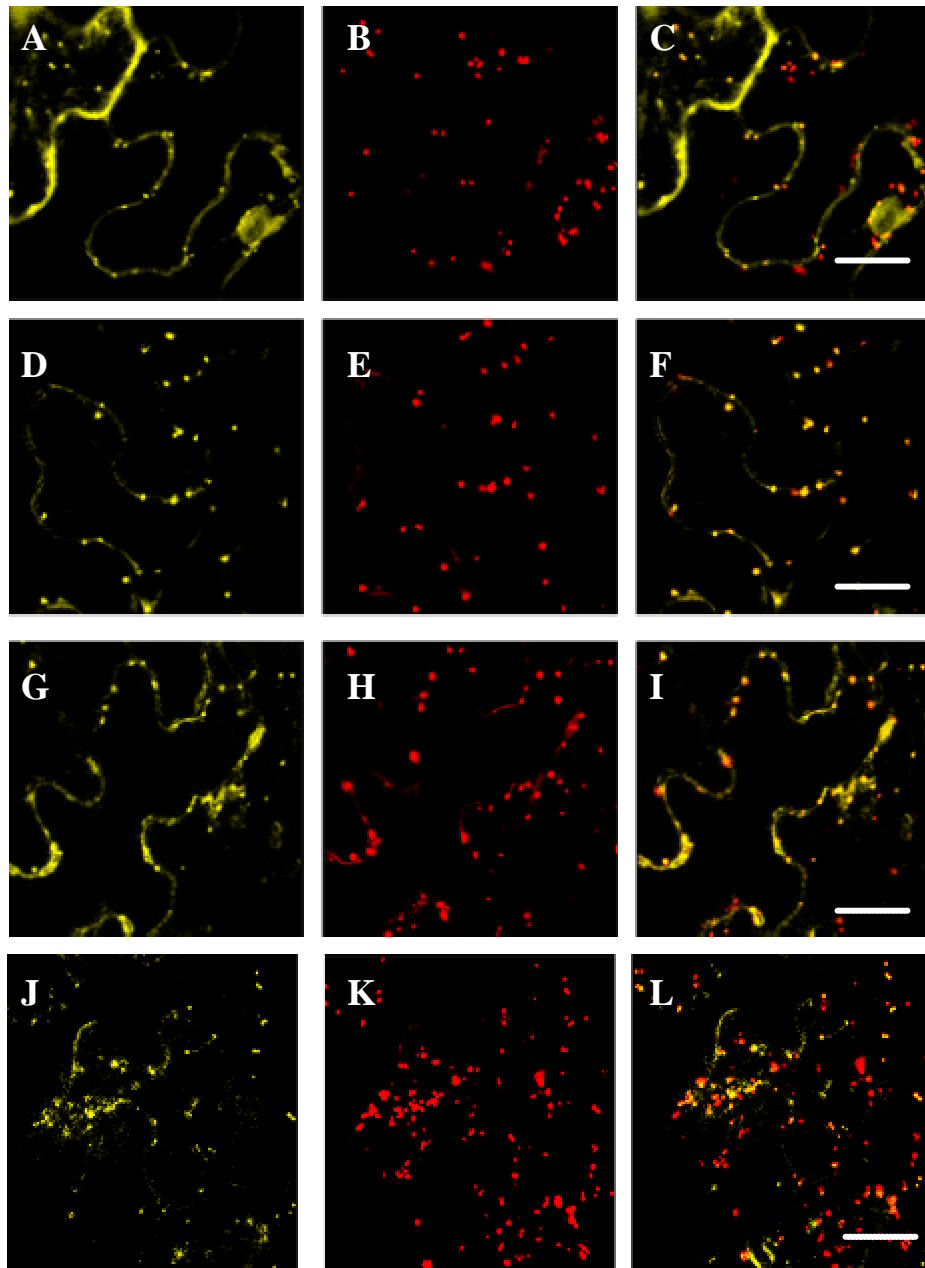


**Figure 3.1.3.1:** Subcellular localization of the DIL and LCP-domains of *A. thaliana* members of class XI subclasses Mya1, Mya2 and Mya4. Respective plasmid constructs containing N-terminal YFP-fusions of At5g20490- DIL (A) , At4g3320 -DIL (D), At5g43900 -LCP (G), At1g4160 DIL (J) and appropriate constructs for the dsRed labeling of peroxisomes (B, E ,H and K) were used for transient expression in *N. benthamiana* leaves. The colocalization in epidermal cells was detected by confocal laser scanning microscopy (C, F, I and L). Bar corresponds to 20  $\mu\text{m}$ .

Further experiments were performed to investigate the capability of the VEA domain (Fig 3.1.1 C) for binding to vesicular structures. For this purpose subfragments just comprising this putative vesicle binding site of the At5g43900 (Mya2) and At4g33200 (Mya4) (Fig 3.1.3.2) as representative for MYA2 and MYA4 subclasses were generated and N-terminally fused to YFP. The subcellular localization of YFP fusion of the VEA domains after transient expression in *N. benthamiana* leaves were analyzed using confocal laser scanning microscopy. Both constructs showed nuclear and cytoplasmic localization (Fig 3.1.3.2 B). For co-localization studies autofluorescence of chloroplasts has been used.

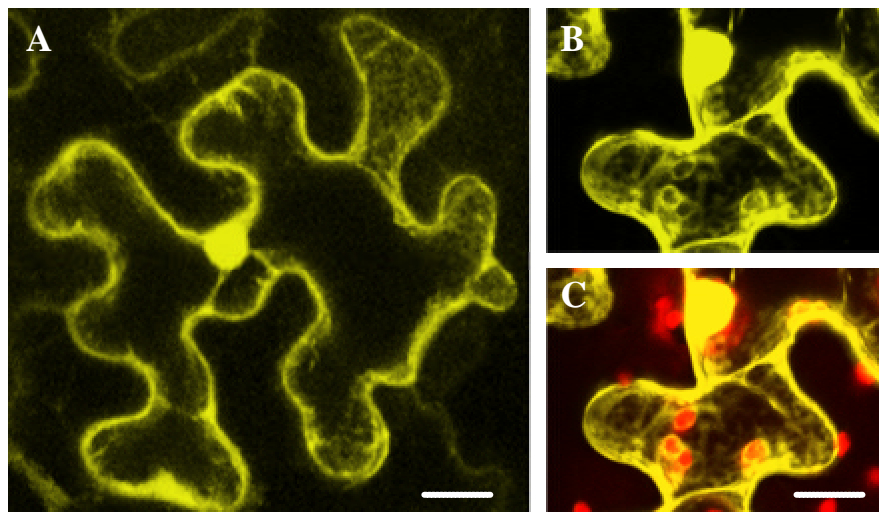


**Figure 3.1.3.2:** Subcellular localization of the VEA domain of *A. thaliana* members of class XI subclass Mya2 and Mya4. The respective plasmid construct containing the N-terminal YFP-fusion of At5g43900VEAK (A) and At4g33200VEAK (B, C) were transiently expressed in epidermis cells of *N. benthamiana*. Both constructs showed nuclear and cytoplasmic localization. Autofluorescence of plastids appeared red (C). Bar corresponds to 10  $\mu$ m.

### 3.1.4 *In planta* expression of selected fragments of *S. cerevisiae* class V myosin, Myo2p

Since the *S. cerevisiae* class V myosin Myo2p harbors within its DIL domain a binding site for secretory vesicles and additionally further upstream to the DIL domain a vacuole binding motif, it was logical to test whether these sequences encode for vesicular targeting also in plant cells. Therefore, the full length DIL domain cDNA from *S. cerevisiae* Myo2p, the subsequence encoding the binding site for secretory vesicles (homologous to the LCP domain of plant class XI myosins) and the vacuole binding sequence (homologous to the VEAK domain of plant class XI myosins) were cloned and fused N-terminally with the YFP cDNA. Appropriate plasmid constructs were then used for transient expression in *N. benthamiana* leaves (Fig 3.1.4). In the co-localization experiments, a clear-cut targeting of the yeast DIL domain to plant peroxisomes was found (Fig 3.1.4 A, B and C).

Remarkably, the secretory vesicle binding and the vacuole binding motives did not label distinct vesicular structures *in planta*, it was just found in the cytoplasm and in the nucleus (Fig. 3.1.4 D and E respectively).

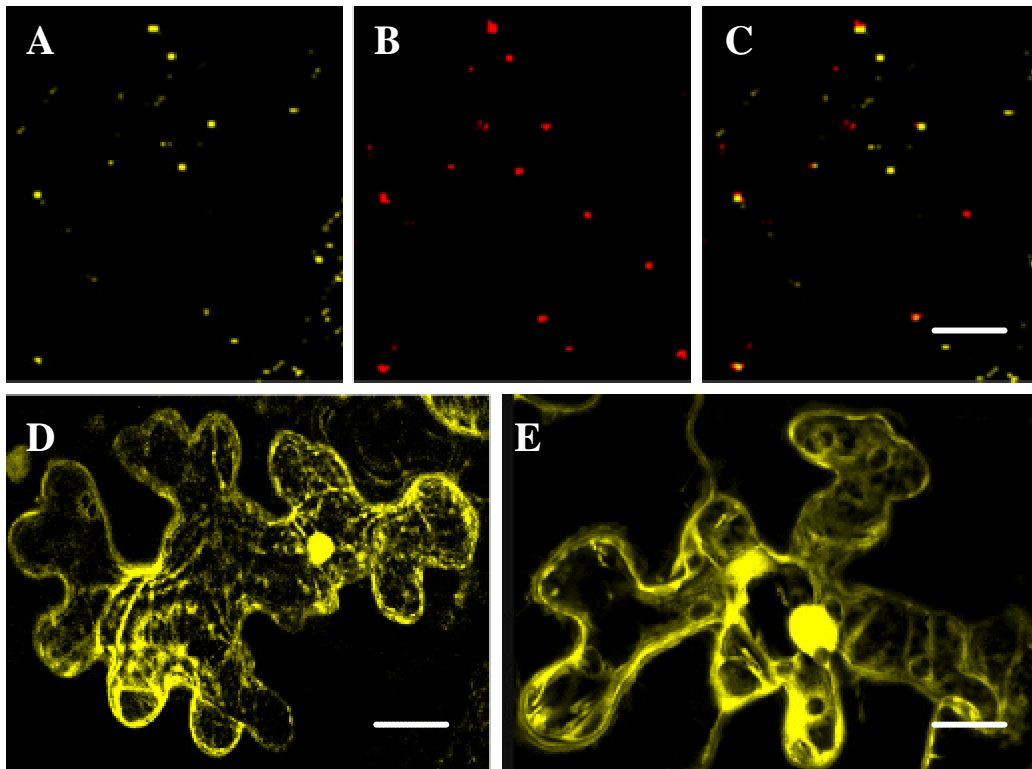


**Figure 3.1.4:** Localization of the vacuole binding motif, DIL domain and secretory vesicle binding motif of the yeast class V myosin Myo2p are shown. The YFP-tagged DIL domain (A), secretory vesicle (D) and vacuole binding motives of the yeast myosin V, Myo2p, were transiently expressed in *Nicotiana bentamiana*. A plasmid construct appropriate for the fluorescent tagging of peroxisomes with dsRed (B) was co-expressed with the DIL domain of the Myo2p. The observed colocalization of Myo2pDIL with peroxisomes is shown in (A-C). In contrast, the secretory vesicles and vacuole binding domains showed cytoplasmic and nuclear localization (D and E). Bar corresponds to 15, 20 and 10  $\mu\text{m}$  in C, D and E respectively.

The reciprocal experiment, to test the targeting of the *A. thaliana* Mya1 DIL domain in *S. cerevisiae*, was not successful. After transformation of a suitable yeast strain with an appropriate plasmid containing the Mya1 DIL domain cDNA fused to YFP, YFP fluorescence was never detectable in yeast cells.

### 3.1.5 Transient expression and subcellular localization of selected fragments of AtMya1

(AtMya1 full length, large tail fragments, a proximal C-terminal fragment and head domain fragments )

In addition to the various tail fragments that were tested with respect to their binding capability to different vesicular populations, the AtMya1 full length protein and two large fragments of the tail domain containing these binding regions (AtMya1316, AtMya1320, Table 3.1.1.2) were examined for subcellular targeting. Although the full length AtMya1 construct, tagged with YFP at the N-terminus, was used for transient expression for several times in *N. benthamiana* and in *A. thaliana*, fluorescent signals due to the presence of YFP could never be detected. However, the two large tail fragments fused N-terminally with YFP showed expression, but they were not colocalizing with vesicular structures. The confocal laser scanning microscopic imaging revealed that both fusion proteins were more or less evenly distributed in the cytoplasm (Fig. 3.1.5). In addition, a fragment from the very C-terminal end of the tail domain of AtMya1, downstream of the DIL domain (AtMya1C), was expressed as N-terminal YFP fusion protein. This part of the C-terminal end of the tail was found also throughout the cytoplasm and in the nucleus (Fig. 3.1.5). A very similar distribution was observed with two head domain fragments fused to YFP (AtMya1-354 and AtMya1-356, Table 3.1.1.2) in the transient expression assay with *N. benthamiana* (Fig. 3.1.5).

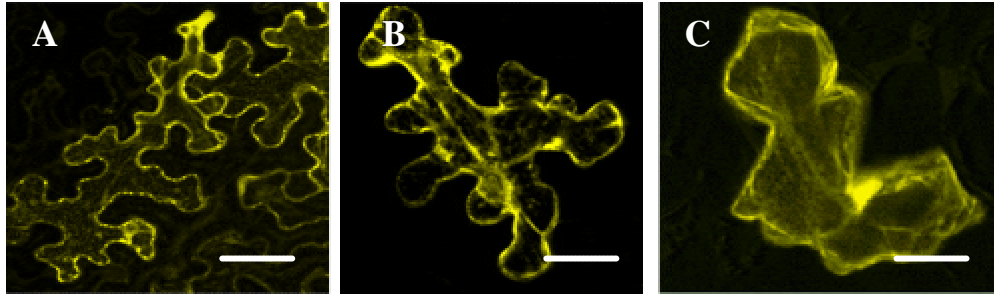


**Figure 3.1.5:** The fragments AtMya1-354, AtMya1-320 and AtMya1C (Table 3.1.1.2) were N-terminally fused to YFP and used for transient expression in *Nicotiana benthamiana*. Their localization in epidermal cells was examined by confocal laser scanning microscopy. A, AtMya1-354 (head domain region); B, AtMya1-320 (large tail fragment); and C, fragment AtMya1C (piece of C-terminal tail). Bar corresponds to 30, 20 and 20  $\mu\text{m}$  in A, B and C respectively.

### 3.2 Characterization of *Arabidopsis thaliana* class VIII myosins

In *A. thaliana*, 4 of the altogether 17 myosin genes belong to class VIII (ATM1 - 4). On the basis of sequence homology of the full-length cDNAs, the *A. thaliana* class VIII myosin genes could be grouped into two different subclasses, ATM A and ATM B (Fig 3.2.1), as was found by performing a phylogenetic tree analysis. ATM A comprises AT3g19960 (ATM1) and AT1g50360, ATM B comprises AT5g54280 (ATM2) and AT4g27370 (Fig. 3.2.1).

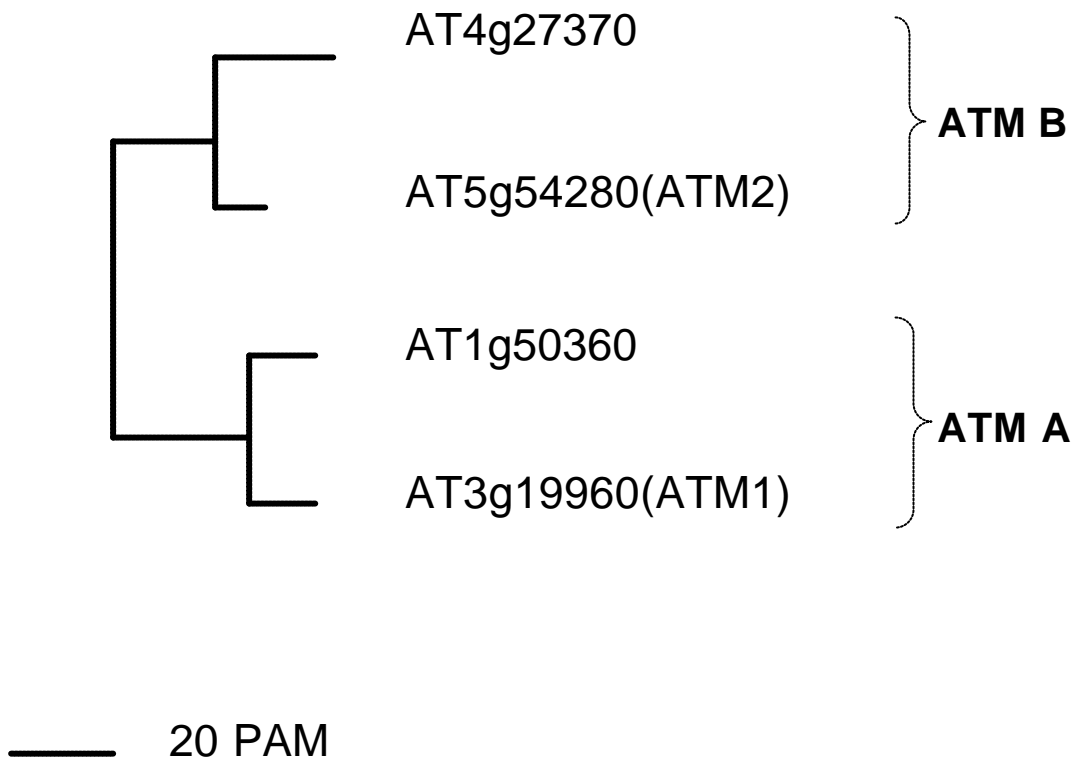


**Figure 3.2.1:** The Alignment of the full length *A. thaliana* class VIII myosins was performed using Multalin (version 5.4.1) and a phylogenetic tree was generated using the hierarchical clustering method (Corpet 1988).

Because of the strong phenotypic effect of the knock-out of the *ATM2* gene in *A. thaliana* plants (as described below in 3.5.3), this myosin was selected for a more detailed analysis concerning subcellular targeting. As a representative of the ATM A subclass the myosin ATM1 was selected for testing of subcellular localization. This was the first myosin from *A. thaliana* that have been characterized at the molecular level (Reichelt et al., 1999). Furthermore, for this myosin detailed immunocytochemical data are available describing the subcellular localization *in situ*. It was interesting to

see whether by the *in vivo* approach applied throughout this thesis corresponding results would be obtained.

### 3.2.1 Subcellular localization of ATM2

Since in the tail region of the *A. thaliana* class XI myosins several domains could be identified that are showing vesicle binding, also in the case of ATM2, in addition to the full length protein, a number of subregions were tested for their subcellular localization (Fig 3.2.1.2).

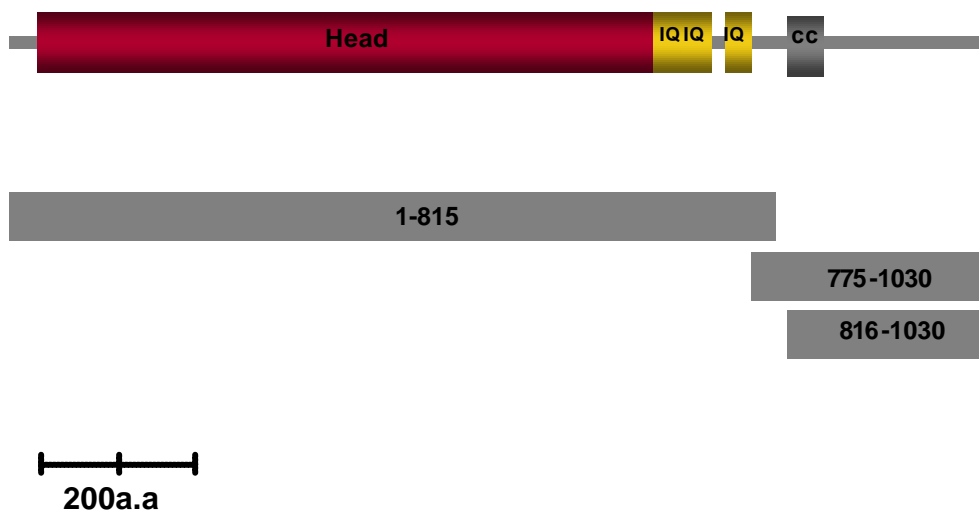


**Figure 3.2.1.2:** Construct generation for *in vivo* testing of subcellular localization of ATM2. Scheme of the ATM2 amino acid sequence and the length and positions of the subfragments generated for testing of subcellular localization. The subcellular localization of ATM2 was determined by means of transient expression of fluorescently tagged proteins in leaves of *N. benthamiana*.

The full length ATM2, fused C-terminally to YFP, labeled mostly filamentous structures and some vesicles along those filaments (Fig 3.2.1.3 A). In contrast the C-terminal 255 a.a. of ATM2 (775-1030) fused C-terminally with YFP localized to a large amount to vesicles along filaments that could be identified as actin filaments by co-localization studies using fimbrin as tag for actin filaments (Fig 3.2.1.3 D) and a pronounced localization within the nucleus (Fig 3.2.1.3 C). However, the N-terminal fusion of the C-terminal tail construct (775-1030) visualized densely packed small vesicles strictly in the cell periphery (Fig. 3.2.1.3 E). These vesicles were of similar size (about 1 $\mu$ m in diameter) and homogeneously distributed in the entire cytoplasm (Fig. 3.2.1.3.1), but not at all in transvacuolar cytoplasmic strands.

In addition, to investigate the potential binding capability for vesicles of the C-terminal part of the tail domain a fragment of 214 a.a. of ATM2 (816-1030) has been generated and fused at the C-terminus to the YFP-cDNA. Interestingly, the subcellular localization of this construct showed that this segment (ATM2-816) labeled vesicular structures which, in contrast to the full-length ATM2 tail domain, were moving (Fig 3-2-1-3 F). Interestingly, deletion of this 214 a.a from full length ATM2 leads to actin filament localization of this protein and no vesicle labeling could be observed (3-2-1-3 B).

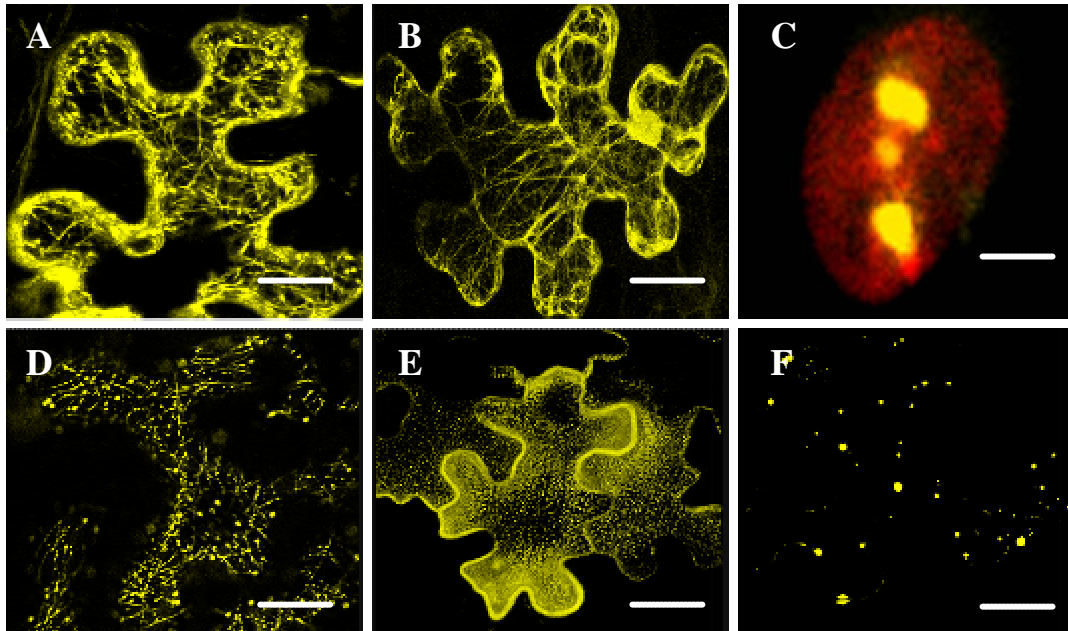


**Figure 3.2.1.3:** Subcellular localization of different fragments (see Figure 3.2.1.2) of the *Aabidopsis thaliana* class VIII myosin ATM2 fused with YFP are shown. (A) The cDNA coding for the full length ATM2 C-terminally fused to YFP. (B) The fragment ATM2-815 coding for the 815 a.a from the N terminal part of the ATM2 tail fused C terminally to YFP. (C) The nuclear localization of the tail domain of the ATM2 fused C terminally to YFP. Nuclei of the cells were counter-stained with Propidium Iodide (Red). (D) The tail domain of ATM2 fused C-terminally to YFP. (E) The tail domain of ATM2 fused N-terminally to YFP (F) The fragment ATM2 816 coding for 214 a.a from the C terminal part of the ATM2 tail fused C terminally to YFP. Bar corresponds to 25, 25, 5, 25, 50 and 25  $\mu\text{m}$  in A, B, C, D, E and F respectively.

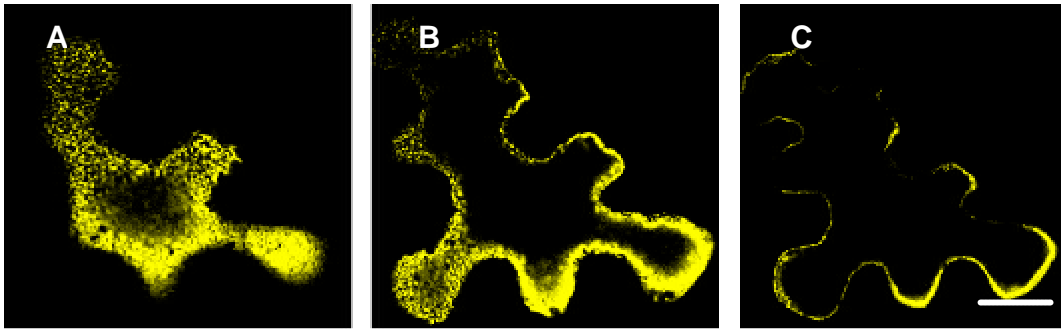


**Figure 3.2.1.3.1:** Subcellular localization of the tail domain of the ATM2 fused N-terminally to YFP by confocal laser scanning microscopy. Subsequent optical sections of the localization of the ATM2 tail fused N terminally to YFP are shown (A, B and C).

In order to investigate the nature of these vesicles labeled with the different segments of the ATM2 tail, the following colocalization studies have been performed.

A) ATM2tail::dsRed (C-terminal) plus YFP::ATM2tail (N-terminal)

B) ATM2tail::dsRed plus YFP::ATM2 816

In contrast to YFP::ATM2 tail alone which showed densely packed small vesicles in the cell periphery (see Fig 3.2.1.3 E), in the coexpression experiment of this construct with ATM2tail::dsRed, colocalization of the labeled vesicles was now observed (Fig 3.2.1.4). Furthermore, upon coexpression of ATM2tail::dsRed and ATM2-816::YFP also colocalization was found.

Obviously, by coexpressing the different ATM2 tail versions, the patterns of labeled vesicular structures merge. This strongly suggests that the tail of ATM2 is binding to one class of vesicles only. The differences in the vesicular labeling patterns resulting from the expression of the individual constructs alone might be due to varying dominant negative inhibition within the transport or processing pathway of these vesicles.

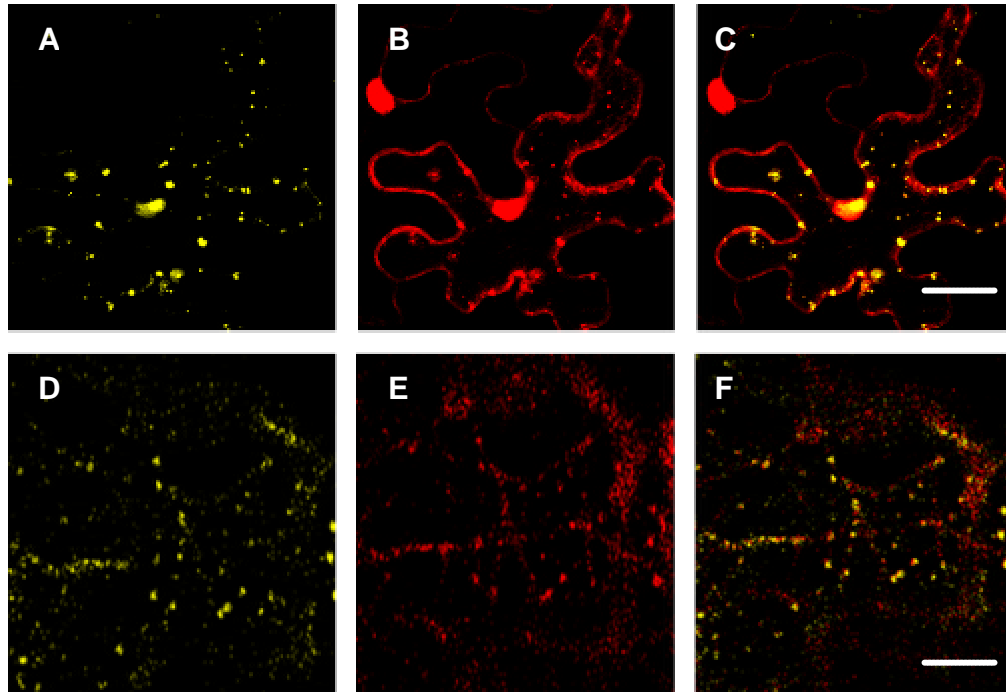


**Figure 3.2.1.4:** Subcellular co-localization experiments using transient co-expression of plasmid constructs coding for ATM2-816::YFP (A), ATM2tail::RFP(B) and YFP:ATM2tail(D), ATM2tail:RFP(E) in *N. benthamiana* epidermis leaves. Corresponding overlay pictures are shown(C and F). Bar corresponds to 20 $\mu$ m.

A striking observation was made, when the YFP::ATM2tail (N-terminal) version was expressed together with the FYVE-dsRed tagged endosomal marker. In cells with lower expression levels of the two fusion proteins, partial colocalization was detected (Fig 3.2.1.5). This indicates that the cargo of ATM2 belongs to the endocytic pathway or at least is strongly related with endosomal membranes.

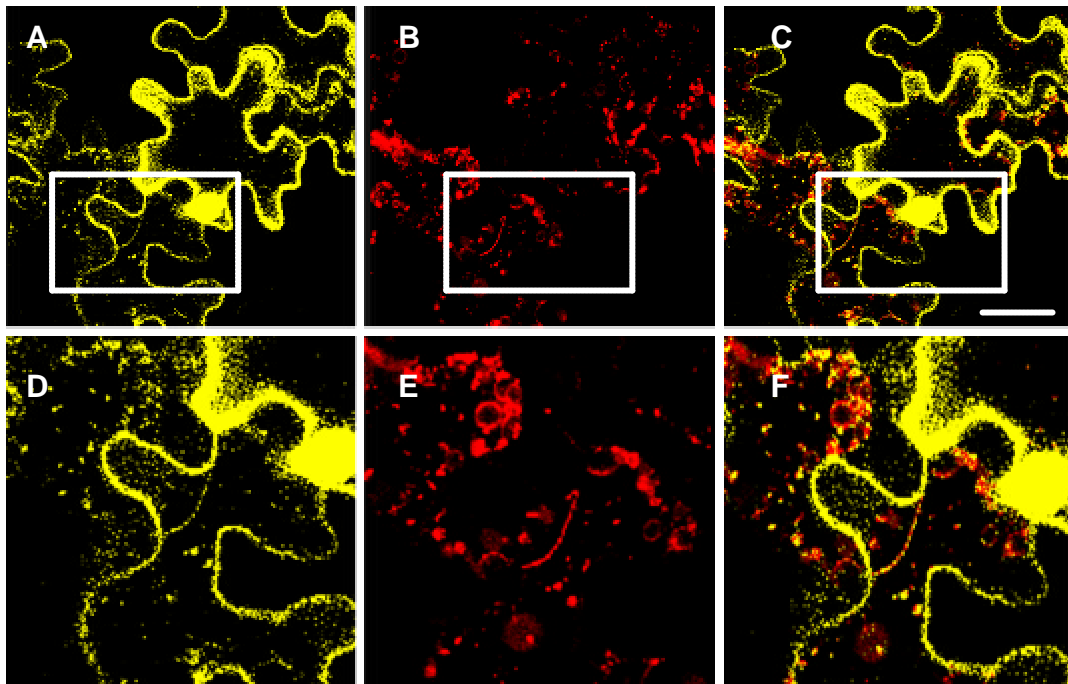


**Figure 3.2.1.5:** Subcellular localization of the tail domain of the ATM2 fused N-terminally to YFP by confocal laser scanning microscopy. Co-localization of the ATM2 tail-YFP with FYVE-dsRed tagged endosomes is shown in A, B and C. Enlargements for the framed regions are shown in D, E and F. Bar, 20  $\mu$ m.

Further colocalization studies between the C terminal YFP fusion of ATM2tail and dsRed tagged early endosomes (Ara6, plant specific early endosomal marker, Fig 3.2.1.6 A-C), late endosomes (FYVE-marker, Fig 3.2.1.6 D-F) and mitochondria Fig 3.2.1.6 G-H) have been performed. In contrast to the observed partial colocalization of the N-terminal YFP fusion of ATM2tail with the FYVE-endosomal marker, no colocalization could be observed with the C-terminal YFP fusion.

The construct ATM2 816 showed in contrast to all other tested ATM2 constructs, targeting to vesicles that were moving (Fig 3.2.1.3 F). In order to identify the nature of these observed moving vesicles additional colocalization studies of construct ATM2-816 with Golgi stacks/vesicles,

peroxisomes, mitochondria, and endosomes were performed. In all these experiments no co-localization with the respective organelles was observed (Fig 3.2.1.7).

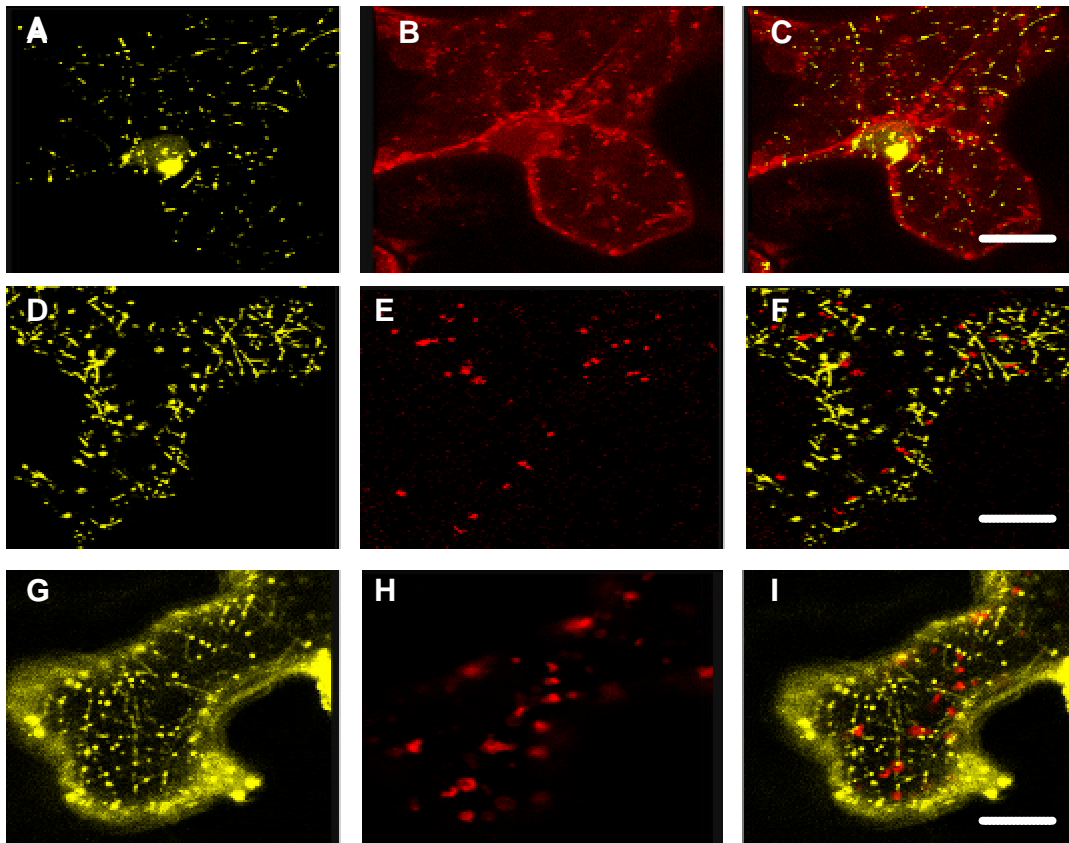


**Figure 3.2.1.6:** Subcellular localization of the tail domain of ATM2 by confocal laser scanning microscopy. Plasmid constructs containing the complete cDNA of the tail region of ATM 2 (A,D,G ) fused C terminally to the YFP cDNA were generated and used for transient co-expression in *Nicotiana bentamiana* epidermis leaves with dsRed tagged early endosomes (B), late endosomes (E) and mitochondria (H). There was no colocalization observed (C, F and I). Bar corresponds to 20  $\mu\text{m}$ .

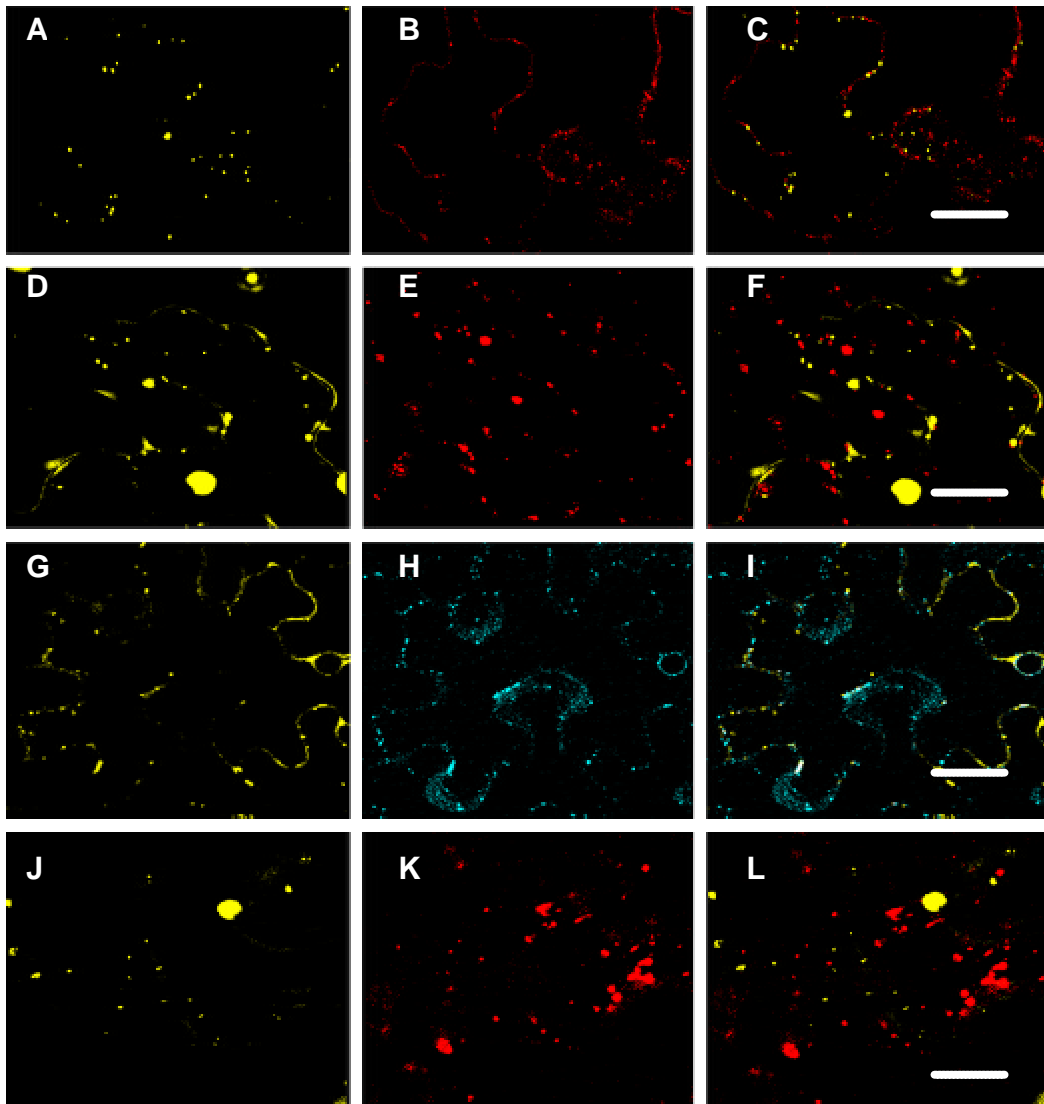


**Figure 3.2.1.7:** Subcellular colocalization experiments with the segment ATM2-816. A plasmid construct containing the cDNA coding for the 214 a.a at the C-terminal end of ATM 2 (A, D, G and J) fused N terminally to the YFP cDNA were generated and used for transient co-expression in *N. bentamiana* epidermis leaves with fluorescently tagged early endosomes (B), late endosomes (E), Golgi stacks/vesicles (H) and mitochondria (K). There was no co-localization observed. Bar corresponds to 20, 15, 30 and 15  $\mu\text{m}$  in C, F, I and L respectively.

### 3.2.2 Subcellular localization of ATM1

A cDNA fragment coding for the last C-terminal 167 a.a. (999-1166) of ATM1 was used for the generation of an N-terminal YFP fusion plasmid construct. In the transient expression assay with *N. benthamiana* leaves the fusion protein labeled intensely the plasma membrane and showed weaker signals in cytoplasmic strands and around the nucleus (Fig 3.2.2).

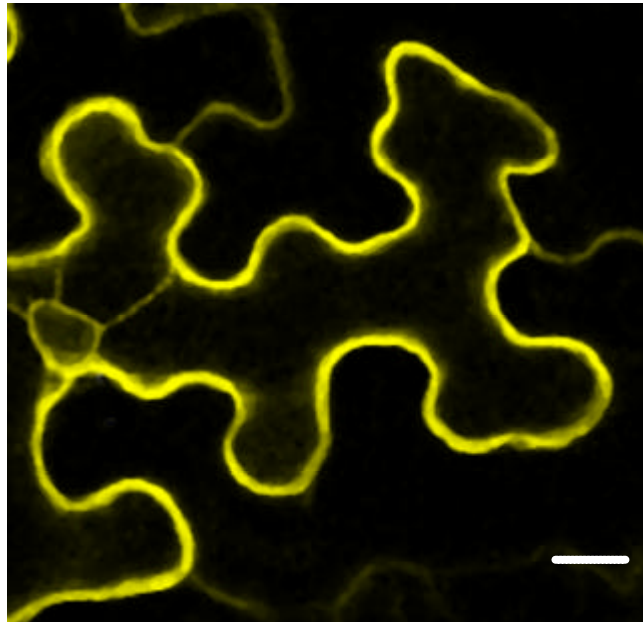


**Figure 3.2.2:** The last C-terminal 167 a.a of the ATM1 sequence was N-terminally fused to YFP and used for transient expression in *Nicotiana benthamiana*. The localization in epidermal cells was examined by confocal laser scanning microscopy. Bar corresponds to 10  $\mu\text{m}$ .

### 3.3 Subcellular localization of selected myosin constructs in *A. thaliana*

As described above, most of the localization and co-localization studies were carried out in a heterologous expression system using *Agrobacterium thumfaciens* based transient transformation of *N. benthamiana* leaves. Nevertheless, some of these constructs were also examined in *A. thaliana* leaves using transient expression in epidermal cells after biolistic transformation (Fig 3.3).

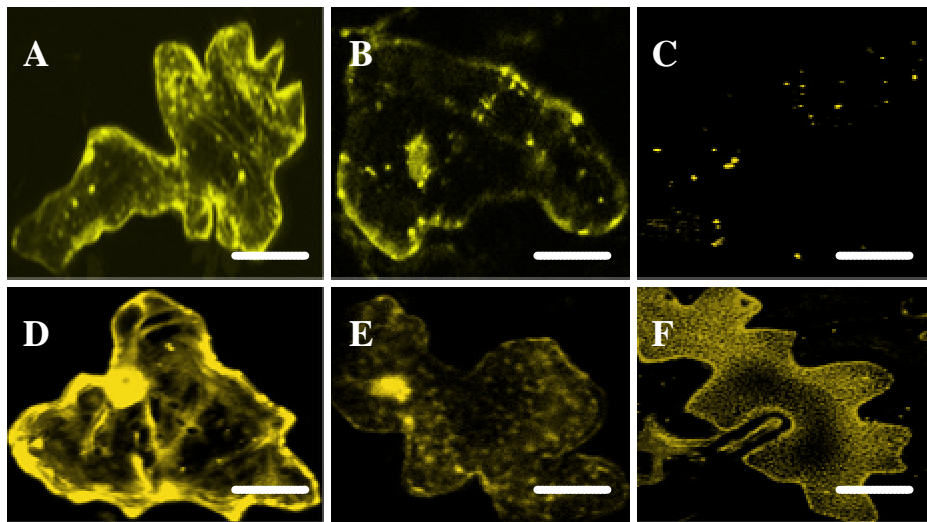


**Figure 3.3:** The subcellular localization of N terminal YFP-fusion proteins of AtMya1-314(A) , AtMya1-DIL(B), AtMya1-LCP (C) and AtMya1-INVQ(D), the DIL domain of At1g4600(E) and the tail domain of ATM2 (N-terminal fusion) (F). Leaves of *A. thaliana* were biolistically transformed (particle bombardment) and transient expression of the various fusion proteins was examined by Confocal Laser Scanning Microscopy. Bar corresponds to 25  $\mu$ m.

The subcellular localization and the pattern of labeled vesicles in *A. thaliana* were very similar to the situation in *N. benthamiana*.

### 3.4 Identification of putative myosin binding proteins by yeast two-hybrid screening

#### 3.4.1 Screening for Mya1

The cDNAs encoding full length AtMya1, the subsegment encoding the DIL domain and the INVQ subfragment (Table 3.1.1.2) were recombined into the bait vector. The recombinant hybrid proteins were tested for self-activation and non-specific protein-binding properties. These myosin proteins were used as bait to screen two different *A. thaliana* cDNA-libraries (one library made from tissue of whole plants, the other one made from a green tissue parts only, these libraries were provided kindly by the group of Dr. Uhrig, MPIZ, Cologne, Germany). After the screening and selection procedure the positive candidates were analyzed by PCR and the insert was sequenced. The identity of the respective proteins was obtained by using the publicly available cDNA data base of *A. thaliana*. Based on the experience with yeast two-hybrid assays available in our institute regarding false positive interactors the most significant and interesting candidates have been selected. The full length cDNAs of these putative Mya1 interactors were cloned and fused at the C-terminus to the YFP cDNA. The subcellular localization of the respective YFP-fusions was examined after transient expression in *N. benthamiana* leaves by confocal laser scanning microscopy. In Table 3.4 representative examples are listed and in Fig 3.4.1 (co-) localization investigations are shown.

Gene code	Identified clones from Y2H	bait	bait specific name
At4g15620	integral membrane protein family	1339-1454	AtMya1 DIL domain
At3g49720	membrane related protein	1339-1454	AtMya1 DIL domain

**Table 3.4.1:** Identified *Arabidopsis thaliana* genes clones from yeast two hybrid screens with respective baits from AtMya1 cDNA are listed.

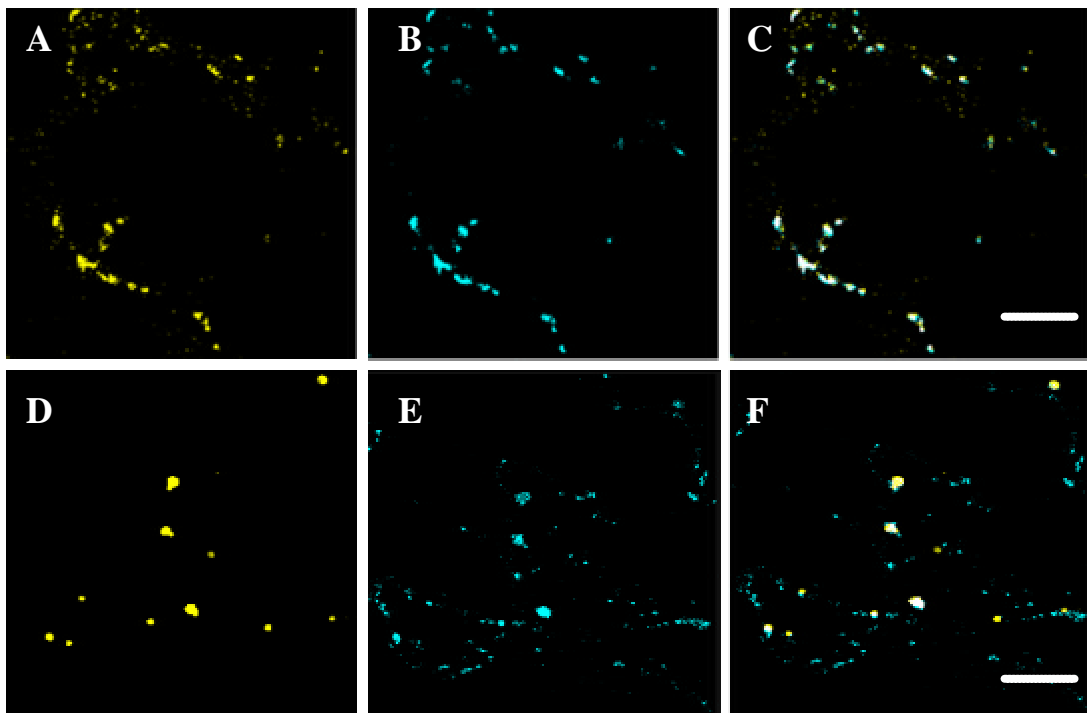


**Figure 3.4.1:** Co-localization studies for the *Arabidopsis thaliana* integral membrane family protein, At4g15620 (A) and a membrane related protein containing START domain, At3g49720 (D) are shown.

The full length of the above mentioned genes which has been identified from yeast two hybrid screens using AtMya1-DIL domain as bait have been c-terminally fused to YFP and transiently coexpressed with plasmid constructs appropriate for the fluorescent tagging of Golgi stacks/vesicles (B and E). The colocalization of these fused proteins with golgi stacks/vesicles are shown in C and F. Bar corresponds to 20  $\mu\text{m}$ .

The C terminal YFP fusion of At4g15620 and At3g49720 were transiently co-expressed in *N. benthamiana* with plasmid constructs appropriate for the fluorescent tagging of Golgi stacks/vesicles (CFP). The results were that At4g15620 (member of the Arabidopsis thaliana integral protein family) and At3g49720 (a putative membrane related protein) co-localized with Golgi stacks/vesicles (Fig 3.4.1)

### 3.4.2 Screening for ATM2

The cDNA encoding the ATM2 tail (775-1030) was used as a bait to screen the two different *A. thaliana* cDNA-libraries mentioned above (3.4.1). From the positive candidates resulting from the screening procedure one most interesting protein (At5g10480, *PEPINO/PASTICCINO2*) which is coding for a protein tyrosine phosphatase has been selected and assayed for subcellular localization in *N. benthamiana* leaves. The C terminal YFP fusion of PAS2 localized on vesicles distributed in the cell prephery, and in addition colocalization experiments with the endosomal marker FYVE-dsRed have been performed, however colocalization was not observed (Fig 3.4.2).

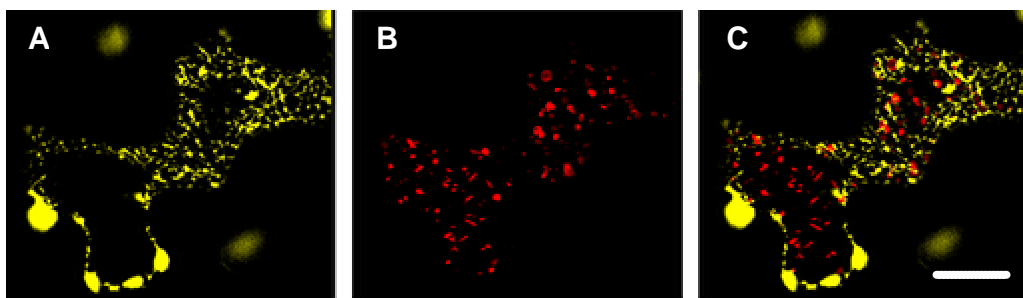


**Figure 3.4.2:** Localization studies for the *A. thaliana* tyrosine phosphatase like protein (At5G10480). The full length cDNA of this gene was C-terminally fused to YFP and was used for transient expression in *N. benthamiana*. Colocalization of the YFP fusion of tyrosine like protein (A) with plasmid constructs appropriate for dsRed tagging of endosomes (B) was performed. No colocalization has been determined. Bar corresponds to 20  $\mu\text{m}$ .

### **3.5 *A. thaliana* myosin knock-out lines**

#### **3.5.1 Selection and identification of *A. thaliana* myosin knock-out lines**

From the T-DNA insertion mutant collections GABI-Kat, Max Planck Institute for Plant Breeding Research, Cologne, Germany, and SIGnAL, Salk Institute Genomic Analysis Laboratory, La Jolla, USA, a number of lines, which mostly had T-DNA insertions in exons of the respective myosin genes have been selected (Table 3.5.1). From each of these lines 15-20 plants were grown and tested for presence of the T-DNA and hetero- or homozygosity with PCR using primers for the T-DNA flanking sequences. Seeds from the identified homozygous plants were collected and used for further growth and propagation.

These homozygous plants were tested by RT-PCR for actual absence of the respective transcripts. In Table 3.5.1 all these homozygous myosin knock-out lines that are listed.

Gene code	class	selected mutant lines	name
At3g19960	VIII	219H11	AtATM
At5g54280	VIII	SALK-104355,SALK-052429	AtATM2
At5g20490	XI	SALK-018764	AtMya14
AT1g17580	XI	SALK-022140,SALK-129106	AtMya1
At1g04160	XI	279F, 403F, 463, 135E, 231E12	AtMya11
At1g04600	XI	622E02	AtMya3
At1g08730	XI	754C	AtMya5
At5g43900	XI	115C01,SALK055785	AtMya2
At4g33200	XI	SALK-084363	AtMya4
At2g32240	XI	SALK-094036	AtMya10
At1g54560	XI	SALK-089338	AtMya6
At2g20290	XI	232D12	AtMya9

**Table 3.5.1:** List of selected T-DNA insertion knock-out mutant lines for *A. thaliana* myosin genes.

### 3.5.2 Phenotypic characterization of *Arabidopsis thaliana* class XI myosin knock-out lines

Fourteen *Arabidopsis thaliana* homozygous knock-out lines for 10 class XI myosin genes have been identified (Table 3.5.1). Phenotypic characterization of these 14 homozygous knock-out lines revealed no drastic effects with respect to growth and development. However various degrees of stunted growth and changes in seed morphology have been observed (Fig 3.5.1 -A/B/C).

Phenotypic characterization of seeds from At1g04160 and At1g04600 knock-out plants (homozygous) showed squashed seed shape compared to WT plants (Fig 3.5.1 C).

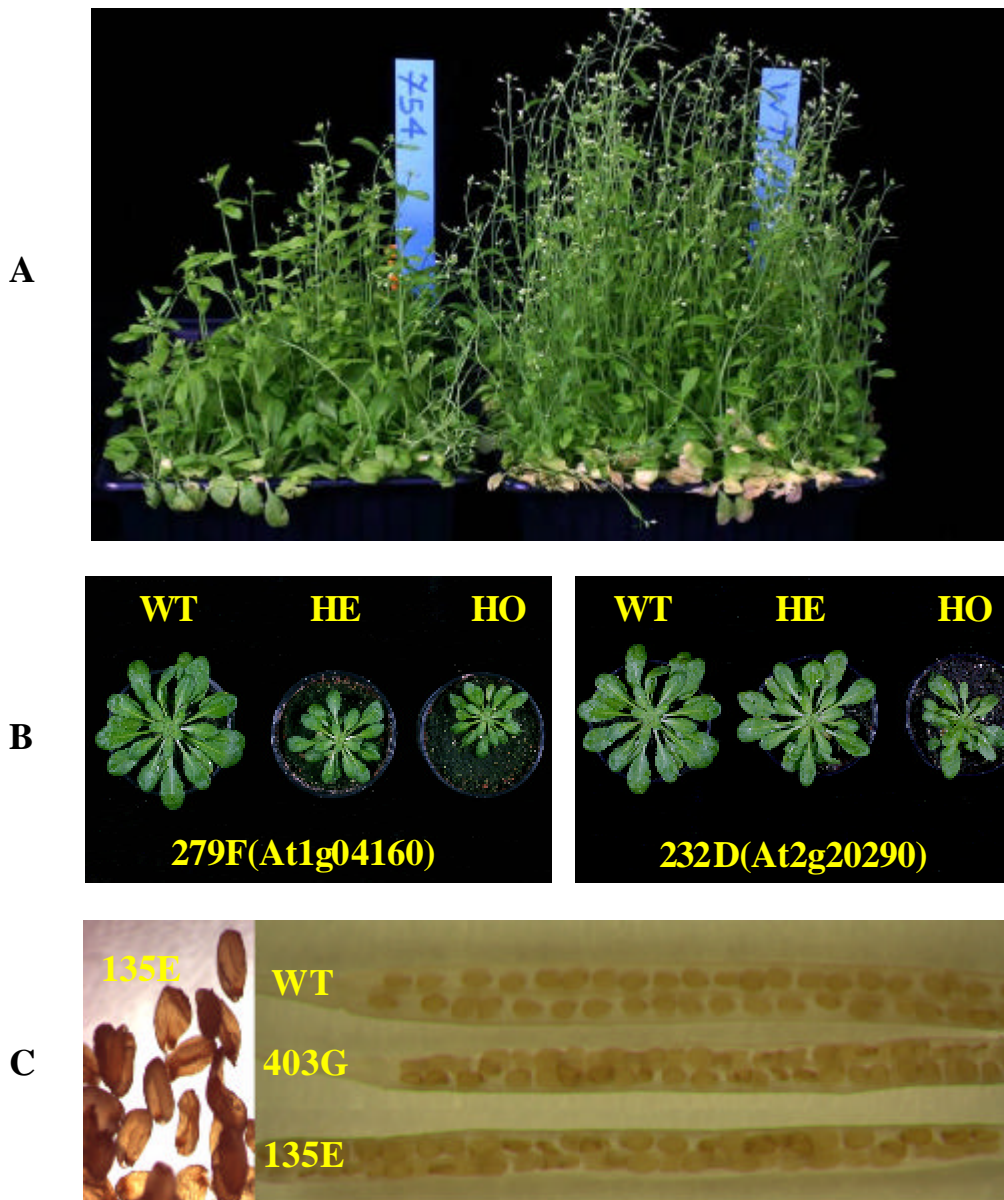


**Fig 3.5.1:** Comparison of *A. thaliana* wild type and knock-out lines for the class XI myosins.

(A) Comparison of *A. thaliana* wild type (WT) and homozygous knock-out line for one member of the class XI myosins (line 754, At1g08730).

(B) Comparison of *A. thaliana* wild type (WT), the heterozygous and homozygous knock-out line for the class XI myosin At1g04160 (line 279F) and At2g20290 (line 232D).

(C) 403G and 135E, homozygous knock-out lines of class XI myosin from *Arabidopsis thaliana* (At1g4160) showing altered seed shape compared to wild-type plants.

### **3.5.3 Phenotypic characterization of *Arabidopsis thaliana* class VIII myosin knock-out lines.**

Based on sequence homology the four class VIII myosins can be grouped into two subgroups as described above (ATM A, ATM B). To investigate the function of this class of plant myosins, knock-out lines corresponding to At1g19960 (ATM1) and At5g54280 (ATM2) have been selected from mutant collections GABI-Kat (line 219 H for ATM1) and SIGnAL, Salk Institute Genomic Analysis Laboratory (lines SALK-104355 and SALK-052429).

For the ATM2 lines homozygous plants could never be identified. The heterozygous plants showed strong deficiencies with respect to growth and development when they were grown on MS agar without sucrose (Fig 3.5.3. A). Surprisingly, on soil the heterozygous plants were growing more or less normally and produced seed. To examine the potential lethality of the homozygous knock-out of this gene, seeds collected from heterozygous plants were sown on MS plates and the numbers of non-germinated seeds, WT seedlings and heterozygous plants were counted (Fig 3.5.3 A, B). This statistic analysis indicated that the homozygous knock-out of ATM2 might be lethal or at least prevent completely germination of seeds. In the case of ATM1 the respective knock out lines showed no visible phenotype, even homozygous plants were growing normally like wild type and produced seed.

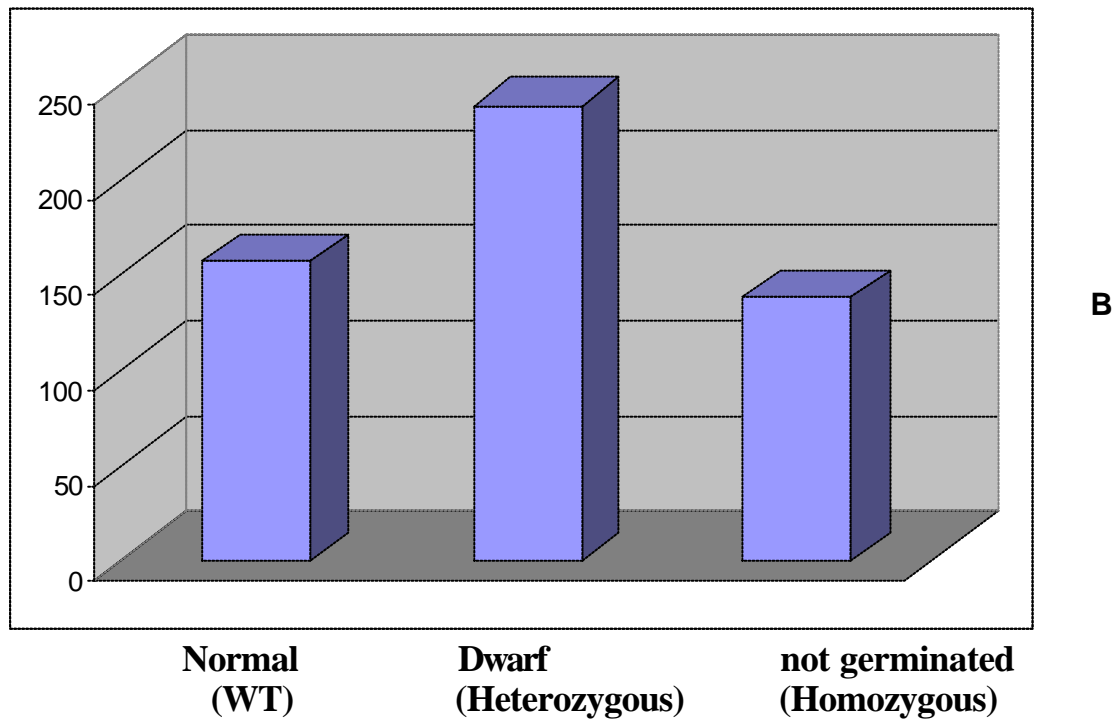
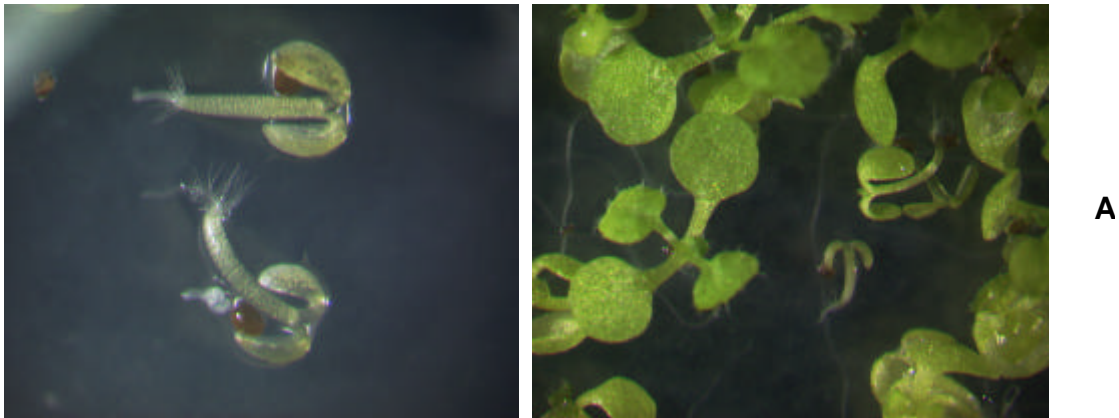


**Figure 3.5.3 A**, Morphology of heterozygous and wild type seedlings grown from seeds of a heterozygous population of ATM2 knock-out plants grown on MS agar without sucrose.

**B**, Statistical distribution of the morphological phenotypes in the F<sub>2</sub> progeny of ATM2 heterozygous knock-out plants (SALK-052429). X axis: Number of plants.

### **3.6 Studies on the involvement of myosins in plant defence responses**

#### **3.6.1 Non-host resistance (powdery mildew of barley)**

On its natural host barley the fungal pathogen *Blumeria graminis* f. sp. *hordei* (*Bgh*, powdery mildew of barley) is able to invade epidermal cells and to form intracellular feeding organs, the so called haustoria, which provide the nutrients for further hyphal growth, colonization of the entire epidermis and propagation by production of conidiospores. The non-host plant *Arabidopsis*, however, is fully resistant against *Bgh*, which is not able to develop and propagate on this plant. Penetration of the cell wall and invasion into epidermal cells is largely hindered by papilla formation. In the relatively rare cases, where the fungus nevertheless penetrates successfully, the plant cell undergoes programmed cell death (hypersensitive reaction, HR) and by this terminates further fungal growth.

All *Arabidopsis* myosin knock-out lines identified in this study (Table 3.5.1) were challenged with *Bgh*. At 24 h and 48 h post inoculation with fungal spores, when the fungus usually has formed haustoria on its host barley, the defence responses of the *Arabidopsis* plants were microscopically inspected and statistically evaluated. In two experiments with 2 week old plants we found an altered defence response, essentially a strong reaction (callose deposition) in mesophyll cells (Fig 3.6.1), in a sub-set of 2 myosin class XI gene *Arabidopsis* knock-out lines (*AtMyA1* and *At1g04160*) out of 10 evaluated. Repeating these experiments with 3 week old plants including

PEN1 (Collins et al., 2003) mutant plants as an additional control, the above described changes in defence responses of the respective myosin knock-out lines could not be obtained. Thus, the observed phenotypic alterations could be due to other factors, most probably to a transient change or weakening of the overall physiology by the defect in one of the myosin XI genes. This might have resulted in a retarded papilla formation and consequently in extension of callose deposition into the mesophyll. Similar mesophyll responses were observed in *A. thaliana* wild type plants upon inoculation with either *Blumeria graminis* f. sp. *tritici* (*Bgt*) or *Erysiphe cichoracearum* (Yun et al., 2003).

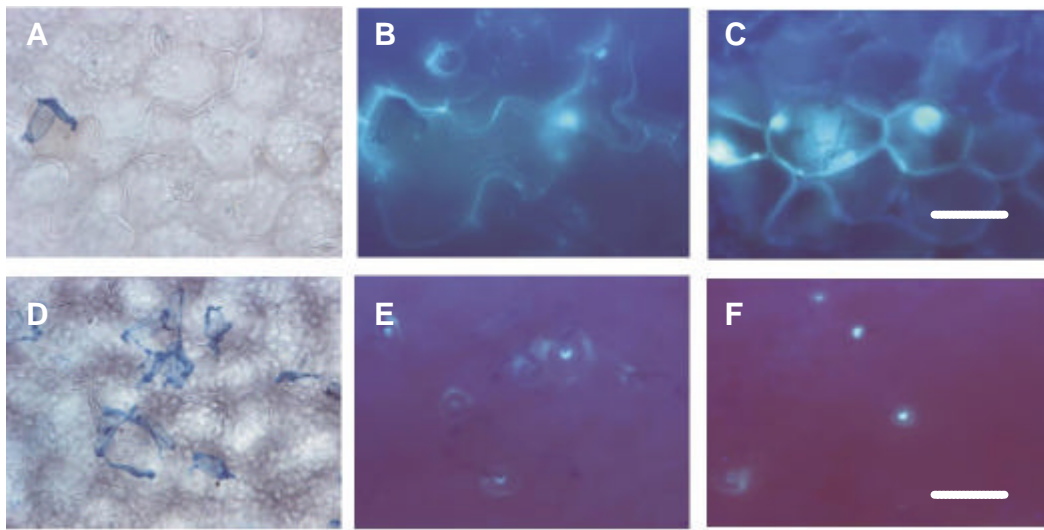


**Figure 3.6.1:** Light microscopic evaluation of Arabidopsis defence responses. Leaves of Col WT (D, E, F) and a myosin knock-out line 403 F GABI-CAT (A, B, C) were inoculated with *Bgh* spores and stained for fungal structures and callose after 2 days. A, D, fungal structures on leaf surface; B, C, callose deposition in epidermis (B, E, F) and mesophyll (C). Bar corresponds to 20  $\mu$ m.

### 3.6.2 Host resistance

*Pseudomonas syringae* pv. *tomato* DC3000 (*Pst*) is a virulent pathogen that causes disease on tomato and *A. thaliana*. The strain DC3000 is known for its race specific incompatible interaction (plant resistant) on the *A. thaliana* ecotype Col0. The identified myosin knock-out lines were also tested with DC3000. As a control for susceptibility the *A. thaliana* mutant line EDS1 was used. The plants were infiltrated with *Pseudomonas syringae* pv. *tomato* DC3000 and disease symptoms were analyzed at 5 days after inoculation. The knock out lines N518 (At5g20490), 754 (At1g08730) and 594 (At4g33240) (Table 3.5.1) were showing significant differences (increased susceptibility) to Col-0 wild type plants (Fig 3.6.2).

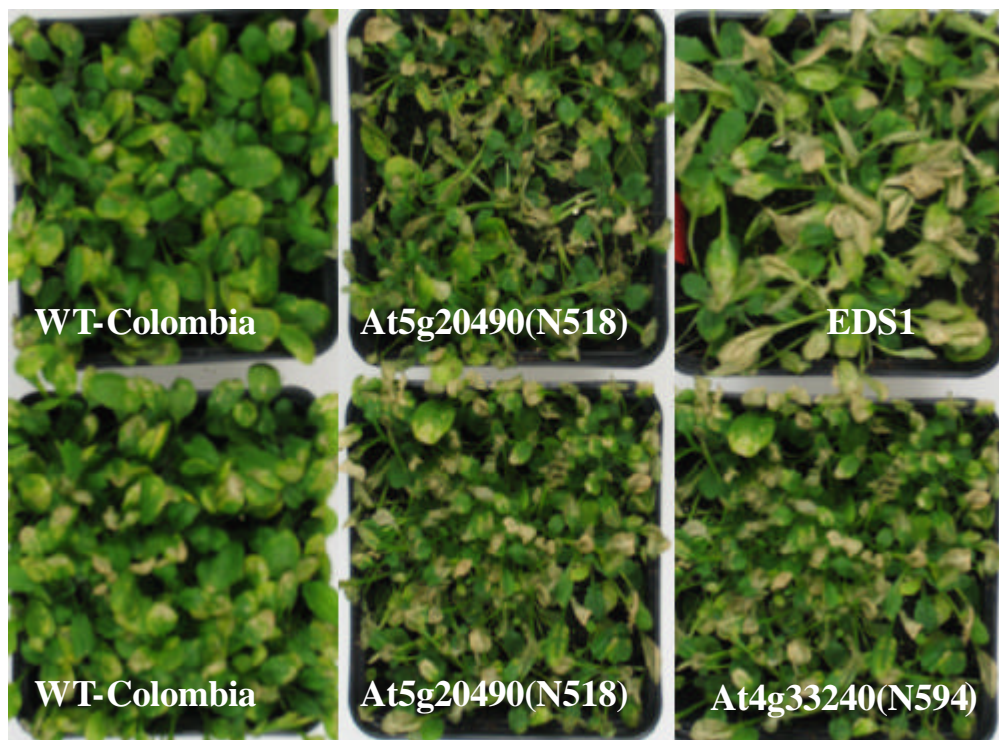


**Figure 3.6.2:** Class XI myosin knock out lines of *Arabidopsi thaliana* (lines 518, and 594 and control lines EDS1 and WT col-0) were examined for disease symptoms 5 days after inoculation.

### 3.6.3 Influence of BDM application on the defence response of barley

To obtain information about potential involvement of myosins in the defence response of barley plants, the inhibitor 2,3-Butanedione 2-Monoxime (BDM) was used in infection experiments with the fungal pathogen *Blumeria graminis* f. sp. *hordei* (*Bgh*, powdery mildew of barley). For these experiments barley plants carrying the broad-spectrum *Mlo*-resistance against *Bgh* have been selected. The resistance response of such plants essentially consists of papilla formation. Adverse effects of the inhibitor on fungal germination and development of infection structures was minimized by application of the inhibitor via the transpiration stream. Leaves of 7 d old barley plants were cut and put with their base into reaction tubes filled with BDM solution. These samples were incubated overnight within a growth chamber under intense airflow to force uptake of the inhibitor into the entire tissue. Subsequently the leaves were taken out of the solution and inoculated with fungal spores. After 24 h of infection the leaves were stained for visualization of fungal germlings and papilla and microscopically inspected. Statistic evaluation revealed a strong impact of BDM on papilla formation. With increasing concentrations of BDM in the reaction tubes the number of papilla drastically decreased. Effective concentrations were 20 – 30 mM BDM which reduced papilla formation up to 80 % (Fig 3.6.3). Interestingly, this inhibition of papilla formation was a transient effect and could not be observed anymore after 48 h of infection. We have tried to avoid inhibition of fungal functions during its growth on the leaf surface by application of BDM via the transpiration stream, however, BDM also affected the fungal development and no increase in haustoria development after application n 30 and 35 mM BDM was observed.

Probably, uptake of BDM by the fungus occurred directly after penetration of the plant cell wall and inhibited further growth and development of infection structures.

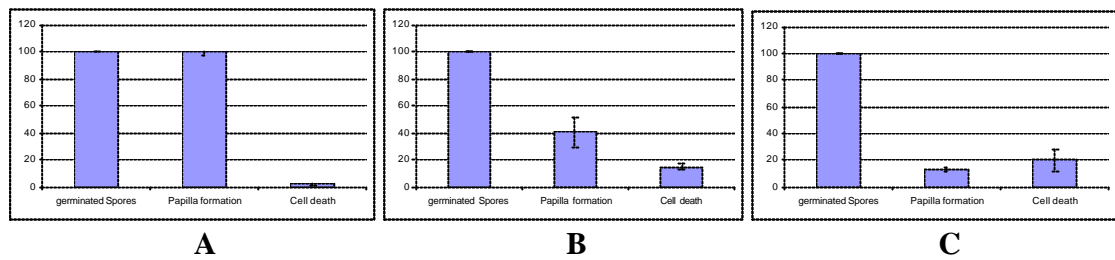


**Fig 3.6.3:** Statistic analysis of defence responses in barley epidermal leaves (*mlo3*) after application of 0 (A), 20 (B) and 30 (C) mM BDM. Leaves of *mlo3* plants were inoculated with spores of *Bgh* and stained for fungus and callose after 2 days.

### 3.7 Effects of BDM on the subcellular localization of the AtMya1 DIL domain

The specificity of the inhibitory effects of BDM on myosin functions was tested by an additional control experiment. Previous *in vivo* studies indicated that the DIL domain of AtMYA1 is labeling Golgi stacks/vesicles (Fig 3.1.2). In this experiment different concentrations of BDM including 0, 20, 25 and 30 mM were infiltrated into leaves of *N. benthamiana* that were expressing the AtMya1 DIL domain fused to YFP. In control plants without BDM treatment expressing transiently the AtMya1 DIL domain, the vesicles were moving rapidly within the cytoplasm (Fig 3.7.A). However, at concentrations of 10-30 mM, the BDM treatment disrupted the normal subcellular distribution and dynamic behavior of the AtMya1DIL domain labeled Golgi stacks/vesicles at 10 h after application in a dose-dependent

manner. The vesicle labeling was drastically changing; large, non-motile vesicles were observed in addition to diffuse labeling throughout the cytoplasm (Fig 3.7 B-C). This inhibition of vesicle dynamics was a transient effect and could not be observed anymore after 24 h of application of BDM.

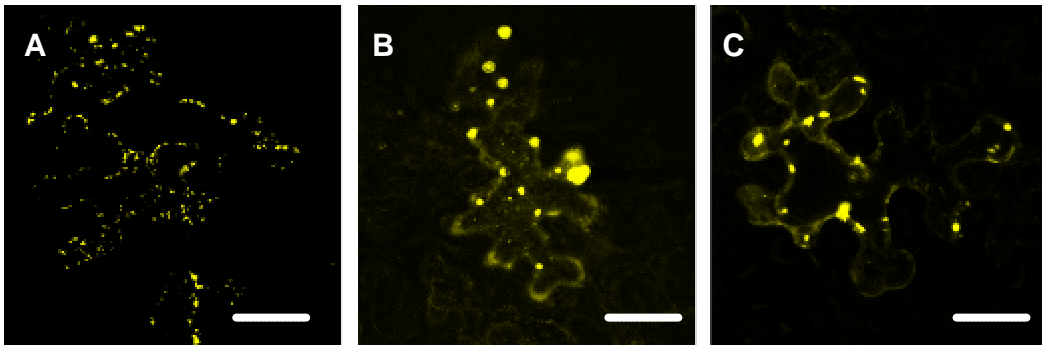


**Fig 3.7:** Effects of 20 mM BDM on class XI myosin distributions in *N.benthamiana* epidermis cells in control (A) and treated cells (B, C) 10 h after BDM application. Bar, corresponds to 30, 20 and 20  $\mu\text{m}$  in A, B and C respectively.

### 3.8 Expression studies of barley myosins

An alternative experimental system for transient expression of proteins and investigation of their subcellular targeting that is well established in our institute is biolistic transformation of barley leaves. Thus, this system was employed to test whether the subcellular targeting of barley myosins gives similar results as the *A. thaliana* myosins. Based on sequence homology with available myosin gene sequences from *A. thaliana* and *Oryza sativa*, the EST database from Barley (IPK Gatersleben) was searched for identification of putative barley myosins. The most significant EST clones showing homology to plant myosins, provided by P. Schweizer, IPK

Gatersleben, were sequenced. It turned out that a number of them covered larger parts or even the complete myosin tail domains. In addition a cDNA library from barley leaf epidermis cells (H. Giese, RNL Roskilde) was screened with a mixture of the EST cDNAs as probes to find additional myosin sequences. The identified and isolated barley myosin gene sequences are listed in Table 3.8.1

<b>Origin (EST or cDNA)</b>	<b>Class</b>	<b>Length (amino acids)</b>
EST (HS17P01)	VIII	800
EST (H V08K01)	VIII	400
cDNA library(41I08)	VIII	500(complete tail)
EST (HX 09A01)	VIII	450
EST (HM11G03)	XI	800
EST (HD01p02)	XI	1000 (complete tail)
EST (HF13O06)	XI	1200 (complete tail)
EST (HO15I 09)	XI	1000
EST (HO02F16)	XI	1400
cDNA library (30p13)	XI	800 (complete tail)
cDNA library (31N06)	XI	1000 (complete tail)
cDNA library (77A01)	XI	200

**Table 3.8.1:** Barley myosin genes that have been identified from EST database and screening of a cDNA library.

### 3.8.1 Subcellular localization of myosins from barley

For the identified myosin cDNAs HF13O06 and 77A01 (see Table 3.8.1) coding for class XI myosins N-terminal translational fusion constructs coding for the DIL domain fused to YFP under control of the ubiquitin promoter as a constitutive strong promoter were generated. These constructs were transiently expressed in barley epidermal cells after biolistic transformation. The localization of the YFP-fusion proteins was studied by confocal laser scanning microscopy. They targeted to small, fast moving vesicles (Fig 3.8.1 A and B).

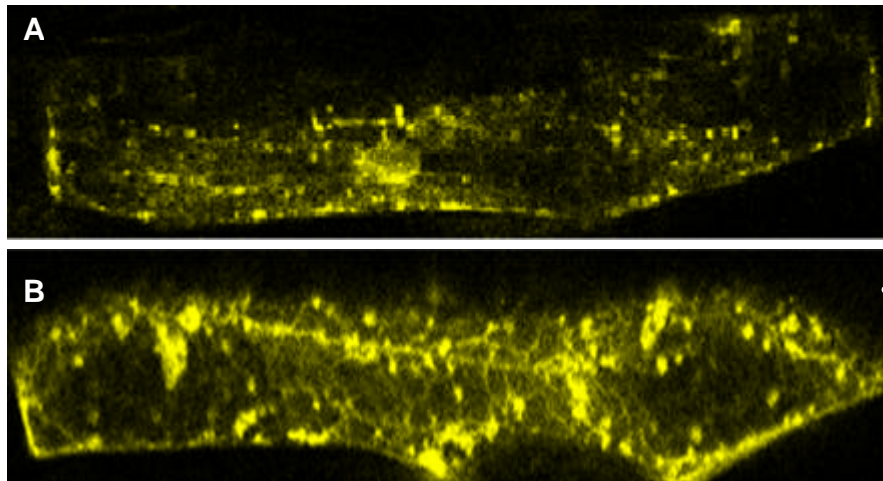


**Fig 3.8.1:** Localization of YFP-tagged DIL domains of barley class XI myosin in living barley epidermal cells after biolistic transformation. DIL domain of identified barley class XI myosins HF13O06 (A) and 77A01 (B) (Table 3.8.1) has been used for transient expression in living barley epidermal cells. Bar, 10  $\mu$ m.

Interestingly, when the barley class XI myosin cDNA HM11G03 which is coding for a C terminal part of the myosin class XI tail domain including the DIL domain was transiently expressed in the *N. benthamiana* assay, it could be clearly shown by co-localization experiments, that peroxisomes were labeled (Fig 3.8.2).

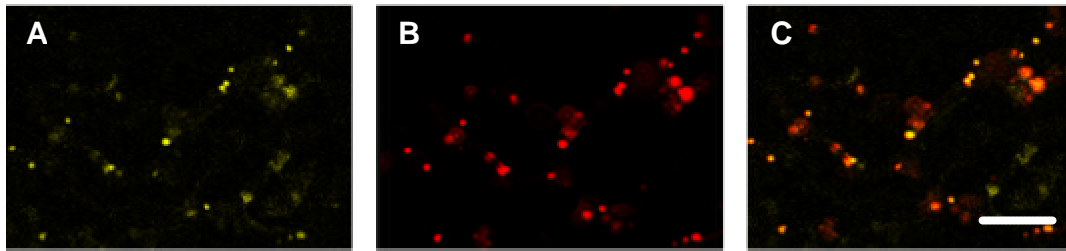


**Figure 3.8.2:** YFP-tagged C terminal part of globular tail domain of the Barley class XI myosin HM11G03 (A) (Table 3.8.1) has been used for transient expression in *Nicotiana benthamiana*. Plasmid construct appropriate for the fluorescent tagging of peroxisomes with dsRed (B) was co-expressed. The observed co-localization is shown in C. Bar, is 20  $\mu\text{m}$ .

In contrast to the targeting of these barley myosin XI constructs the C terminal 261 a.a. of the tail domain of the identified class VIII myosin 41I08 (Table 3.8.1) fused N-terminally to YFP was resulting in labeling of the cytoplasm and nucleus (Fig 3.8.3).

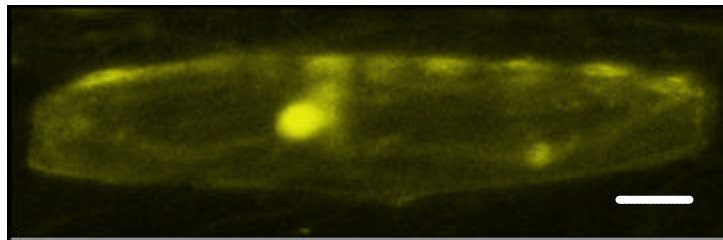


**Fig 3.8.3:** YFP-tagged 261 a.a. of C terminal tail domain of the identified barley class VIII myosin (LR4c) were used for transient expression in living barley epidermal cells after biolistic transformation. Bar, 10  $\mu\text{m}$

The transient expression experiments with myosin tail regions in barley showed that the transformation rates in comparison to *Agrobacterium* mediated transient expression in *N. benthamiana* were unusually low and the expression levels rather weak.

## 4 Discussion

### 4.1 Transient overexpression of myosin fluorescence protein (FP) fusions as assay system for the *in vivo* analysis of cargo binding sites

In this dissertation transient overexpression of selected *A. thaliana* myosins and a variety of respective subregions fused to fluorescent proteins as markers was applied for the microscopic *in vivo* investigation of their subcellular localization and potential binding capacity to cellular compartments or organelles. Two assay systems for transient expression of proteins are widely used: biolistic transformation (Sanford et al., 1987; Sanford, 1988) and *Agrobacterium tumefaciens*-mediated transformation of *Nicotiana benthamiana* leaf tissue (Zupan and Zambryski, 1997). As the method of choice the *A. tumefaciens* transformation of *N. benthamiana* was routinely employed in this dissertation for a number of reasons. Due to infiltration of bacteria into the leaves large tissue areas were transformed and showed considerable expression levels over several days. The expression was substantially improved concerning level and duration by employing co-expression of a virus-encoded suppressor of gene silencing, the p19 protein of tomato bushy stunt virus (TBSV), that prevents post-transcriptional gene silencing (PTGS) in the infiltrated tissues (Voinnet et al., 2003). With this, the expression levels were usually high. In rare cases of relatively low expressions, within the infiltrated area at least a number of individual cells or cell clusters in the epidermis possessed easily detectable amounts of fusion proteins. This turned out to be particularly important in

co-expression experiments where always cells could be found that were equally transformed with both constructs. In contrast, biolistic transformation of *A. thaliana* as well as barley leaves was much more troublesome especially with respect to our myosin constructs. Often transformation rates (i.e. number of cells displaying expression) and expression levels were very poor resulting in only very few cells per leaf that were worthwhile to be analyzed. Several of the cDNA myosin – FP – fusion constructs could even be never expressed. In addition the time window for expression was rather narrow, usually 1 – 1.5 days only. In co-expression experiments frequently only one of the fusion proteins or markers was detectable within a cell rendering it impossible to test for co-localization. Hence, many of the data presented in this thesis could be only obtained by using the *A. tumefaciens* mediated transformation of *N. benthamiana* leaves. However, it must be clearly taken into account, that the *A. thaliana* cDNA constructs were heterologously expressed in *N. benthamiana*. Thus, the possibility for miss-targeting of fusion proteins due to sequence differences between the two plant species can not be ruled out completely, although in all cases tested the subcellular localization data from the heterologous and homologous (biolistic transformation in *A. thaliana* and barley) expression of equivalent constructs was similar. For example, as shown in chapter 3.3 the transient over-expression of the AtMya1DIL domain and ATM2 tail fused N-terminally to YFP in epidermis cells of leaves of *A. thaliana* and *N. benthamiana* resulted exactly in the same pattern (Fig 3.3). Therefore, it might well be that presence of distinct binding sites for specific cargo in individual myosin molecules is a fundamental feature conserved among plant species. Several studies used

successfully the tobacco transient expression system as a heterologous system (Gallois and Marinho, 1995; Verdelhan Des Molles et al., 1999; Yamaguchi et al., 2005).

Transient expression is generally driven by a strong promoter, usually the 35S CMV promoter (Odell et al., 1985). For expression of the barley constructs the promoter of ubiquitin was used (Christensen et al., 1992). These strong promoters produce high amounts of the respective protein product which is certainly wanted on the one hand, but on the other hand can disturb the steady-state physiology of the cell or even tissue. This effect can actually be expected when a non-functional variant of a protein is expressed up to high levels in a cell and is known as dominant-negative effect (Reck-Peterson et al., 1999; Aschenbrenner et al., 2004). By interference with the function of the native, endogenous protein the whatever pathway, where the respective function is integrated, will be inhibited. Since in this work mostly domains and sub-domains of myosins were expressed not possessing the full molecular motor function, dominant negative effects certainly occurred for several constructs. Most probably this was the case for the various tail regions of the class VIII myosin ATM2 (see 3.2). As in this instance, emerging dominant negative effects can give clues for the function of the native protein. A possible consequence of overexpression can be mis-targeting (Gnanasambandam and Birch, 2004) or the development of vesicular deposits (Voigt et al., 2005). An example might be the vesicular accumulations of the ATM2 tail domains within the nuclei (see Fig 3.2.1.3). Another consequence of dominant negative or toxic effects might be the failure of expression of certain constructs if this is not due to improper transcription and translation and subsequent proteolytic

degradation. Results of this type are rarely described in the literature, but there are some examples (Waldo et al., 1999; Feilmeier et al., 2000). This might have happened with expression of the Mya1 full length protein (see 3.1.5). It is possible that the overexpression of the full length Mya1 protein caused a severe poisonous effect on the cells and was thus rapidly removed by proteolysis or even caused cell death. It has been shown in yeast that overexpression of the wild-type Myo2 globular tail (myosin class V) disrupts secretory-vesicle movement and causes cell death (Reck-Peterson et al., 1999).

*In vivo* imaging approaches bare other problems not directly related to overexpression but to employing of fluorescence protein tagging technology. The fusion proteins, in this dissertation myosin molecules or their domains and subdomains fused N- or C-terminally with YFP or other related fluorescent proteins, might suffer from misfolding or stereochemical hinderance as reviewed in (Hanson and Kohler, 2001). This might cause abolishment or masking of binding sites and loss of function.

Thus it might happen that a particular fusion protein is missing the correct subcellular targeting. Such an effect was for instance observed with the ATM2tail domain-CFP fusion protein, which did not show any binding preference, whereas its fusion to YFP clearly bound to vesicular structures (see 3.2.1). Similar problems might have arisen with some other myosin fusions for example the longer tail version of Mya1 (see 3.1.5).

Of course, subcellular localization of proteins and binding capacities to subcellular compartments, organelles or other proteins can be approached alternatively by immunocytochemistry, cell fractionation and biochemical

binding assays. However, these approaches do not offer the inestimable advantage of monitoring the *in vivo* situation. In particular for the investigation of molecular motors only the employment of living cells allows studying the dynamic aspects of movement of cargo. Furthermore there are quite a number of problems appearing related with the production of specific antibodies and disruption of tissue and cellular morphology.

An alternative for a transient transformation and expression assay is the generation and analysis of stably transformed plants. However, in this thesis multiple constructs coding for a systematic array of domains and sub-domains were screened for their subcellular localization and binding capabilities. Not only that the generation and analysis of transgenic plants for all these constructs would have been impossible within the available time, there would appear severe difficulties in connection with dominant negative effects and sufficiently high expression levels in microscopically accessible tissues (epidermis). Transgenic plants will certainly be valuable tools for further studies concerning physiological aspects, for instance endocytosis or plant defence responses.

Altogether, for the purpose of obtaining a survey of the subcellular localization, the dynamic behavior and the identification of cargo and its potential binding site(s) in myosin tails in this dissertation the transient overexpression assay including fluorescence protein tagging was the most appropriate tool. It is a combination of high resolution *in vivo* microscopy (confocal laser scanning microscopy), molecular biology and *in vivo* biochemistry (testing of binding domains). Such an integrated approach was so far not applied for plant myosin investigations, even in non-plant systems

there is only one publication using equivalent methodology (Lister et al., 2006). Most of the presently available data were generated by immunocytochemistry, genetics, or biochemistry (Grolig et al., 1988; Braun, 1996; Baluska et al., 2000; Wang and Pesacreta, 2004; Hashimoto et al., 2005; Hashimoto k and E, 2005).

#### **4.2 Systematic analysis of *A. thaliana* myosin class XI cargo binding sites**

As described in the results, by multiple alignments of the amino acid sequences of the tail domains of plant class XI myosins (which are equivalent to myosin V motors in non-plants), several conserved sequences were identified in the tail domain of these genes, the VEAk, DIL and LCP domain (see 3.1.1). Based on the sequence homology between these domains in the plant (*A. thaliana*) class XI myosins and the vacuole and secretory vesicle binding sites of the yeast class V myosin Myo2p (Schott et al., 1999; Catlett et al., 2000) we suggested that these identified conserved plant domains might have the capability to bind to vesicular structures. Additionally we proposed that the nature of vesicles associated with each of these domains might be different. Actually, the findings in this thesis show that the *A. thaliana* class XI myosin Mya1 (AT1g17580) might possess 2 distinct binding sites. These are subregions of the DIL domain, the KVFG domain at the N-terminal end and the LCP domain downstream at the C-terminal end of the DIL domain (Table 3.1.4, Fig 3.1.1 C). Remarkably, one of those, the KVFG domain is binding to Golgi stacks/vesicles, whereas the LCP domain is binding to peroxisomes (Table 3.1.4, Fig 3.1.2). In another

tested class XI myosin, Mya2, (AT5g43900) the LCP domain is also binding to peroxisomes (Fig 3.1.3.1). Thus, also because this domain is highly conserved among the class XI myosins, the LCP domain might represent a common peroxisome binding sequence so that class XI myosins could be redundant in the capability to transport these organelles. The second subregion of the DIL domain, the KVFG domain, was identified as Golgi stacks/vesicle binding sequence only in Mya1 (AT1g17580) by the experiments employing the INVQ segment (DIL domain missing the C-terminal 8 amino acids) and the segment bearing a single amino acid exchange (G to T) at position 4 from the C-terminal end of the DIL domain. These two mutated segments lost the binding capacity for Golgi stacks/vesicles (Fig 3.1.2.1). Interestingly, the DIL domains of 3 other class XI myosins, one representative of each subclass Mya2 and Mya4 and even the highly homologous isoform AT5g20490 of the same subclass (Mya1) localized to peroxisomes and not to Golgi stacks/vesicles (Fig 3.1.3.1 A-C). All these 3 candidates differed from Mya1 (AT1g17580) in the above mentioned G to T exchange in the C-terminal region. From these data one can conclude that the G and not T in this position is essential for Golgi stacks/vesicle binding. However, since there are other exchanges in this position (S, H, C; see Fig 3.1.1 B) in other myosins of class XI that were not tested, it remains open whether in this position only G is required for Golgi stacks/vesicle targeting.

It is an interesting question, why the two Mya1 DIL domain segments which are mutated in respect of the Golgi stacks/vesicle targeting KVFG sequence (deletion, single a.a. exchange) showed just cytoplasmic localization and were not binding to peroxisomes although they should still

possess an intact LCP domain. This might be related to the observation that Mya1 (AT1g17580) was the only myosin tested whose DIL domain was localizing to Golgi stacks/vesicles, the others were binding to peroxisomes. This preference of the Mya1 DIL domain for Golgi stacks/vesicles could be encoded by any of the subtle amino acid differences along the whole DIL domain sequence including the LCP domain that might be involved in modulation of the binding to peroxisomes. As was shown for the yeast class V myosin Myo2p, this could be achieved by regulated phosphorylation (Legesse-Miller et al., 2006). Further experiments using a series of respectively mutated DIL domain constructs might provide a solution to this problem.

For the VEAK domain, although among the class XI myosins there exist high homology in this region and in addition almost complete identity at exact 5 positions with the yeast myosin class V (Myo2p)(Fig 3.1.1 B), there was no specific vesicle or organelle binding observed, at least in the two examples tested (Fig 3.1.3.2). However, only the sequence stretch corresponding in length with the vacuole binding motif from the yeast myosin V was investigated. Since the homology of class XI myosins extends about 20 amino acids further downstream in this region it is possible that an accordingly longer construct would actually display binding capability.

From the data obtained in this thesis it can be concluded that the myosin class XI from plants fulfills important functions in organelle transport similar to myosin class V in animal and yeast cells. For Mya1(AT1g17580) two binding sites were identified whose specificity might be differentially regulated similar to the class V myosin Myo2p from yeast (Pashkova et al.,

2005). Because of the high sequence homology of these binding regions among class XI myosins this might be valid also for other members of class XI. A strong indication for this comes from the experiments with the barley class XI myosin tail constructs where in two examples also in this plant species vesicular targeting was found and, interestingly enough, the barley tail domain was colocalizing with peroxisomes when expressed in *N. benthamiana*. This shows that the respective binding motif might be conserved and works also in other plant species. From these data it can be postulated that there exist a certain degree of redundancy in class XI myosin functions and a tight regulation concerning organelle or vesicle binding specificity. Further regulation is taking place at the level of transcription. According to the RNA macroarray database (TAIR homepage) several members of *A. thaliana* class XI myosins show preferential expression in certain organs or tissues, as for instance in stamen and mature pollen (AT3g58160), in carpels and mature pollen (AT1g04160) or in mature pollen only (AT1g04600). Others are expressed throughout the whole plant as for instance AT1g17580 (Mya1) and AT4g33200 (Mya4).

### **4.3 *In planta* expression and localization of the yeast class V myosin (Myo2p) cargo binding domains**

As described above, the yeast class V myosin Myo2p was selected as model for the functional analysis of the plant class XI myosins. When the Myo2p DIL domain was transiently expressed in *N. benthamiana* leaves, surprisingly it colocalized with peroxisomes as most of the plant DIL

domains of the class XI myosins (Fig 3.1.4 A-C). However, for the Myo2p secretory binding motif (equivalent to the plant class XI LCP domain) and the Myo2p vacuole binding motif (plant class XI VEAK domain), only cytoplasmic localization was seen (Fig 3.1.4 D and E). Thus, the two yeast motives for specific organelle binding do not show any binding specificity *in planta* in contrast to the whole yeast DIL domain. Thus, the yeast DIL domain obviously contains in addition to the known secretory binding site another domain which has in plant cells the ability to specifically bind to peroxisomes. Because it was shown by mutant analysis that the myosin V (*myo2p*) locus is responsible for peroxisome movement and inheritance also in yeast (Hoepfner et al., 2001), the respective binding site localized within the DIL domain sequence might be functioning also in yeast.

#### **4.4 Subcellular localization of plant class VIII myosins**

On the basis of sequence homology of the full-length cDNAs, the *A. thaliana* class VIII myosin genes were grouped into two subclasses, ATM A and ATM B each with two members (Fig 3.2.1). The ATM B subclass was selected for the *in vivo* binding investigations in this dissertation because investigations have been performed already for one member (ATM1, AT1g19960) of the ATM A subclass by using immunocytology with antibodies against the tail domain. Thus the subcellular localization of this myosin is known (Reichelt et al., 1999).

In subclass ATM B, ATM2 was selected here for further analysis because of the observed lethality of the homozygous knock-out lines of ATM2

(AT5g54280). Since for the second member of the ATM B subgroup (AT4g27370) no EST so far has been reported. Therefore, in course of this thesis, investigations concentrated mostly on the subcellular localization and phenotypical analysis of AT5g54280 (ATM2). By application of the *in vivo* binding assay as described above, the capability of ATM2 full length, tail domain and subsegments of the ATM2 tail for binding to subcellular compartments, organelles and vesicular structures was analyzed (see 3.2.1 and Fig 3.2.1.2).

As described above in the results, the labeling patterns of the different constructs are looking somewhat diverse. The full length ATM2 was preferentially localizing to filaments, probably actin filaments, whereas the ATM2 tail showed vesicular localization (Fig 3.2.1.3). This could be explained by the different functionality of the head and tail domain. The head domain is responsible for force production and movement and binds to actin filaments, yet the tail domain binds to cargo. Assuming that the binding to actin filaments somehow prevails when the full length ATM2 is expressed this will result in the observed filament labeling. Expressing the tail only would reveal the cargo binding which were vesicular structures (Fig 3.2.1.3). Interestingly, for the different tail domain constructs binding to apparently different vesicle populations was detected. The N-terminal YFP-fusion labeled small, densely packed, immotile vesicles throughout the entire cell periphery (Fig 3.2.1.3.1), while the C-terminal YFP-fusion decorated immotile small vesicles along filaments like beads on a string (Fig 3.2.1.3 D). The shorter tail domain (a.a. 816-1030) surprisingly was found on motile vesicles (Fig 3.2.1.3 F). However, in coexpression experiments these different patterns converged. Coexpression of the N and C-terminal

tail FP-fusions resulted in colocalization as well as coexpression of the C-terminal FP-fusion of the tail and the shorter tail domain (816-1030) (Fig 3.2.1.4). This observation of colocalization suggests that the tail domain of ATM2 probably possesses binding capability to one vesicular cargo only. The different localization of the three constructs might be due to dominant negative blocking of a vesicular transport pathway at slightly different positions. This would interrupt the native vesicular flow and vesicles would accumulate at certain stages resulting in the observed labeling patterns.

The respective binding region should reside in the C terminal part of the ATM2 tail between a.a. residues 816-1030. This is supported by the filamentous localization of the construct comprising the N-terminal half of ATM2 including the head domain but missing exactly this C-terminal tail region (Fig 3.2.1.3). Strikingly, a 160 amino acid stretch within this subsegment ATM2-816 is showing high homology (E.value=0.008) with a domain of the tumor susceptibility 101 protein (*Tsg101*). The *Tsg101* gene encodes a 43 kDa protein containing a coiled-coil domain, a proline-rich region and an N-terminal domain with homology to ubiquitin-conjugating enzymes (Ponting et al., 1997). Among various biological functions of *Tsg101* including a role in ubiquitination (Koonin and Abagyan, 1997; Ponting et al., 1997), transcriptional regulation (Watanabe et al., 1998) and cell proliferation (Xie et al., 1998; Zhong et al., 1998), it is, most importantly, involved in endosomal trafficking (Babst et al., 2000; Garrus et al., 2001). Because of this remarkable homology of part of the ATM2 tail and the observation in this dissertation that ATM2 tail-labeled vesicles partially colocalized with endosomes (Fig 3.2.1.5) and never with any of the other tested organelles and vesicles (Golgi stacks/vesicles, peroxisomes,

mitochondria; Fig 3.2.1.6), it is postulated that ATM2 participates in endocytosis. Baluska et al. (2004) suggested already class VIII myosins as candidate motors for endocytosis in plant cells because class VIII myosins appear to be the only plant myosins that are localized in the cell periphery in contrast to the cytoplasmic distribution of class XI myosins. Furthermore, results from pharmacological studies implicate a role for myosins in endocytosis of plants (Baluska et al., 2004; Samaj et al., 2005). In animal cells myosin VI has an important function, it is binding to early endosomes just after clathrin uncoating and facilitates further transportation and through the endocytotic pathway (Morris et al., 2002; Aschenbrenner et al., 2004). Overexpression of the tail domain causes a severe dominant negative inhibition of this pathway; the uncoated early endosomes are not processed further and accumulate in the cell periphery. This strongly resembles the picture after overexpression of the ATM2 tail- N- terminal YFP – fusion in *N. benthamiana* and in *A. thaliana* cells (see results, Fig 3.2.1.3 E, Fig 3.2.1.3.1 A and Fig 3.3 F). Interestingly, myosin VI is the only myosin that moves into the minus end direction of actin filaments, opposite to all other myosins. The structural features, essentially two characteristic inserts within the amino acid sequence (Wells et al., 1999), enabling this directionality are however missing in ATM2.

Surprisingly, the tail domain of ATM2 was found also in the nucleus in larger vesicular structures (Fig 3.2.1.3 C). These vesicles might represent a sort of deposits due to overexpression of the fusion protein of ATM2tail; however the specific localization in the nucleus might indicate a specific function for ATM2. It has been shown that actin is also present in nucleus (Prat and Cantiello, 1996; Rando et al., 2000; Gettemans et al., 2005).

Recently, it was demonstrated that an isoform of myosin I is localized in the nucleus of mouse cells and colocalizes with RNA polymerase II in an alpha-amanitin- and actinomycin D-sensitive manner (Pestic-Dragovich et al., 2000). Antibodies specific for this myosin coimmunoprecipitated RNA polymerase II and blocked *in vitro* RNA synthesis. Based on these observations the authors suggested that this isoform of myosin I appears to form a complex with RNA polymerase II and may participate in transcription (Pestic-Dragovich et al., 2000).

ATM1, the tested member of the other Myosin VIII subgroup (ATMA) in this thesis, displayed strict association with the plasma membrane (Fig 3.2.2). This result is in agreement with previous data (Reichelt et al., 1999) based on immunofluorescence and immunoelectron microscopy using an anti-ATM1 antibody. The authors could show that the ATM1 is concentrated along the plasma membrane at newly forming transverse cell walls. This suggested that ATM1 may have some role in the phragmoplast and the formation of new cell walls. Hence, this totally different subcellular localization of the members of the two myosin VIII subgroups indicates that they might have different functions in plant cells.

## **4.5 Functions of plant myosins in subcellular transport**

### **4.5.1 Class XI myosins**

As described above systematic mapping of organelle specific binding regions in the tail domain of class XI myosins have shown that specific binding sites for Golgi vesicles and peroxisomes reside within the C-terminal part. These data also demonstrate that small sequence changes can lead to binding to different cargo; however these binding sequences appear to be conserved enough to function similarly in a heterologous plant. In summary one can postulate that the C-terminal tail domain of class XI myosins bears probably multiple binding sites each for distinct cargo. These binding sites would interact with organelle/vesicle-specific receptors. Receptor-regulatory proteins could then facilitate the temporal and spatial regulation of transport (Karcher et al., 2002; Ishikawa et al., 2003). This view agrees well with the current model for the function of class V myosins in animal and yeast (Pruyne et al., 2004; Futter, 2006; Weisman, 2006).

#### **4.5.1.1 Transportation of Peroxisomes**

Plant peroxisomes are subdivided into three different classes in higher plants: glyoxysomes, leaf peroxisomes and unspecialized peroxisomes (Beevers, 1979). They have been extensively studied and some of their functions are fatty-acid  $\beta$ -oxidation, photorespiration, peroxisomal biogenesis (Hayashi and Nishimur, 2003), biogenesis of ER-derived proteins and oil bodies (Lin et al., 1999) and more recently involvement in plant-pathogen interactions (Lipka et al., 2005). Using the peroxisome-targeting signal (PTS) fused to GFP, four groups independently discovered

that peroxisomes move actively in various cell types of *A. thaliana* (Jedd and Chua, 2002; Mano et al., 2002) and also in epidermal cells of onion (Mathur et al., 2002) or leek (Collings et al., 2002). The motility of peroxisomes can differ according to the plant cell-types including slow or rapid directional movement, random oscillations or stop-and-go movements (Collings et al., 2002; Jedd and Chua, 2002; Mano et al., 2002; Mathur et al., 2002). Furthermore, pharmacological studies using an actin-depolymerizing drug (Latrunculin-B) and an inhibitor of myosin activity (2,3-butanedione monoxime; BDM), have indicated that the actin–myosin system is involved in the movement of peroxisomes in plant cells (Jedd and Chua, 2002; Mano et al., 2002). In contrast, studies on peroxisomal motility in animal cells have demonstrated microtubules as the preferred tracks for peroxisome movement (Rapp et al., 1996; Schrader et al., 1996; Wiemer et al., 1997). In this thesis, colocalization of five different isoforms of the *A. thaliana* class XI myosins with peroxisomes was observed (Table 3.1.3). Importantly, the presented results here indicate an important role for the DIL/LCP domain of class XI myosins in this process. As described in the results, all these five isoforms were selected as representatives for each subclass of class XI myosins and, strikingly, in all these molecules the peroxisome binding site resided in the DIL domain or LCP domain as a part of the DIL domain. Hashimoto et al., (2005) used an affinity-purified antibody raised against MYA2 (AT5g43900) for immunolocalization studies. These experiments showed punctate signals which mostly colocalized with actin filaments in leaf epidermal cells, root hair cells and suspension-cultured cells, and some relatively large sized signals overlapped with GFP-labeled peroxisomes in leaf epidermal cells and guard cells. The

nature of the fine dots is to date unclear. These data obtained by a completely different method are in agreement with the *in vivo* observations in this dissertation and support the view that Mya2 (AT5g43900) transports peroxisomes.

#### **4.5.1.2 Transportation of Golgi stacks/vesicles**

In contrast to the highly ordered Golgi complex in animal cells (Rambourg and Clermont, 1997) the Golgi apparatus of plant cells consists of a large number of small, independent stack-trans-Golgi network units (TGN) (Nebenfuhr et al., 1999). The stacks and/or vesicles are moving around the cytoplasm (Boevink et al., 1998; Nebenfuhr et al., 1999). Pharmacological studies showed that the movement of the Golgi stacks in plant cells is along actin filaments instead of microtubules (Boevink et al., 1998; Nebenfuhr et al., 1999). In this thesis a fusion protein of the transmembrane domain of a rat sialyl transferase (STtmd) with Cyan fluorescence protein (CFP) has been used for visualization of Golgi stacks in *N.Benthamiana* epidermis cells of leaves. It was reported that the GFP-fusion protein decorates Golgi stacks in plant cells (Boevink et al., 1998).

The results presented here show for the first time the association of an *A. thaliana* class XI myosin (Mya1) with Golgi stacks/vesicles. This strongly indicates that myosins XI are the motors that transport Golgi stacks/vesicles in plant cells. Surprisingly, Mya1 (AT1g17580) was the only class XI myosin among the tested class XI myosins from *A. thaliana* that showed colocalization with Golgi stacks in this study. Phenotypic analysis of Mya1 (AT1g17580) homozygous knock-out lines did not show any drastic effects in growth and development (see 3.5.2). This rather speaks for some

redundancy in the function of Golgi stack transportation by class XI myosins. This discrepancy could be explained by the fact, that not all of the class XI myosins were tested in this work and that the nature of the regulation of cargo binding might be highly complex. Interestingly, immunofluorescent studies recently showed that an isoform of the *A. thaliana* kinesin family (AtKinesin-13A) localized to entire Golgi stacks. Although in both wild-type and *kinesin-13a* mutant cells (knock-out), the Golgi stacks were frequently associated with microtubules as well as with actin microfilaments. However, aggregation/clustering of Golgi stacks were often observed in the *kinesin-13a* mutant trichomes and other epidermal cells. This was unexpected because previous pharmacological studies indicated that only actin filaments are involved in Golgi stack translocation. The authors suggested that the distribution of the Golgi apparatus in the cell cortex might require microtubules and kinesin-13A (Lu et al., 2005). There are several indications in animal cells that there is a co-operation between actin filament and microtubule based motor proteins for the transport of membranous organelles. A model proposes that organelles involve both myosin and microtubule motor proteins allowing them to be associated with actin filaments as well as with microtubules (Allan and Schroer, 1999; Brown, 1999).

Thus, based on this model, in plant cells Mya1 could play a role in driving long distance transport of Golgi stacks, and kinesin-13A may mediate local dispersal of the stacks (Fig 4.1).

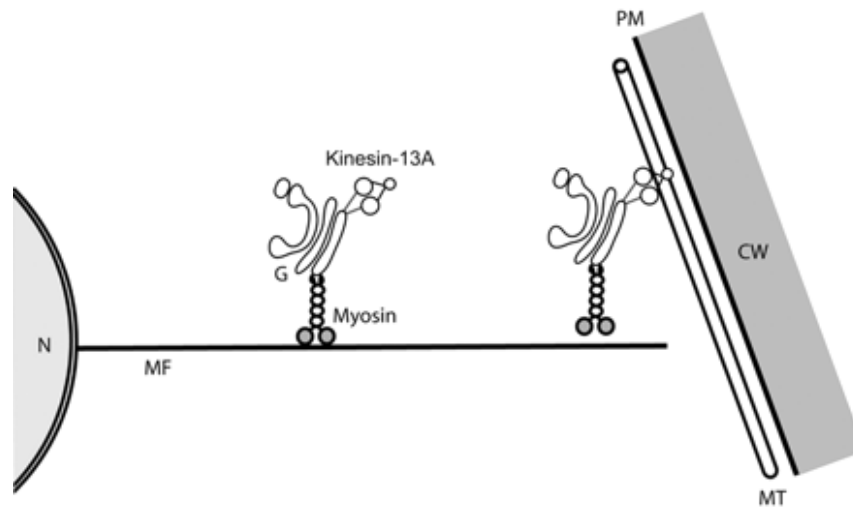


**Figure 4.1:** Proposed model for Myo1 and Kinesin-13A functions in plant cells. The plant Golgi apparatus is associated with Myo1 and Kinesin-13A. It has been suggested that from the perinuclear region to the cell cortex, the motility of Golgi stacks depends on Myo1. In the cell cortex, Kinesin-13A plays a role in either the dispersal of the Golgi apparatus along cortical microtubules. CW, cell wall; G, Golgi apparatus; MF, actin microfilaments; MT, microtubules; N, nucleus (Proposed model from Ling et al. 2005).

#### 4.5.1.3 Motility of mitochondria and endoplasmic reticulum (ER) in plant cells

In addition to the above described plant specific features of Golgi stacks and peroxisomes, the movement of higher plant mitochondria is also different from yeast or animals and dependent on actin filaments but not microtubules (Quader and Schnepf, 1989; Hawes and Satiat-Jeunemaitre, 2001; Van Gestel et al., 2002). Evidence is coming mostly from pharmacological studies demonstrating that mitochondrial transport in plant cells needs intact F-actin and is myosin based (Quader and Schnepf, 1989; Van Gestel et al.,

2002). More recently, immunofluorescence studies in maize showed that an isoform of class XI myosins is localized on mitochondria (Wang and Pesacreta, 2004). Furthermore, one of the major characteristic features of the plant secretory system is the mobility of the ER. Several pharmacological studies were showing that actomyosin complexes, but not the microtubule cytoskeleton, are responsible for endocellular movements of ER elements in higher plant cells (Quader et al., 1987; Kachar and Reese, 1988; Quader and Schnepf, 1989; Knebel et al., 1990; Liebe and Menzel, 1995; Runions et al., 2006). Actin-disrupting drugs also prevent the ER from further remodeling (Runions et al., 2006) confirming previous indications of a connection between the ER and the actin–myosin system (Volkman and Baluska, 1999). So far there is no direct evidence for this and during this study, no colocalization of mitochondria and ER with the tested class XI myosins has been observed. It is certainly possible, that in this dissertation, binding sites have been overlooked or have not been recognized, because not all parts of the class XI tail regions were subjected to a detailed fine mapping and not all members of the class XI were investigated.

#### 4.5.2 Class VIII myosins

The functions of the members of class VIII myosins are probably quite diverse. According to immunocytological investigations ATM1 might have a role within the phragmoplast by being involved in formation of the new cell wall and the positioning of plasmodesmata (Reichelt et al., 1999). In this thesis an ATM1 tail construct was labeling in particular the entire plasma membrane and was never found in any vesicular structures (see Fig 3.2.2). This indicates a function which requires intimate association with the plasma membrane rather than transport of vesicles or organelles. The other myosin class VIII member investigated in this work, ATM2, displayed a completely different subcellular localization. It was labeling always vesicular structures. Although the pattern was varying with respect to the type of tail construct (full length protein, N- or C-terminal FP-fusion, shorter tail version) these vesicles were clearly related as was shown by colocalization in the coexpression experiments. Furthermore, at least one of the tail fusion proteins (N-terminal YFP fusion) displayed partial colocalization with an RFP-fluorescent marker of early endosomes (FYVE). Remarkably, this colocalization was seen in cells showing lower expression levels of both the ATM2 tail and the endosomal marker (Fig 3.2.1.5). These vesicles carrying both tags (ATM2 tail-YFP and RFP-FYVE) were small and rapidly moving. They could be clearly distinguished from late endosomes, as for instance multivesicular bodies, which were also labelled by the FYVE-RFP-tag in the *N. benthamiana* cells. In further studies with tagged mitochondria, Golgi stacks and peroxisomes absolutely no colocalization was observed with ATM2 tail constructs. Finally, the pattern

of vesicles labelled by the overexpressed N-terminal YFP ATM2 tail fusion is similar to the one obtained after overexpression of an equivalent tail construct of the animal myosin VI in mouse cells (Aschenbrenner et al., 2004). Myosin VI is known to play an important role in endocytosis of mammals. Research on endosomal trafficking in plants is far behind that which is known in animals and yeast. The occurrence of endocytotic processes in plants has been discovered only recently (Baluska et al., 2002; Geldner et al., 2003; Murphy et al., 2005; Robatzek et al., 2006). From this it became clear that in plants, as in animals and yeast, membrane proteins as receptors and receptor like kinases are internalized. Thus, in analogy to the concept of endocytosis in animals and yeast, also in plants regulated vesicle trafficking to and from the surface probably controls the levels and activities of receptors, transporters and other plasma membrane proteins. This analogy could hold true also for the involvement of myosin in early endocytosis. Accordingly, ATM2 could bind to early endosomes and mediate transportation through the endocytic pathway. However, two of the observations made in the course of the ATM2 studies are puzzling. First, in coexpression experiments of the ATM2 tail with the marker Ara6, which is known to bind to early plant endosomes (Ueda et al., 2001), no colocalization was found. Second, in coexpression experiments with the FYVE-marker, partial colocalization was found in cells with lower expression levels, but in cells with high expression levels there was neither a change in the pattern of the FYVE marker nor in the pattern of the ATM2 tail as compared to the pattern in cells expression just one of the two constructs. Thus, there was no obvious change or disturbance of the endocytotic dynamics by overexpression and, hence, of the ATM2 tail. This

suggests that overexpression of the ATM2 tail does not necessarily lead to complete dominant negative blocking of the endocytic pathway. Another explanation for the lack of a total endocytic block is that an alternative way for endocytic vesicle movement may be activated. This movement could be microtubule based or involve other myosin motors, thereby allowing endocytosis to proceed.

## **4.6 Potential myosin interacting proteins**

### **4.6.1 Myosin class XI**

Two interesting putative binding proteins were found by yeast two-hybrid screening employing the Mya1 DIL domain as bait (see 3.4.1). The first one, At4g15620 exhibits the characteristics of an integral membrane protein (The Arabidopsis Information Resource, TAIR). It has 190 amino acids and is predicted to contain 4 membrane-spanning regions (amino acids 29-48, 80-102, 122-144 and 165-187). The colocalization studies showed Golgi stack association (Fig 3.4.1). However, more detailed experiments are needed to explore the nature of interaction of this integral membrane protein with Golgi stacks and potentially Mya1 (AT1g17580). There is the possibility that this integral membrane protein acts as a Mya1 receptor either directly or indirectly. It is known that class V myosins attach to their cargoes by interacting with adaptor molecules on the surface of a target organelle. Only three such receptors have been characterized: melanophilin on melanosomes (Wu et al., 2002), Vac17p on yeast vacuoles (Ishikawa et al., 2003) and recently Inp2p on peroxisomes (Fagarasanu et al., 2006). It has been shown

that Inp2p is a peroxisomal membrane protein that interacts directly with the cargo binding globular tail of Myo2p and is essential for the segregation of peroxisomes to growing buds (Fagarasanu et al., 2006). This distinguishes this protein from the two other myosin V receptors, melanophilin and Vac17p, which are peripheral membrane proteins that require an additional membrane protein to mediate their attachment to the organelle membrane (Wu et al., 2002; Tang et al., 2003).

The second interesting candidate for a putative Mya1 interacting protein, At3g49720, contains a START domain. The steroidogenic acute regulatory protein (StaAR) – related lipid transfer (START) domain is a protein domain spanning 210 residues. It is conserved throughout plants and animals and serves as a versatile binding interface for lipids that function in many different processes (Soccio and Breslow, 2003; Schrick et al., 2004). This domain is absent from yeast and archaea but found in some protists and bacteria. In plants, the START domain is more common than in animals and is often found in homeodomain transcription factors (Schrick et al., 2004). The identity of the lipids that bind each START domain is known for only a few members of the family, however recent work has implicated START proteins in the control of several aspects of lipid biology, including lipid trafficking, lipid metabolism and cell signaling reviewed by (Alpy and Tomasetto, 2005). The colocalization of the full length protein with Golgi stacks (Fig 3.4.1) might imply the potential interaction with Mya1.

#### 4.6.2 Myosin class VIII

Using the ATM2 tail domain as bait, the *pas2* tyrosine phosphatase was found in the yeast 2 hybrid screening as interesting candidate for interactions (see 3.4.2). The *pas* mutants were isolated in a screen for uncontrolled growth in presence of cytokines, resulting in cell proliferation and callus formation. *Pas* mutants had an altered development leading to abnormal leaf and root morphology (Faure et al., 1998). The subcellular localization experiments showed labeling of vesicular structures with different size and possibly endoplasmic reticulum (Fig 3.4.2). However, in a preliminary experiment colocalization with the ATM2 tail was not observed.

The fact that the most characteristic feature of myosin VIII sequences is their unique C-terminus that contains several phosphorylation sites (Baluska et al., 2001) including one highly conserved tyrosin. This might hint to PAS2 as interacting partner for the ATM2 functioning in regulation by phosphorylating this residue. In animal cells it has been shown recently that myosin is an *in vivo* substrate of the protein tyrosine phosphatase SHP-1 (Baba et al., 2003). The authors demonstrated that cytoskeletal molecules such as myosin and actin are phosphorylated and dephosphorylated by SHP-1. They postulate that dephosphorylation of actin/myosin by SHP-1 may play a critical role in the mechanism(s) involved in signal transduction and cytoskeleton reorganization.

## 4.7 Analysis of myosin knock out lines

Gene knock-outs, or null mutations, are providing a direct tool to determine the function of a gene product *in vivo*. Most other approaches to analyze gene function are correlative and do not necessarily prove a causal relationship between gene sequence and function (Bouche and Bouchenz, 2001). The use of knock-out lines for class VIII and XI myosin genes in the *A. thaliana* data base facilitates the investigation of the complex plant myosin function by analysis of phenotypes. Considering that actin is utilized by myosin for motility, it was assumed that the possible functions of myosins in plants are closely linked to the functions of actin. The actin cytoskeleton has been shown to be involved in many processes in plants including transportation, signaling, cell division, cytoplasmic streaming, morphogenesis and plant defence response (Williamson, 1986; Volkmann and Baluska, 1999; Volkmann D, 1999).

### 4.7.1 Class XI myosins

Phenotypic characterization of class XI homozygous knock-out lines revealed no drastic effects with respect to growth and development (see 3.5.2). Only various degrees of stunted growth and changes in seed morphology have been observed (Fig 3.5.1B and C). The absence of drastic phenotypic effects in the characterized myosin knock-out lines could be due to different reasons. Functional redundancy among the members of the class XI myosin genes is a likely reason. This is supported by several studies in non-plant cells where mutations in a single myosin isoform generally show no or only mild phenotypes. For example, *Dictyostelium discoideum* cells

lacking one member of the myosin class I show no or weak phenotypic defects, indicative of functional redundancy among myosin I isoforms (Ostap and Pollard, 1996; Falk et al., 2003).

Another possible reason for the lack of drastic phenotypes for single member knock-outs of class XI myosins is that individual members of class XI may function only under specific physiological conditions. Thus, unless the mutant plant is placed under a condition in which the target gene is required, no phenotype is observed (Hirsch et al., 1998). To test for conditional phenotypes in a gene of unknown function, one must employ a broad panel of physiologically meaningful conditions. In contrast to the findings for *Mya2* knock-out lines in this thesis, recently Holweg and Nick, (2004) reported that a T-DNA insertion in the 29<sup>th</sup> intron (*mya2-1* allele) or in the 30<sup>th</sup> exon (*mya2-2* allele) of *Mya2* causes pleiotropic defects, including dwarf growth and sterility (Holweg and Nick, 2004). The *mya2-2* homozygote was reported by these authors to be lethal. However, in contrast, Hashimoto et al., (2005) reported that their T-DNA insertion line for *Mya2* did not show any obvious morphological and developmental abnormalities. In this dissertation the analysis of two different *Mya2* knock out lines clearly confirmed the results obtained by Hashimoto et al., (2005). In class XI myosin knock-out lines for the *At1g04160* and *At1g17580*, the only visible mutant phenotype was a defect in seed morphology (Fig 3.5.1 C). In future experiments these lines can be used for the production of double or triple mutant lines. Such lines should show stronger phenotypes and could be employed for the investigation of pathogen resistance or other morphogenetic or developmental traits.

#### **4.7.2 Class VIII myosins**

No obvious phenotype was found for the ATM1 homozygous knock-out lines. In contrast, homozygous plants could never be identified in two ATM2 knock-out lines (SALK-104355 and SALK-052429). The segregation pattern in the progeny of ATM2 heterozygous plants was examined. If the ATM2 homozygous knock-out is lethal, one quarter of the progeny from heterozygous plants will not grow ( $Aa \times Aa \rightarrow 1/4AA:1/2AA:1/4aa$ ), another quarter should exhibit WT phenotype and half of the progeny will be heterozygous plants. The numbers of 138/533 and 60/221 non-germinated seeds counted from heterozygous plants of the SALK-104355 and SALK-052429 lines, respectively, indicate that most probably the ATM2 homozygous knock-out is lethal. Further analysis indicated that the ATM2 heterozygous lines are showing severe developmental defects under sucrose limitation (Fig 3.5.3 A). Recently it has been shown that uptake and accumulation of external solutes into the storage vacuole of heterotrophic cultured cells are largely mediated by an endocytic mechanism which is induced by sucrose (Etxeberria et al., 2005). In other words, sucrose itself functions as a signal molecule that triggers the endocytic mechanism.

#### **4.8 Application of BDM as myosin inhibitor**

In this dissertation the real time effect of BDM on plant class XI myosins was studied. It has been shown that BDM stabilizes the ADP·Pi-bound state of myosins and thus prevents the release of Pi which normally would

produce the power stroke (McKillop et al., 1994). Cramer and Mitchison, 1995 showed that the ATPase activity of nonmuscle myosins is inhibited by BDM. In contrast, (Ostap, 2002) questions the use of BDM as a “general” myosin inhibitor. In addition to its direct effect on the ATPase function of myosins, BDM also affects kinase related proteins. Valentijn et al. (2000) have shown for pancreatic acinar cells that BDM stabilizes actin filaments which prevent their depolymerization by cytochalasin D and latrunculin B. In spite of this, BDM has been successfully used in plants to test the participation of myosins in a range of cellular functions such as cytoplasmic streaming in *Chara corallina* (Nagai, 1979), plasmodesmatal closure, maturation of cell plates (Radford and White, 1998), cell elongation (Baskin and Bivens, 1995), cell division (Holweg et al., 2003), the movement of Golgi stacks (Nebenfuhr et al., 1999), movement of peroxisomes (Jedd and Chua, 2002; Mathur et al., 2002) and in endocytosis (Voigt et al., 2005). Clearly the results obtained in this thesis have to be taken with care because of potential side effects of the drug. Based on the presented data here, BDM appears to be a useful drug for myosin-related observations and additional experiments are needed to test the effect of BDM on class VIII myosins.

## **4.9 Potential role of myosins in pathogen defence**

### **4.9.1 Effect of BDM on plant-pathogen interaction**

As described, the application of BDM showed a strong effect on papilla formation in barley epidermis cells of leaves (see 4.9.1). Plants build physical barriers to enclose pathogens and exclude them from nutrient access. Thus, an initial defence response against the attack by a fungal pathogen represents the massive, local thickening of the cell wall, termed papilla, at the site where the fungal infection hypha tries to penetrate and to invade the cell (reviewed by Schmelzer, 2002). A clear-cut relationship was shown between changes in cytoskeleton architecture, in particular actin filaments, cytoplasmic rearrangements, formation of papillae and defence of fungal invasion (Gross et al., 1993; Kobayashi et al., 1997; Schmelzer, 2002). Cytochalasin-induced fragmentation of actin filaments correlated with enhanced penetration efficiency of a whole number of non-host pathogenic fungi, which normally fail to invade the plant cells in such interactions. These data provide strong evidence that preferentially actin filament functions are absolutely necessary for papilla formation. Thus, it is possible that actin based transport processes including myosin action are involved in papilla formation (Schmelzer, 2002). In course of this thesis it was tried to avoid inhibition of fungal functions during its growth on the leaf surface by application of BDM via the transpiration stream, nevertheless adverse effects on the penetration process can not be fully excluded. The fact that the penetrated fungus failed to develop haustoria

point into this direction. Furthermore the effective concentrations of BDM appear rather high, however it might well be that only a small proportion of this is present within the cytoplasm of epidermal cells. Nevertheless, our results might be considered as indication for a functional link between myosin action and papilla formation.

#### **4.9.2 Involvement of plant class XI myosins in host resistance**

Many plant pathogenic bacteria, such as *Pseudomonas syringae*, hold a type III secretion system (TTSS), which delivers effector proteins into the plant cell and translocation of these effectors is required for bacterial pathogenesis (Alfano and Collmer, 1996; Lindgren, 1997; He, 1998). The TTSS of the bacterial strain *P. syringae* DC3000 secretes and/or translocates several effector proteins into the host cell (Grant et al., 2006). These effectors alter host cellular processes and support disease development through largely unknown mechanisms. Although the primary function of type III effectors is to support plant susceptibility, some effectors are recognized by the corresponding plant disease resistance proteins in resistant plants and cause defense responses, including the hypersensitive response (HR) (Goodman and Novacky, 1994; Greenberg, 1997).

As shown, the *Arabidopsis thaliana* myosin class XI knock-out lines (homozygous plants) appear to be more susceptible compared to wild type plants. The reason for this might be a potential role of myosins in the defence response, in particular wall thickening or papilla formation. It has been shown that *hrp* mutants of *Xanthomonas campestris* pv. *vesicatoria* and *P. syringae* pv. *phaseolicola* (defective in *the type III secretion*) as well

as a saprophytic bacterium, cause the plant cell wall to thicken, forming a papilla (Bestwick et al., 1995; Brown et al., 1998). In contrast, the type III secretion-competent wild-type *X. campestris* pv. *vesicatoria* does not induce papillae formation (Brown et al., 1995). In addition, it has been reported that *P. syringae* TTSS down-regulated the expression of a set of *A. thaliana* genes encoding putatively secreted cell wall and defense proteins in a salicylic acid-independent manner and interestingly, transgenic expression of AvrPto (type III effector protein), repressed a similar set of host genes, compromised defense-related callose deposition in the host cell wall, and permitted substantial multiplication of an *hrp* mutant (Hauck et al., 2003). Therefore, it could be postulated that a knock-out in a class XI myosin causes a defect in wall thickening or papilla formation and by this increased susceptibility.

## 5 SUMMARY

### 5.1 Summary (English)

Myosins are actin-based molecular motors of eucaryotic organisms that play fundamental roles in many forms of motility. In addition to the well known muscle myosin a large number of myosins exist, that are essential for movement at the cellular and subcellular level. Such processes are for instance cell migration, cytokinesis, endo-/phagocytosis, exocytosis, growth cone extension, remodelling of cell shape and morphology, and organelle/particle trafficking. More recent evidence implicates myosins as important actors even in processes such as signal transduction and polymerization of actin. Based on alignment and tree production by comparing the core motor domain sequences of the myosins (myosin heavy chains) from the public databases, all known myosins were grouped into 17 or 18 classes. Remarkably, the myosins from higher plants exclusively fall into two classes, VIII and XI. In an additional class, class XIII, myosins from the alga *Acetabularia cliftonii* are grouped.

Knowledge about structure and in particular about function of plant myosins is very limited. Major sources of information about higher plant myosin genes are the completed genome sequences of the model plants *Arabidopsis thaliana* and *Oryza sativa* (rice). 17 myosin genes were identified in the *Arabidopsis* genome, 4 of them belong to class VIII and 13 to class XI; the rice genome encodes for 14 genes (2 class VIII and 12 class XI).

Besides the fact that plant myosins appear to form a clade of their own, the available sequence data nevertheless suggest that they follow the domain

pattern typical for all myosins: the highly conserved N-terminal head (motor) domain responsible for ATP hydrolysis, binding to actin and production of force, the neck domain containing characteristic repeat motifs (IQ repeats), and the C-terminal tail domain. The IQ motifs of the neck domain are binding sites for calmodulin or regulatory light chains, which are unknown for plant myosins. The tail domain usually contains one or more coiled-coil regions responsible for dimerization. In the case of class XI myosins the tail domain contains additionally the DIL domain at the C-terminal end. In mammals and yeast this domain is present in class V myosins. Data from yeast shed light on its function, since it was demonstrated that this domain contains a distinct binding region for movement of vesicular cargo. However, cargo binding sites must not necessarily be localized only within the DIL domain, since also in yeast another region, putatively binding vacuoles, was found considerably upstream.

In this dissertation a survey of the subcellular localization, the dynamic behavior, the transported cargoes and their potential binding site(s) in myosin tails was obtained. For this investigation transient overexpression of selected *A. thaliana* class VIII and XI myosins and a variety of respective subregions fused to fluorescent proteins as markers was used as assay system. The approach combined high resolution *in vivo* microscopy, molecular biology and *in vivo* biochemistry. Such an integrated approach was so far not applied for plant myosins. The data showed that specific binding sites for Golgi stacks/vesicles and peroxisomes which are highly conserved among all *A. thaliana* class XI myosins reside within the C-terminal part of class XI myosins (DIL domain). In addition, studying the

tail domain of barely class XI myosins revealed that the identified cargo binding sites are highly conserved in monocots and dicots. The peroxisomal localization of the DIL domain of the yeast myosin V (Myo2p) in plant cells was a strong indication for the involvement of the DIL domain as cargo binding site among class V and XI myosins. The phenotypic characterization of 10 out of 13 class XI homozygous knock-out lines revealed no drastic effects with respect to growth and development or pathogen defence. Only various degrees of stunted growth, changes in seed morphology and a slight increase in susceptibility to bacterial infection were observed. Altogether, these results demonstrate considerable functional redundancy among class XI myosins.

For two selected class VIII myosins (ATM1 and ATM2), each as a representative for one myosin VIII subclass, it appeared that only ATM2 localized on vesicles which later showed partial colocalization with endosomes. The detailed analysis of the ATM2 tail domain showed that in contrast to class XI myosins, ATM2 probably binds only one cargo. For the involvement of ATM2 in such an important process like endocytosis would also speak the fact that the homozygous knock out of this gene results in lethality. The other class VIII myosin investigated, ATM1, showed plasma membrane localization in agreement with previous studies where by immunocytochemistry this myosin was found in the cell plate associated with the plasma membrane in particular at plasmodesmata. These data suggest a role in the formation of the new cell wall and the generation and maintenance of plasmodesmata. Thus, the functions of class VIII myosins might be quite diverse.

## 5.2 Zusammenfassung (Deutsch)

Myosine sind Aktin-abhängige Motorproteine, die in allen Eukaryonten vorkommen und in grundlegenden Funktionen wie Zellmotilität, intrazellulärer Transport, Signalübermittlung, Zellteilung und Morphogenese eine zentrale Rolle spielen. Über Myosine bei Pflanzen ist wenig bekannt, besonders hinsichtlich ihrer zellulären Funktionen. Auf jeden Fall bilden sie eine eigene Gruppe und gehören den Klassen VIII und XI der insgesamt 18 Klassen der Myosin-Superfamilie an. Die verfügbaren Sequenzdaten lassen vermuten, dass die Struktur der pflanzlichen Myosine dem myosintypischen Muster folgt: die hochkonservierte N-terminale Kopf (head)- oder Motordomäne, verantwortlich für ATP-Hydrolyse und die damit verbundene Bewegung entlang Aktinfilamenten, die Hals (neck-)domäne für die Kraft-bzw. Bewegungsübertragung und -Verstärkung und die Bindung von regulatorischen Proteinen wie z. BSP Calmodulin, sowie die Schwanz (tail-)domäne, die gewöhnlich für Dimerisierung und an ihrem C-terminalen Ende für die Bindung an „Cargo“ verantwortlich ist.

In der vorliegenden Doktorarbeit wurde ein erster Überblick über die subzelluläre Lokalisation und deren Dynamik sowie die Art des transportierten Cargos und die Bindungsstellen in den Schwanzregionen pflanzlicher Myosine erarbeitet. Für diese Untersuchungen wurde als Testsystem transiente Überexpression in Verbindung mit Fluoreszenzprotein-Markierungstechnologie an ausgewählten Myosinen und einer Anzahl ihrer verschiedenen Unterregionen und Domänen verwendet. Ein derartig integrierter Versuchsansatz wurde für pflanzliche Myosine bisher nicht eingesetzt. Die Resultate zeigten, dass in der C-terminalen

Region von Myosinen der Klasse XI spezifische Bindungsstellen für Peroxisomen und Golgi Stapel/Vesikel zu finden sind, vorwiegend im C-terminalen Teil, der sogenannten DIL Domäne. Es stellte sich heraus, dass diese Region und die Bindungsstellen innerhalb der Klasse XI untereinander und zwischen verschiedenen Pflanzen stark konserviert sind. Sogar die Bindungsstelle des homologen Myosins aus Hefe, Myosin V (Myo2p) funktionierte in Pflanzenzellen als Bindungsstelle zu Peroxisomen. Dies lässt die Schlussfolgerung zu, dass die pflanzlichen Myosine der Klasse XI in Organelltransport (Golgiapparat, Peroxisomen) involviert sind, wobei gewisse Redundanz vorliegt. In Funktion und Struktur sind die Myosine der Klasse XI den pilzlichen und tierischen Myosinen der Klasse V am ähnlichsten.

Für zwei ausgewählte Vertreter (ATM2, ATM1) der anderen Klasse pflanzlicher Myosine, der Klasse VIII, zeigte nur ATM2 Bindungskapazität an Vesikel, die teilweise mit Endosomen kolokalisierten. Man kann auf Grund der Daten annehmen, dass ATM2 in der pflanzlichen Endozytose eine Rolle spielt, allerdings bleibt unklar an welcher Stelle im Gesamtprozess. Für die Beteiligung an einem solch wichtigen Geschehen wie Endozytose würde auch der Befund sprechen, dass homozygote knock-out Pflanzen in diesem Gen nicht keimungsfähig und damit nicht lebensfähig sind. Das untersuchte zweite Myosin der Klasse VIII, ATM1, war eng mit der Plasmamembran assoziiert und zeigte keinerlei vesiculäre Lokalisierung. Dieses Ergebnis ist in Übereinstimmung mit publizierten Lokalisierungen, die mit Immunocytologie erhoben wurden. Hier war Bindung an Plasmamembran, vorwiegend im Bereich von Plasmodesmata, in der sich neu entwickelnden Zellplatte nach Zellteilung gefunden worden.

Dies spricht für eine Funktion von ATM2 bei der Bildung der neuen transversalen Zellwand und ihrer Zell-Zellverbindungen (Plasmodesmata). Die Funktionen der Myosine der Klasse VIII sind daher wahrscheinlich recht verschieden.

## **6 OUTLOOK**

### **6.1 Class XI myosins:**

Since the AtMya1 (AT1g17580) was the only isoform of class XI myosins that showed localization with golgi vesicles/stacks in course of this thesis, it would be highly interesting to monitor the trafficking of Golgi stacks/vesicles in Mya1 knock-out lines. For this purpose analysis of crosses of the Mya1 single knock-out lines with the transgenic line labeled for golgi stacks/vesicles with GFP could further strengthen the obtained data and would provide final evidence that class XI myosins (Mya1) are the motors that transport Golgi stacks/ vesicles in plant cells.

In respect to experimental continuation of subcellular localization studies for class XI myosins, further analysis of the highly conserved domain downstream of the VEAK domain in the tail domain of class XI myosins and further detailed characterization of the DIL domain of Mya1 by mutagenesis will be needed. This should finally allow a fine-mapping of the binding sites for the vesicular cargoes and might reveal additional binding sites. Concerning investigations on the involvement of class XI myosins in defence responses the generation of double and triple knock-out lines will certainly be needed.

### **6.2 Class VIII myosins**

The results available so far for the ATM2 (AT5g54280) require extended and detailed experimental continuation. The ongoing generation and characterization of the ATM2 complementation lines would provide genetic proof for the lethality of ATM2 knock-out lines. In order to provide genetic proof for the involvement of ATM2 in endocytosis, generation of transgenic

lines expressing an RFP fusion of ATM2tail in the genetic background of FLS2-GFP would be helpful. Recently Robotzeck et al. (2006) have generated transgenic plants expressing a functional GFP fusion of FLS2, the receptor for the recognition of the bacterial flagelin. They showed that after treatment with the flagellin epitope flg22 the transfer of FLS2 into intracellular mobile vesicles by endocytosis was induced. A dominant negative interference of the ATM2 tail with the internalization of the FLS2 would provide evidence for the participation of ATM2 in endocytosis.

From RNA macroarray data it is evident that ATM2 is relatively highly expressed in root cells. Therefore, it would be worthwhile to perform transient colocalization studies of ATM2 tail constructs in cell cultures of roots using dyes (FM-64) specific for endosomes as marker. This might provide further insight into the involvement of ATM2 in endocytosis.

Preliminary subcellular localization studies showed a cytoplasmic localization for the subsegment (867-1030) of the ATM2 tail domain. However, the construct ATM2 816-1030 was localized on vesicles. Considering that the missing 54 amino acids represent a coiled-coil domain this result might indicate that this domain has an important role in binding of ATM2 to his cargo. Thus, investigations of the participation of coiled-coil domains could complement the mapping of cargo binding sites.

### **6.3 Yeast-two-hybrid**

The above described preliminary results of the yeast-two-hybrid screening and further subcellular localization studies suggested some potential myosin interacting proteins. Further confirmation of the obtained data will be needed.

## 7 LITERATURE

- Alfano, J.R., and Collmer, A.** (1996). Bacterial pathogens in plants: life up against the wall. *Plant Cell*. **8**, 1683-1698.
- Allan, V., and Schroer, T.** (1999). Membrane motors. *Curr Opin Cell Biol*. **11**, 476-482.
- Alpy, F., and Tomasetto, C.** (2005). Give lipids a START: the StAR-related lipid transfer (START) domain in mammals. *J Cell Sci*. **118**, 2791-2801.
- Anson, M., Geeves, M.A., Kurzawa, S.E., and Manstein, D.J.** (1996). Myosin motors with artificial lever arms. *EMBO J*. **15**, 6069-6074.
- Aschenbrenner, L., Naccache, S., and Hasson, T.** (2004). Uncoated endocytic vesicles require the unconventional myosin, Myo6, for rapid transport through actin barriers. *Mol Biol Cell*. **15**, 2253-2263.
- Baba, T., Fusaki, N., Shinya, N., Iwamatsu, A., and Hozumi, N.** (2003). Myosin is an in vivo substrate of the protein tyrosine phosphatase (SHP-1) after mIgM cross-linking. *Biochemical and Biophysical Research Communications*, 67-72.
- Babst, M., Odorizzi, G., Estepa, E.J., and Emr, S.D.** (2000). Mammalian tumor susceptibility gene 101 (TSG101) and the yeast homologue, Vps23p, both function in late endosomal trafficking. *Traffic* **1**, 248-258.
- Bagshaw, C.R., Eccleston, J.F., Eckstein, F., Goody, R.S., Gutfreund, H., and Trentham, D.R.** (1974). The magnesium ion-dependent adenosine triphosphatase of myosin. Two-step processes of adenosine triphosphate association and adenosine diphosphate dissociation. *Biochem. J*. **141**, 351-364.
- Baluska, F., Polsakiewicz, M., Peters, M., and Volkmann, D.** (2000). Tissue-specific subcellular immunolocalization of a myosin-like protein in maize root apices. *Protoplasma*. **212**, 137-145.

- Baluska, F., Cvrckova, F., Kendrick-Jones, J., and Volkmann, D.** (2001). Sink Plasmodesmata as Gateways for Phloem Unloading. Myosin VIII and Calreticulin as Molecular Determinants of Sink Strength? *Plant Physiol.* **126**, 39-46.
- Baluska, F., Samaj, J., Hlavacka, A., Kendrick-Jones, J., and Volkmann, D.** (2004). Actin-dependent fluid-phase endocytosis in inner cortex cells of maize root apices. *J Exp Bot.* **55**, 463-473.
- Baluska, F., Hlavacka, A., Samaj, J., Palme, K., Robinson, D., Matoh, T., McCurdy, D., Menzel, D., and Volkmann, D.** (2002). F-actin-dependent endocytosis of cell wall pectins in meristematic root cells. Insights from brefeldin A-induced compartments. *Plant Physiol.* **130**, 422-431.
- Baskin, T., and Bivens, N.** (1995). Stimulation of radial expansion in *Arabidopsis* roots by inhibitors of actomyosin and vesicle secretion but not by various inhibitors of metabolism. *Planta.* **197**, 514-521.
- Beach, D., Thibodeaux, J., Maddox, P., Yeh, E., and Bloom, K.** (2000). The role of the proteins Kar9 and Myo2 in orienting the mitotic spindle of budding yeast. *Curr. Biol.* **10**, 1497-1506.
- Beevers, H.** (1979). Microbodies in higher plants. *Annu Rev Plant Physiol.* **30**, 159-193.
- Berg, J.S., Powell, B.C., and Cheney, R.E.** (2001). A millennial myosin census. *Mol. Biol. Cell.* **12**, 780-794.
- Bestwick, C., Bennett, M., and Mans, J.** (1995). *Hrp* mutant of *Pseudomonas syringae* pv. *phaseolicola* induces cell wall alterations but not membrane damage leading to the hypersensitive reaction in lettuce. *Plant Physiol.* **108**, 503-516.
- Boevink, P., Oparka, K., Santa Cruz, S., Martin, B., Betteridge, A., and Hawes, C.** (1998). Stacks on tracks: the plant Golgi apparatus traffics on an actin/ER network. *Plant J.* **15**, 441-447.

- Boevink, P., Oparka, K., Santa Cruz, S., Martin, B., Betteridge, A., and Hawes, C.** (1998). Stacks on tracks: the plant Golgi apparatus traffics on an actin/ER network. *Plant J.* **15**, 441-447.
- Boldogh, I., Ramcharan, S., Yang, H., and Pon, L.** (2004). A type V myosin (Myo2p) and a Rab-like G-protein (Ypt11p) are required for retention of newly inherited mitochondria in yeast cells during cell division. *Mol Bio Cell.* **15**, 3994-4002.
- Bouche, N. and Bouchenz, D.** (2001). Arabidopsis gene knock out: phenotype wanted. *Curr. Opin. Plant Biol.* **4**, 111-7
- Braun, M.** (1996). Immunolocalization of myosin in rhizoids of *Chara globularis* Thuill. *Protoplasma* **191**, 1-8.
- Brown, I., Mans, e.J., and Bonas, U.** (1995). *hrp* genes in *Xanthomonas campestris* pv. *vesicatoria* determine ability to suppress papilla deposition in pepper mesophyll cells. *Mol. Plant Microbe Interact.* **8**, 825-836.
- Brown, I., Trethowan, J., Kerry, M., Mansfield, J., and Bolwell, G.P.** (1998). Localization of components of the oxidative cross-linking of glycoproteins and of callose synthesis in papillae formed during the interaction between non-pathogenic strains of *Xanthomonas campestris* and French bean mesophyll cells. *Plant J.* **15**, 333-343.
- Brown, S.** (1999). Cooperation between microtubule- and actin-based motor proteins. *Annu Rev Cell Dev Biol.* **15**, 63-80.
- Cain, F., and Davies, R.** (1962). Breakdown of adenosine triphosphate during a single contraction of working muscle. *Biochem Biophys Res Commun.* **7**, 361-366.
- Catlett, N.L., and Weisman, L.S.** (1998). The terminal tail region of a yeast myosin -V mediates its attachment to vacuole membranes and sites of polarized growth. *Proc. Natl. Acad. Sci. U.S.A.* **95**, 14799-14804.

- Catlett, N.L., Duex, J.E., Tang, F., and Weisman, L.S.** (2000). Two distinct regions in a yeast myosin-V tail domain are required for the movement of different cargoes. *J. Cell Biol.* **150**, 513-525.
- Cheney, R., and Mooseker, M.** (1992). **Unconventional myosins**. *Curr Opin Cell Biol.* **4**, 27-35.
- Christensen, A., Sharrock, R., and Quail, P.** (1992). Maize polyubiquitin genes: structure, thermal perturbation of expression and transcript splicing, and promoter activity following transfer to protoplasts by electroporation. *Plant Mol Biol* **18**, 675-689.
- Collings, D.A., Harper, J.D.I., Marc, J., Overall, R.L., and Mullen, R.T.** (2002). Life in the fast lane: actin-based motility of plant peroxisomes. *Can.J.Bot.* **80**, 430-441.
- Cope, M.J.T., Whisstock, J., Rayment, I., and Kendrick-Jones, J.** (1996). Conservation within the myosin motor domain: implications for structure and function. *Structure* **4**, 969-987.
- Cramer, L., and Mitchison, T.** (1995). Myosin is involved in postmitotic cell spreading. *J Cell Biol* **131**, 179-189.
- Desnos, C., Schon, J., Huet, S., Tran, V., and El-Amraoui, A.** (2003). Rab27A and its effector MyRIP link secretory granules to F-actin and control their motion towards release sites. *J. Cell Biol* **163**, 559-570.
- Etxeberria, E., Baroja-Fernandez, E., José Muñoz, F., and Pozueta-Romero, J.** (2005). Sucrose-inducible Endocytosis as a Mechanism for Nutrient Uptake in Heterotrophic Plant Cells. *Plant Cell Physiol.* **46**, 474-481.
- Fagarasanu, A., Fagarasanu, M., Eitzen, G., Aitchison, J., and Rachubinski, R.** (2006). The peroxisomal membrane protein Inp2p is the peroxisome-specific receptor for the myosin V motor Myo2p of *Saccharomyces cerevisiae*. *Dev Cell.* **10**, 587-600.
- Falk, D., Wessels, D., Jenkins, L., Pham, T., Kuhl, S., Titus, M., and Soll, D.** (2003). Shared, unique and redundant functions of three members of the

- class I myosins (MyoA, MyoB and MyoF) in motility and chemotaxis in *Dictyostelium*. *J Cell Sci.* **116**, 3985-3999.
- Faure, J., Vittorioso, P., Santoni, V., Fraisier, V., Prinsen, E., Barlier, I., Van Onckelen, H., Caboche, M., and Bellini, C.** (1998). The PASTICCINO genes of *Arabidopsis thaliana* are involved in the control of cell division and differentiation. *Development.* **125**, 909-918.
- Feilmeier, B., Iseminger, G., Schroeder, D., Webber, H., and Phillips, G.** (2000). Green fluorescent protein functions as a reporter for protein localization in *Escherichia coli*. *J Bacteriol.* **182**, 4068-4076.
- Fischer, R., Stoger, E., Schillberg, S., Christou, P., and Twyman, R.** (2004). Plant-based production of biopharmaceuticals. *Curr Opin Plant Biol.* **7**, 52-58.
- Futter, C.** (2006). The molecular regulation of organelle transport in mammalian retinal pigment epithelial cells. *Pigment Cell Res.* **19**, 104-111.
- Gallois, P., and Marinho, P.** (1995). Leaf disk transformation using *Agrobacterium tumefaciens*-expression of heterologous genes in tobacco. *Methodes Mol Biol.* **49**, 39-48.
- Garrus, J.E., von Schwedler, U.K., Pornillos, O.W., Morham, S.G., Zavitz, K.H., Wang, H.E., Wettstein, D.A., Stray, K.M., Cote, M., Rich, R.L., Myszka, D.G., and Sundquist, W.I.** (2001). Tsg101 and the vacuolar protein sorting pathway are essential for HIV-1 budding. *Cell.* **107**, 55-65.
- Geeves, M., Fedorov, R., and Manstein, D.** (2005). Molecular mechanism of actomyosin-based motility. *Cell Mol Life Sci.* **62**, 1462-1477.
- Geeves, M.A., Goody, R.S., and Gutfreund, H.** (1984). Kinetics of acto-S1 interaction as a guide to a model for the crossbridge cycle. *J. Muscle Res. Cell Motil.* **5**, 351-361.
- Geldner, N., Anders, N., Wolters, H., Keicher, J., Kornberger, W., Muller, P., Delbarre, A., Ueda, T., Nakano, A., and Jurgens, G.** (2003). The

- Arabidopsis GNOM ARF-GEF mediates endosomal recycling, auxin transport, and auxin-dependent plant growth. *Cell*. **112**, 219-230.
- Gettemans, J., Van Impe, K., Delanote, V., Hubert, T., Vandekerckhove, J., and De Corte, V.** (2005). Nuclear actin-binding proteins as modulators of gene transcription. *Traffic*. 847-857.
- Gietz, R., Schiestl, R., Willems, A., and Woods, R.** (1995). Studies on the transformation of intact yeast cells by the LiAc/SS-DNA/PEG procedure. *Yeast*. **11**, 355-360.
- Gnanasambandam, A., and Birch, R.** (2004). Efficient developmental mistargeting by the sporamin NTPP vacuolar signal to plastids in young leaves of sugarcane and Arabidopsis. *Plant Cell Rep.* **23**, 435-447.
- Goldman, Y.E.** (1987). Kinetics of the actomyosin ATPase in muscle fibers. **49**, 637-654.
- Goodman, R.N., and Novacky, A.J.** (1994). The fungus induced Hypersensitive Reaction in plants to pathogens. In *The Hypersensitive Reaction in plants to pathogens.*, R.N. Goodman and A.J. Novacky, eds (St. Paul, Minn.: APS Press), 3-74.
- Govindan, B., and Bowser, R.** (1995). The role of Myo2, a yeast class V myosin, in vesicular transport. *J Cell Biol.* **128**, 1055-1068.
- Govindan, B., Bowser, R., and Novick, P.** (1995). The role of Myo2, a yeast class V myosin, in vesicular transport. *J. Cell Biol* **128**, 1055-1068.
- Grant, S.R., Fisher, E.J., Chang, J.H., Mole, B.M., and Dangl, J.L.** (2006). Subterfuge and Manipulation: Type III Effector Proteins of Phytopathogenic Bacteria. *Annu.Rev.Microbiol.* **60**, 425-449.
- Greenberg, J.** (1997). Programmed cell Death in plant-pathogen interactions. *Annu Rev Plant Physiol Plant Mol Biol.* **48**, 525-545.
- Grolig, F., Schroder, J., Sawitzky, H., and Lange, U.** (1996). Partial characterization of a putative 110 kDa myosin from the green alga Chara

corallina by in vitro binding of fluorescent F-actin. *Cell Biol Int.* **20**, 365-373.

- Grolig, F., Williamson, R., Parke, J., Miller, C., and Anderton, B.** (1988). Myosin and Ca<sup>2+</sup>-sensitive streaming in the alga *Chara*: detection of two polypeptides reacting with a monoclonal anti-myosin and their localization in the streaming endoplasm. *Eur J Cell Biol.* **47**, 22-31.
- Gross, P., Julius, C., Schmelzer, E., and Hahlbrock, K.** (1993). Translocation of cytoplasm and nucleus to fungal penetration sites is associated with depolymerization of microtubules and defense gene activation in infected, cultured parsley cells. *EMBO J.* **12**, 1735-1744.
- Hales, C., Vaerman, J., and Goldenring, J.** (2002). Rab11 family interacting protein 2 associates with myosin Vb and regulates plasma membrane recycling. *J. Biol. Chem.* **277**, 50415-50421.
- Hanahan, D.** (1983). Studies on transformation of *Escherichia coli* with plasmids. *J Mol Biol.* **166**, 557-580.
- Hanson, M., and Kohler, R.** (2001). GFP imaging: methodology and application to investigate cellular compartmentation in plants. *J Exp Bot.* **52**, 529-539.
- Harper, J., Adami, G., Wei, N., Keyomarsi, K., and Elledge, S.** (1993). The p21 Cdk-interacting protein Cip1 is a potent inhibitor of G1 cyclin-dependent kinases. *Cell.* **75**, 805-816.
- Hashimoto, k., Igarashi, H., Mano, S., Nishimura, M., Shimmen, T., and Yokota, E.** (2005). Peroxisomal localization of a myosin XI isoform in *Arabidopsis thaliana*. *Plant Cell Physiol.* **46**, 782-789.
- Hashimoto k, I.H., Mano S, Nishimura M, and E, S.T.a.Y.** (2005). Peroxisomal localization of a myosin XI isoform in *Arabidopsis thaliana*. *Plant Cell Physiol.* 782-789.
- Hauck, P., Thilmony, R., and He, S.** (2003). A *Pseudomonas syringae* type III effector suppresses cell wall-based extracellular defense in susceptible *Arabidopsis* plants. *Proc.Natl.Acad.Sci. USA* **100**, 8577-8582.

- Hawes, C.** (2005). Cell biology of the plant Golgi apparatus. *New Phytol.* **165**, 29-44.
- Hawes, C., and Satiat-Jeunemaitre, B.** (2001). Trekking along the cytoskeleton. *Plant Physiology*. **125**, 119-122.
- Hayashi, M., and Nishimur, M.** (2003). Entering a new era of research on plant peroxisomes. *Current Opinion in Plant Biology.* **6**, 577-582.
- He, S.** (1998). Type III protein secretion systems in plant and animal pathogenic bacteria. *Annu Rev Phytopathol.* **36**, 363-392.
- Heintzelman, M., and Schwartzman, J.** (1997). A novel class of unconventional myosins from *Toxoplasma gondii*. *J Mol Biol.* **8**, 139-146.
- Heslop-Harrison, J., and Heslop-Harrison, Y.** Myosin associated with the surfaces of organelles, vegetative nuclei and generative cells in angiosperm pollen grains and tubes. *J Cell Sci.* **94**, 319-325.
- Hill, K., Catlett, N., and Weisman, L.** (1996). Actin and myosin function in directed vacuole movement during cell division in *Saccharomyces cerevisiae*. *J. Cell Biol.* **135**, 1535-1549.
- Hirsch, R., Lewis, B., Spalding, E., and Sussman, M.** (1998). A role for the AKT1 potassium channel in plant nutrition. *Science* **280**, 918-921.
- Hodge, T., and Cope, M.J.** (2000). A myosin family tree. *J. Cell Sci.* **113**, 3353-3354.
- Hoepfner, D., Van den Berg, M., Philippsen, P., Tabak, H., and Hettema, E.** (2001). A role for Vps1p, actin, and the Myo2p motor in perox-isome abundance and inheritance in *Saccharomyces cerevisiae*. *J. Cell Biol.* **155**, 979-990.
- Holweg, C., and Nick, P.** (2004). Arabidopsis myosin XI mutant is defective in organelle movement and polar auxin transport. *Proc. Natl. Acad. Sci. U.S.A.* **101**, 10488-10493.
- Holweg, C., Honsel, A., and Nick, P.** (2003). A myosin inhibitor impairs auxin-induced cell division. *Protoplasma.* **222**, 193-204.

- Howard, J.** (2001). Mechanics of Motor Proteins and the Cytoskeleton.
- Huxley, H.E.** (1969). The mechanism of muscular contraction. *Science*. **164**, 1356-1365.
- Ishikawa, K., Catlett, N., Novak, J., Tang, F., Nau, J., and Weisman, L.** (2003). Identification of an organelle-specific myosin V receptor. *J. Cell Biol.* **160**, 887-897.
- Ito, H., Fukuda, Y., Murata, K., and Kimura, A.** (1983). Transformation of intact yeast cells treated with alkali cations. *J Bacteriol.***153**, 163-168.
- Itoh, T., Tohe -E, A., and Matsui, Y.** (2004). Mmr1p is a mitochondrial factor for Myo2p-dependent inheritance of mitochondria in the budding yeast. *EMBO J.* **23**, 2520-2530.
- James, C., Indge, K., and Oliver, S.** (1995). DNA sequence analysis of a 35 kb segment from *Saccharomyces cerevisiae* chromosome VII reveals 19 open reading frames including RAD54, ACE1/CUP2, PMR1, RCK1, AMS1 and CAL1/CDC43. *Yeast*. **11**, 1413-1419.
- Jedd, G., and Chua, N.-H.** (2002). Visualization of peroxisomes in living plant cells reveals acto-myosin-dependent cytoplasmic streaming and peroxisome budding. *Plant Cell Physiol.* **43**, 384 392.
- Jiang, S., and Ramachandran, S.** (2004). Identification and molecular characterization of myosin gene family in *Oryza sativa* genome. *Plant Cell Physiol.* **45**, 590-599.
- Johnston, G., Prendergast, J., and Singer, R.** (1991). The *Saccharomyces cerevisiae* MYO2 gene encodes an essential myosin for vectorial transport of vesicles. *J Cell Biol.* **113**, 539-551.
- Kachar, B., and Reese, T.** (1988). The mechanism of cytoplasmic streaming in *Characean* algal cells: sliding of endoplasmic reticulum along actin filaments. *J Cell Biol* **106**, 1545-1552.
- Karcher, R., Deacon, S., and Gelfand, V.** (2002). Motor-cargo interactions: the key to transport specificity. *Trends Cell Biol.* **12**, 21-27.

- Karcher, R., Roland, J., Zappacosta, F., Huddleston, M., Annan, R., Carr, S., and Gelfand, V.** (2001). Cell Cycle Regulation of Myosin-V by Calcium/Calmodulin Dependent Protein Kinase II. *Science*. **293**, 1317-1320.
- Kinkema, M., and Schiefelbein, J.** (1994). A myosin from a higher plant has structural similarities to class V myosins. *J. Molec. Biol.* **239**, 591-597.
- Knebel, W., Quader, H., and Schnepf, E.** (1990). Mobile and immobile endoplasmic reticulum in onion bulb epidermis cells: short- and long-term observations with a confocal laser scanning microscope. *Eur J Cell Biol.* **52**, 328-340.
- Kobayashi, Y., Yamada, M., Kobayashi, I., and Kunoh, H.** (1997). Actin microfilaments are required for the expression of nonhost resistance in higher plants. *Plant Cell Physiol.* **38**, 725-733.
- Koncz, C., Mayerhofer, R., Koncz-Kalman, C., Reiss, B., Redei, G.P., and Schell, J.** (1990). Isolation of a gene encoding a novel chloroplast protein by T-DNA tagging in *Arabidopsis thaliana*. *EMBO J.* **9**, 1337-1346.
- Koncz, C., Mayerhofer, R., Koncz-Kalman, Z., Nawrath, C., Reiss, B., Redei, G., and Schell, J.** (1990). Isolation of a gene encoding a novel chloroplast protein by T-DNA tagging in *Arabidopsis thaliana*. *EMBO J.* **9**, 1337-1346.
- Koonin, E.V., and Abagyan, R.A.** (1997). TSG101 may be the prototype of a class of dominant negative ubiquitin regulators. *Nat. Genet.* **16**, 330-331.
- Lapierre, L., Kumar, R., Hales, C., Navarre, J., and Bhartur, S.** (2001). Myosin vb is associated with plasma membrane recycling systems. *Mol. Biol. Cell.* **12**, 1843-1857.
- Legesse-Miller, A., Zhang, S., Santiago-Tirado, F., Van Pelt, C., and Bretscher, A.** (2006). Regulated Phosphorylation of Budding Yeast's Essential Myosin V Heavy Chain, Myo2p. *Molecular Biology of the Cell.* **17**, 1812-1821.

- Legesse-Miller A, Zhang S, Santiago-Tirado FH, Van Pelt CK, and A., B.** (2006). Regulated phosphorylation of budding yeast's essential myosin V heavy chain, Myo2p. *Mol Biol Cell.* **17**, 1812-1821.
- Liebe, S., and Menzel, D.** (1995). Actomyosin-based motility of endoplasmic reticulum and chloroplasts in *Vallisneria* mesophyll cells. *Biol Cell.* **85**, 207-222.
- Lin, Y., Sun, L., Nguyen, L., Rachubinski, R., and Goodman, H.** (1999). The Pex16p homolog SSE1 and storage organelle formation in *Arabidopsis* seeds. *Science.* **284**, 328-330.
- Lindgren, P.** (1997). The role of *hrp* genes during plant-bacterial interactions. *Annu Rev Phytopathol.* **35**, 129-152.
- Lipka, V., Dittgen, J., Bednarek, P., Bhat, R., Wiermer, M., Stein, M., Landtag, J., Brandt, W., Rosahl, S., Scheel, D., Llorente, F., Molina, A., Parker, J., Somerville, S., and Schulze-Lefert, P.** (2005). Pre- and postinvasion defenses both contribute to nonhost resistance in *Arabidopsis*. *Science.* **310**, 1180-1183.
- Lister, I., Tolliday, N., and Li, R.** (2006). Characterization of the minimum domain required for targeting budding yeast myosin ii to the site of cell division. *BMC Biology .* **4**, 19-
- Liu, L., Zhou, J., and Pesacreta, T.C.** (2001). Maize myosins: diversity, localization, and function. *Cell Motil. Cytoskelet.* **48**, 130-148.
- Lombardi, V., Piazzesi, G., Ferenczi, M.A., Thirlwell, H., Dob-bie, and Irving, M.** (1995). Elastic distortion of myosin heads and repriming of the working stroke in muscle. *Nature.* **374**, 553-555.
- Long, R., Singer, R., Meng, X., Gonzalez, I., Nasmyth, K., and Jansen, R.** (1997). Mating type switching in yeast controlled by asymmetric localization of *ASH1* mRNA. *Science.* **277**, 383-387.
- Lu, L., Lee, Y., Pan, R., Maloof, J., and Liu, B.** (2005). An Internal Motor Kinesin Is Associated with the Golgi Apparatus and Plays a Role in

- Trichome Morphogenesis in *Arabidopsis*. *Molecular Biology of the Cell*. **16**, 811-823.
- Lynn, R.W., and Taylor, E.W.** (1971). Mechanism of adenosine triphosphate hydrolysis by actomyosin. *Biochemistry*. **10**, 4617-4624.
- Mano, S., Nakamori, C., Hayashi, M., Kato, A., Kondo, M., and Nishimura, M.** (2002). Distribution and characterization of peroxisomes in *Arabidopsis* by visualization with GFP: dynamic morphology and actin-dependent movement. *Plant Cell Physiol*. **43**, 331-341.
- Mathur, J., Mathur, N., and Hülskamp, M.** (2002). Simultaneous visualization of peroxisomes and cytoskeletal elements reveals actin and not microtubule-based peroxisome motility in plants. *Plant Physiol*. **128**, 1031-1045.
- Mathur, J., Mathur, N., Kernebeck, B., and Hülskamp, M.** (2003). Mutations in actin-related proteins 2 and 3 affect cell shape development in *Arabidopsis*. *Plant Cell*. **15**, 1632-1645.
- Mathur, J., Mathur, N., Kirik, V., Kernebeck, B., Purushottam Srinivas, B., and Hülskamp, M.** (2003). *Arabidopsis* CROOKED encodes for the smallest subunit of the ARP2/3 complex and controls cell shape by region specific fine F-actin formation. *Development*. **130**, 3137-3146.
- McKillop, D., Fortune, N., Ranatunga, K., and Geeves, M.** (1994). The influence of 2,3-butanedione monoxime (BDM) on the interaction between actin and myosin in solution and in skinned muscle fibres. *J Muscle Res Cell Motil*. **15**, 309-318.
- Meagher, R., and Fechheimer, M.** (2003). The *Arabidopsis* Cytoskeletal Genome. *The Arabidopsis Book*.
- Mercer, J., Seperack, P., Strobel, M., Cope-land, N., and Jenkins, N.** (1991). Novel myosin heavy chain encoded by murine dilute coat colour locus. *Nature*. **349**, 709-713.

- Mermall, V., Post, P., and Mooseker, M.** (1998). Unconventional myosins in cell movement, membrane traffic, and signal transduction. *Science*. **23**, 527-533.
- Miller, D., Scordilis, S., and Hepler, P.** (1995). Identification and localization of three classes of myosins in pollen tubes of *Lilium longiflorum* and *Nicotiana glauca*. *J Cell Sci*. **108**, 2549-2653.
- Morris, S., Arden, S., Roberts, R., Kendrick-Jones, J., Cooper, J., Luzio, J., and Buss, F.** (2002). Myosin VI binds to and localises with Dab2, potentially linking receptor-mediated endocytosis and the actin cytoskeleton. *Traffic*. **3**, 331-341.
- Murphy, A., Bandyopadhyay, A., Holstein, S., and Peer, W.** (2005). Endocytotic cycling of PM proteins. *Annu Rev Plant Biol*. **56**, 221-251.
- Nagai, R.** (1979). Cytoplasmic streaming in plant cells. *Plant Physiology*. **10**, 45-48.
- Nagai, R.** (1993). Regulation of intracellular movements in plant cells by environmental stimuli. *Internat. Rev. Cytol*. **145**, 251-310.
- Nebenfuhr, A., Gallagher, L.A., Dunahay, T.G., Frohlick, J.A., Mazurkiewicz, A.M., Meehl, J.B., and Staehelin, L.A.** (1999). Stop-and-go movements of plant Golgi stacks are mediated by the actin-myosin system. *Plant Physiol*. **121**, 1127-1141.
- Odell, J., Nagy, F., and Chua, N.** (1985). Identification of DNA sequences required for activity of the cauliflower mosaic virus 35S promoter. *Nature*. **313**, 810-812.
- Oliver, T.N., Berg, J.C., and R.C., C.** (1999). **Tails of unconventional myosins.** *Cell. Mol. Life Sci*. **56**, 243-257.
- Ostap, E., and Pollard, T.** (1996). Overlapping functions of myosin-I isoforms? *J Cell Biol*. **133**, 221-224.
- Ostap, E.M.** (2002). 2,3-Butanedione monoxime (BDM) as a myosin inhibitor. *Journal of Muscle Research and Cell Motility*. **23**, 305-308.

- Parke, J., Miller, C., and Anderton, B.** (1986). Higher plant myosin heavy-chain identified using a monoclonal antibody. *Eur J Cell Biol.* **41**, 9-13.
- Pashkova, N., Catlett, N.L., Novak, J.L., Wu, G., Lu, R., Cohen, R.E., and Weisman, L.S.** (2005). Myosin V attachment to cargo requires the tight association of two functional subdomains. *J. Cell Biol.* **168**, 359-364.
- Pesaresi, P., Masiero, S., Eubel, H., Braun, H., Bhushan, S., Glaser, E., Salamini, F., and Leister, D.** (2006). Nuclear photosynthetic gene expression is synergistically modulated by rates of protein synthesis in chloroplasts and mitochondria. *Plant Cell.* **18**, 970-991.
- Pestic-Dragovich, L., Stojiljkovic, L., Philimonenko, A., Nowak, G., Ke, Y., Settlage, R., Shabanowitz, J., Hunt, D., Hozak, P., and de Lanerolle, P.** (2000). A myosin I isoform in the nucleus. *Science.* **290**, 337-341.
- Piazzesi, G., Reconditi, M., Linari, M., Lucii, L., Sun, Y.B., and Narayanan, T.** (2002). Mechanism of force generation by myosin heads in skeletal muscle. *Nature.* **415**, 659-662.
- Ponting, C.** (1995). AF-6/cno: neither a kinesin nor a myosin, but a bit of both. *Trends in Biochemical. Sciences.* **20**, 265-266.
- Ponting, C., Cai, Y., and Bork, P.** (1997). The breast cancer gene product TSG101: a regulator of ubiquitination? *J Mol Med.* **75**, 467-469.
- Prat, A., and Cantiello, H.** (1996). Nuclear ion channel activity is regulated by actin filaments. *Am J Physiol.* **270**, 1532-1543.
- Prekeris, R., and Terrian, D.** (1997). Brain myosin V is a synaptic vesicle-associated motor protein: evidence for a Ca<sup>2+</sup>-dependent interaction with the synaptobrevin-synaptophysin complex. *J. Cell Biol.* **137**, 1589-1601.
- Pruyne, D., Legesse-Miller, A., Gao, L., Dong, Y., and Bretscher, A.** (2004). Mechanisms of polarized growth and organelle segregation in yeast. *Annu Rev Cell Dev Biol.* **20**, 559-591.

- Qiao, L., Grolig, F., Jablonsky, P., and Williamson, R.** (1989). Myosin heavy chains: detection by immunoblotting in higher plants and localization by immunofluorescence in the alga *Chara*. *Cell Biol Int Rep.* **13**, 107-117.
- Qiao, L., Jablonsky, P., Elliott, J., and Williamson, R.** (1994). A 170 kDa polypeptide from mung bean shares multiple epitopes with rabbit skeletal myosin and binds ADP-agarose. *Cell Biol Int.* **18**, 1035-1047.
- Quader, H., and Schnepf, E.** (1989). Actin filament array during side branch initiation in protonema cells of the moss *Funaria hygrometrica*: an actin organizing center at the plasma membrane. *Protoplasma.* **151**, 167-170.
- Quader, H., Hofmann, A., and Schnepf, E.** (1987). Shape and movement of the endoplasmic reticulum in onion bulb epidermis cells: possible involvement of actin. *Eur J Cell Biol.* **44**, 17-26.
- Radford, J.E., and White, R.G.** (1998). Localization of a myosin-like protein to plasmodesmata. *Plant J.* **14**, 743-750.
- Rambourg, A., and Clermont, Y.** (1997). Three-dimensional structure of the Golgi apparatus in mammalian cells. *In* EG Berger, J Roth, eds *The Golgi Apparatus*. Birkhaeuser Verlag, Basel, 37-61.
- Rando, O., Zhao, K., and Crabtree, G.** (2000). Searching for a function for nuclear actin. *Trends Cell Biol.* **10**, 92-97.
- Rapp, S., Saffrich, R., Anton, M., Jäkle, U., Ansorge, W., Gorgas, K., and Just, W.W.** (1996). Microtubule-based peroxisome movement. *Cell Sci.* **109**, 837-849.
- Rayment, I., Holden, H.M., Whittaker, M., Yohn, C.B., Lorenz, M., and Holmes, K.C.** (1993). Structure of the actin-myosin complex and its implications for muscle contraction. *Science.* **261**, 58-65.
- Reck-Peterson, S., Novick, P., and Mooseker, M.** (1999). The tail of a yeast class V myosin, myo2p, functions as a localization domain. *Mol Biol Cell.* **10**, 1001-1017.

- Reddy, A.S.N., and Day, I.S.** (2001). Analysis of the myosins encoded in the recently completed *Arabidopsis thaliana* genome sequence. *Genome Biol.* **2**, 0024.0021-0024.0017.
- Reedy M. K., H.K.C.a.T.R.T.** (1965). Induced changes in orientation of the cross-bridges of glycerinated insect flight muscle. *Nature.* **207**, 1276-1280.
- Reichelt, S., Knight, A.E., Hodge, T.P., Baluska, F., Samaj, J., Volkmann, D., and Kendrick-Jones, J.** (1999). Characterization of the unconventional myosin VIII in plant cells and its localization at the post-cytokinetic cell wall. *Plant J.* **19**, 555-567.
- Reilein, A., Rogers, S., Tuma, M., and Gelfand, V.** (2001). Regulation of molecular motor proteins. *Int Rev Cytol.* **204**, 179-238.
- Robatzek, S., Chinchilla, D., and Boller, T.** (2006). Ligand-induced endocytosis of the pattern recognition receptor FLS2 in *Arabidopsis*. *Genes Dev.* **20**, 537-542.
- Robinson, D.** (2003). *The Golgi Apparatus and the Plant Secretory Pathway*  
**ISBN: 1841273295.**
- Rodriguez, O., and Cheney, R.** (2002). Human myosin-Vc is a novel class V myosin ex-pressed in epithelial cells. *J. Cell Sci* **115**, 991-1004.
- Rossanese, O., Reinke, C., Bevis, B., Ham-mond, A., and Sears, I.** (2001). A role for actin, Cdc1p, and Myo2pin the inheritance of late Golgi elements in *Saccharomyces cere-visiae*. *J. Cell Biol.* **153**, 47-62.
- Rudolf, R., Kogel, T., Kuznetsov, S., Salm, T., and Schlicker, O.** (2003). Myosin Va facili-tatesthe distribution of secretory granules inthe F-actin rich cortex of PC12 cells. *J. CellSci.* **116**, 1339-1348.
- Runions, J., Brach, T., Kühner, S., and Hawes, C.** (2006). Photoactivation of GFP reveals protein dynamics within the endoplasmic reticulum membrane. *J. Exp. Bot.* **57**, 43-50.
- Samaj, J., Read, N., Volkmann, D., Menzel, D., and Baluska, F.** (2005). The endocytic network in plants. *TRENDS in Cell Biology.* **15**, 425-433.

- Sanford, J.** (1988). The biolistic process. *Trends Biotech* **6**, 299-302.
- Sanford, J., Klein, T., Wolf, E., and Allen, N.** (1987). Delivery of substances into cells and tissues using particle bombardment process. *J. Part. Sci. Tech* **5**, 27-37.
- Schliwa, M. and Woehlke, G.** (2003). Molecular motors. *Nature*. **422**, 759-765
- Schmelzer, E.** (2002). Cell polarization, a crucial process in fungal defence. *Trend. Plant Science*. **7**, 411-15
- Schneider, K., Kienow, L., Schmelzer, E., Colby, T., Bartsch, M., Miersch, O., Wasternack, C., Kombrink, E., and Stuible, H.** (2005). A new type of peroxisomal acyl-coenzyme A synthetase from *Arabidopsis thaliana* has the catalytic capacity to activate biosynthetic precursors of jasmonic acid. *J Biol Chem*. **280**.
- Schott, D., Ho, J., Pruyn, D., and Bretscher, A.** (1999). The COOH-terminal domain of Myo2p, a yeast myosin V, has a direct role in secretory vesicle targeting. *J. Cell Biol*. **147**, 791-807.
- Schrader, M., Burkhardt, J.K., Baumgart, E., Lüers, G., Spring, H., Völkl, A., and Fahimi, H.D.** (1996). Interactions of microtubules with peroxisomes. Tubular and spherical peroxisomes in HepG2 cells and their alterations induced by microtubule-active drugs. *Eur. J. Cell Biol*. **69**, 24-35.
- Schrack, K., Nguyen, D., Karlowski, W.M., and Mayer, K.F.** (2004). START lipid/sterol-binding domains are amplified in plants and are predominantly associated with homeodomain transcription factors. *Genome Biology* **5**, 41.
- Seller, J.R.** (1999). *Myosins*. Oxford University Press, ISBN: 0198505094 .
- Sellers, J.R.** (2000). Myosins: a diverse superfamily. *Biochim. Biophys. Acta* **1496**, 3-22.

- Shahjahan, R., Hughes, K., Leopold, R., and DeVault, J.** (1995). Lower incubation temperature increases yield of insect genomic DNA isolated by the CTAB method. *Biotechniques*. **19**, 332-334.
- Shimmen, T., and Yokota, E.** (1994). Physiological and biochemical aspects of cytoplasmic streaming. *Int Rev Cytol*. **155**, 97-140.
- Shimmen, T., and Yokota, E.** (2004). Cytoplasmic streaming in plants. *Current Opinion in Cell Biology*. **16**, 68-72.
- Soccio, R., and Breslow, J.** (2003). StAR-related lipid transfer (START) proteins: mediators of intracellular lipid metabolism. *J Biol Chem*. **278**, 22183-22186.
- Spudich, J.A.** (2001). The myosin swinging cross-bridge model. *Nat. Rev. Mol. Cell Bio*. **2**, 387-392.
- Stoger, E., Sack, M., Fischer, R., and Christou, P.** (2002). Plantibodies: applications, advantages and bottlenecks. *Current Opinion in Biotechnology*. **13**, 161-166.
- Suzuki, Y., Yasunaga, T., Ohkura, R., Wakabayashi, T., and Sutoh, K.** (1998). *Nature*. **396**, 380-383.
- Takagishi, Y., Oda, S., Hayasaka, S., Dekker-Ohno, K., and Shikata, T.** (1996). The *dilute-lethal (dl)* gene attacks a Ca<sup>2+</sup> store in the dendritic spine of Purkinje cells in mice. *Neurosci. Lett*. **215**, 169-172.
- Takizawa, P., Sil, A., Swedlow, J., Herskowitz, I., and Vale, R.** (1997). Actin-dependent localization of an RNA encoding a cell-fate determinant in yeast. *Nature*. **389**, 90-93.
- Tang, F., Kauffman, E., Novak, J., Nau, J., Catlett, N., and Weisman, L.** (2003). Regulated degradation of a class V myosin receptor directs movement of the yeast vacuole. *Nature* **422**, 87-92.
- Tang, X., Hepler, P., and Scordilis, S.** (1989). Immunochemical and immunocytochemical identification of a myosin heavy chain polypeptide in Nicotiana pollen tubes. *J Cell Sci*. **92**, 569-574.

- Thomson, R., and Langford, G.** (2002). Myosin superfamily evolutionary history. *268*, 276-289.
- Tirlapur, U., Cai, G., Faleri, C., Moscatelli, A., Scali, M., Casino, C., Tiezzi, A., and Cresti, M.** (1995). Confocal imaging and immunogold electron microscopy of changes in distribution of myosin during pollen hydration, germination and pollen tube growth in *Nicotiana tabacum*. *L. Eur J Cell Biol.* **67**, 209-217.
- Tominaga, M., Kojima, H., Yokota, E., Orii, H., Nakamori, R., Katayama, E., Anson, M., Shimmen, T., and Oiwa, K.** (2003). Higher plant myosin XI moves processively on actin with 35 nm steps at high velocity. *EMBO J.* **22**, 1263-1272.
- Ueda, T., Yamaguchi, M., Uchimiya, H., and Nakano, A.** (2001). Ara6, a plant-unique novel type Rab GTPase, functions in the endocytic pathway of *Arabidopsis thaliana*. *EMBO.* **20**, 4730-4741.
- Uyeda T. Q., A.P.D.a.S.J.A.** (1996). The neck region of the myosin motor domain acts as a lever arm to generate movement. *Proc. Natl. Acad. Sci.* **93**, 4459-4464.
- Vallee, R., and Sheptner, H.** (1990). Motor proteins of cytoplasmic microtubules. *Annu Rev Biochem.* **59**, 909-932.
- Van Gestel, K., Koehler, R., and Verbelen, J.-P.** (2002). Plant mitochondria move on F-actin, but their positioning in the cortical cytoplasm depends on both F-actin and microtubules. *J Exp Bot.* **53**, 659-667.
- Verdelhan Des Molles, D., Gomord, V., Bastin, M., Faye, L., and Courtois, D.** (1999). Expression of a carrot invertase gene in tobacco suspension cells cultivated in batch and continuous culture conditions. *J. Biosci Bioeng.* **87**, 302-306.
- Vitale, A., and Pedrazzini, E.** (2005). Recombinant pharmaceuticals from plants: the plant endomembrane system as bioreactor. *Mol Interv.* **5**, 216-225.

- Voigt, B., Timmers, A., Samaj, J., Muller, J., Baluska, F., and Menzel, D.** (2005). GFP-FABD2 fusion construct allows in vivo visualization of the dynamic actin cytoskeleton in all cells of Arabidopsis seedlings. *Eur J Cell Biol.* **84**, 595-608.
- Voigt, B., Timmers, A., Samaj, J., Hlavacka, A., Ueda, T., Preuss, M., Nielsen, E., Mathur, J., Emans, N., Stenmark, H., Nakano, A., Baluska, F., and Menzel, D.** (2005). Actin-based motility of endosomes is linked to the polar tip growth of root hairs. *Eur J Cell Biol.* **84**, 609-621.
- Voinnet, O., Rivas, S., Mestre, P., and Baulcombe, D.** (2003). An enhanced transient expression system in plants based on suppression of gene silencing by the p19 protein of tomato bushy stunt virus. *Plant J.* **33**, 949-956.
- Volkman, D., and Baluska, F.** (1999). Actin cytoskeleton in plants: from transport networks to signaling networks. *Microsc. Res. Tech.* **47**, 135-154.
- Volkman D, B., F.** (1999). Actin cytoskeleton in plants: from transport networks to signaling networks. *Microsc Res Tech* **47**, 135-154.
- Wada, M., and Suetsugu, N.** (2004). Plant organelle positioning. *Current Opinion in Plant Biology.* **7**, 626-631.
- Waldo, G., Standish, B., Berendzen, J., and Terwilliger, T.** (1999). Rapid protein-folding assay using green fluorescent protein. *Nat Biotechnol.* **17**, 691-695.
- Wang, Z., and Pesacreta, T.C.** (2004). A subclass of myosin XI is associated with mitochondria, plastids and the molecular chaperone subunit TCP-1a in maize. *Cell Motil. Cytoskel.* **57**, 218-232.
- Watanabe, M., Yanagi, Y., Masuhiro, Y., Yano, T., Yoshikawa, H., Yanagisawa, J., and Kato, S.** (1998). A putative tumor suppressor, TSG101, acts as a transcriptional suppressor through its coiled-coil domain. *Biochem. Biophys. Res. Commun.* **245**, 900-905.

- Weisman, L.** (2006). Organelles on the move: insights from yeast vacuole inheritance. *Nat Rev Mol Cell Biol.* **7**, 243-252.
- Wells, A., Lin, A., Chen, L., Safer, D., Cain, S., Hasson, T., Carragher, B., Milligan, R., and Sweeney, H.** (1999). Myosin VI is an actin-based motor that moves backwards. *Nature.* **30**, 505-508.
- Wells, A.L., Lin, A.W., Chen, L.-Q., Safer, D., Cain, S.M., Hasson, T., Carragher, B.O., Milligan, R.A., and Sweeney, H.L.** (1999). Myosin VI is a myosin that moves backwards. *Nature.* **401**, 505-508.
- Whalen, M., Innes, R., Bent, A., and Staskawicz, B.** (1991). Identification of *Pseudomonas syringae* pathogens of *Arabidopsis* and a bacterial locus determining avirulence on both *Arabidopsis* and soybean. *Plant Cell.* **3**, 49-59.
- Wiemer, E.A.C., Wenzel, T., Deerinck, T.J., Ellisman, M.H., and Subramani, S.** (1997). Visualization of the peroxisomal compartment in living mammalian cells: dynamic behavior and association with microtubules. *J. Cell Biol.* **136**, 71-80.
- Williamson, R.** (1986). Organelle Movements along Actin Filaments and Microtubules. *Plant Physiology.* **82**, 631-634.
- Williamson, R.E.** (1993). Organelle movements. *Annu. Rev. Plant Physiol. Plant Mol. Biol.* **44**, 181-202.
- Wu, X., Wang, F., Rao, K., Sellers, J., and Hammer, J.** (2002). Rab27a is an essential component of melanosome receptor for myosin Va. *Mol. Biol. Cell* **13**, 1735-1749.
- Xie, W., Li, L., and Cohen, S.N.** (1998). Cell cycle-dependent subcellular localization of the TSG101 protein and mitotic and nuclear abnormalities associated with TSG101 deficiency. *Proc. Natl. Acad. Sci. USA* **95**, 1595-1600.
- Yamaguchi, M., Sasaki, T., Sivaguru, M., Yamamoto, Y., Osawa, H., Ju Ahn, S., and Matsumoto, H.** (2005). Evidence for the Plasma Membrane

Localization of Al-activated Malate Transporter (ALMT1). *Plant and Cell Physiology*. **46**, 812-816.

- Yin, H., Pruyne, D., Huffaker, C., and Bretscher, A.** (2000). Myosin V orientates the mitotic spindle in yeast. *Nature*. **406**, 1013-1015.
- Yokota, E.** (2000). Identification and characterization of higher plant myosins responsible for cytoplasmic streaming. *J Plant Res*. **113**, 511-519.
- Yokota, E., Yukawa, C., Muto, S., Sonobe, S., and Shimmen, T.** (1999). Biochemical and immunochemical characterization of two types of myosins in cultured tobacco bright yellow-2 cells. *Plant Physiol*. **121**, 525-534.
- Yun, B., Atkinson, H., Gaborit, C., Greenland, A., Read, N., Pallas, J., and Loake, G.** (2003). Loss of actin cytoskeletal function and EDS1 activity, in combination, severely compromises non-host resistance in *Arabidopsis* against wheat powdery mildew. *Plant J*. **34**, 768-777.
- Zhao, H., Liu, A., Liu, G., and Yen, L.** (2002). Purification and characterization of myosin from wheat mitochondria. *Chinese Science Bulletin*. **47**, 315-318.
- Zhong, Q., Chen, Y., Jones, D., and Lee, W.H.** (1998). Perturbation of TSG101 protein affects cell cycle progression. *Cancer Res*. **58**, 2699-2702.
- Zupan, Y., and Zambryski, P.** (1997). The *Agrobacterium* DNA transfer complex. *Crit. Rev. Plant Sci*. **16**, 279-295.

## 8 Acknowledgements

It is a pleasure to thank the many people who gave me the possibility to complete this thesis. With a deep sense of gratitude, I would like to express my most cordial thanks to my supervisor, PD. Dr. Elmon Schmelzer for his patient, his enthusiasm, his inspiration, and his great efforts to explain things clearly and simply, his immense help in all the time of research for and writing of this thesis.

I have been very fortunate to have him as my advisor. His enthusiasm and dedication toward science are an inspiration in my life, and his personal support has meant much to me. Throughout my thesis-writing period, he provided encouragement, sound advice, good teaching, good company, and lots of good ideas, insightful conversations during the development of the ideas in this thesis, and for helpful comments on the text. I would have been lost without him.

My sincere thanks are due to Prof. Dr. Paul Schulze-Lefert, the Head of the Department, for taking personal interest in my project and providing me the constant encouragement, constructive discussions and productive pieces of advice. I extend my sincere gratitude and appreciation to all CeMic lab members: Rainer Franzen, ILa Rohara, Ulrich Martin and Rolf Hirtz. Most particularly Rainer Franzen for his excellent assistance during this project and for providing nice atmosphere in the lab. The cooperation I received from other members of Max-Planck Institute for plant breeding during my PhD study is gratefully acknowledged, particularly: Dr. Agim Ballvora, Dr. Riyaz Baht, Dr. Muhammad Shahid Mukhtar, Dr. Ralf Panstruga, Klaus Richter, Dr. Uachim Uhrig, Dr. Konstanz Brühl, Dieter Becker, Farshad

Roodbaraki, Doris Birker, Dr. Imre Somsich, Dr. Michael Bartsch, Dr. Jan Dittgen, Dr. Marco Mikilis and Simone Pajonk.

I would also like to thank all the rest of the academic and support staff of the Max-Planck Institute for Plant Breeding in Cologne particularly staff member of Green house, ADIS, SUSAN groups.

I am also grateful to our external collaborators, Prof. Chris Hawes, Dr. Baluska, Dr. Boris Voigt.

Many thanks are due to IMPRS coordinator Dr. Guntram Bauer and particularly Dr Ralf Petri, for excellent scientific and administrative support and IMPRS class mates for friendly atmosphere. For financial support, I thank DFG and Max-Planck Society.

Finally, I would like to give my special thanks to my wife who endured this long process with me, always offering support and love.

This thesis is dedicated to my parents, without whom none of this would have been even possible.

## **9 Eidesstattliche Erklärung**

Ich versichere, dass ich die von mir vorgelegte Dissertation selbständig angefertigt, die benutzten Quellen und Hilfsmittel vollständig angegeben und die Stellen der Arbeit einschließlich Tabellen, Karten und Abbildungen - die anderen Werken im Wortlaut oder dem Sinn nach entnommen sind, in jedem Einzelfall als Entlehnung kenntlich gemacht habe; dass diese Dissertation noch keiner anderen Fakultät oder Universität zur Prüfung vorgelegen hat; dass sie abgesehen von unten angegebenen Teilpublikationen noch nicht veröffentlicht worden ist sowie, dass ich eine solche Veröffentlichung vor Abschluss des Promotionsverfahrens nicht vornehmen werde. Die Bestimmungen dieser Promotionsordnung sind mir bekannt. Die von mir vorgelegte Dissertation ist von Prof. Paul Schulze-Lefert betreut worden.

Köln, im August 2006

(Amirali Sattarzadeh Mohammadi)

## 10 Lebenslauf

### • Persönliche Daten

**Name:** Amirali Sattarzadeh Mohammadi  
**Anschrift:** Kolibriweg 14, Vogelsang, 50829 Köln  
**Email:** asattarzadeh@gmail.com  
**Geburtsdatum:** 22.04.1974  
**Geburtsort:** Tabriz, Iran  
**Familienstand:** Verheiratet  
**Staatsangehörigkeit:** Iraner

### • Ausbildung

**1980 – 1984** Grundschule, Tabriz, Iran  
**1985 – 1991** Allgemeine Höhere Schule, Tabriz, Iran  
**1993– 1997** Studium der Pflanzenbau und Pflanzenzüchtung an der Universität Oroumyeh/Iran mit Bacheloreabschluss

**2001-2003** Hauptstudium: Agrarwissenschaften in Universität-Bonn mit Schwerpunkt Bio-/und Gentechnologie und Züchtung (Gesamtnote 1,9)

**2002-2003** Diplomarbeit am Max-Planck Institut für Züchtungsforschung/Köln im Labor von PD.Dr.Gebhardt in der Abteilung von Professor Salamini

Thema: „ SNP markers in analysis of quantitative resistance against the potato root cyst nematode *Globodera pallida* “.

**2003-2006** Doktorarbeit am Max-Planck Institut für Züchtungsforschung/Köln im Labor von PD.Dr. Schmelzer